Process understanding of photosynthetic fluxes underlying ocean acidification responses in the coccolithophore *Emiliania huxleyi*

Dissertation zur Erlangung des akademischen Grades
eines Doktors der Naturwissenschaften

- Dr. rer. nat. -

am Fachbereich 2 (Biologie/Chemie)
der Universität Bremen

Dorothee Marie Kottmeier

September 2015

Acknowledgements

This work would not have been possible without the support of so many people. In particular, I would like to thank:

Björn Rost for the excellent supervision - Thank you for sharing your expertise and your enthusiasm, for providing support in any situation, for your time, your trust and your kindness.

Sebastian Rokitta for completing our "trio". From my very first day at the AWI you gave me all the support and time I needed. Our passionate discussions, your interest and your patience always motivated me and contributed to this work significantly.

Anya Waite for her willingness to review this thesis and to be part of my thesis committee.

Dieter Wolf-Gladrow for being such a kind and relaxed boss, for the support and being part of my thesis committee. I also thank you for the exchange of ideas about statistics and carbonate chemistry.

Lena Holtz for the discussions and giving feedback on my work - I have always appreciated your critical view and your perspectives on my ideas and the methodology.

Silke Thoms for helping me to get through some "fights" with carbonate chemistry calculations, especially for "tearing apart" the ^{14}C disequilibrium method.

The Biogeosciences group - Thank you for the warm and friendly working environment, your cooperation and all support during my time at the AWI.

All current and former Phytochange members - I really enjoyed working with you. Thank you for the scientific and personal exchange of ideas, for sharing the enthusiasm, and for always being willing to give each other a hand.

My friends - Thank for all your support, for the fun and for the dialogues. Thank you for sharing the "real" (and scientific) life with me and for always reminding me of what really matters.

My family - Thank you for being there for me unconditionally.

Contents

I. Abbreviations

Abbreviations

CA	Carbonic anhydrase
Ca^{2+}	Calcium
$CaCO_3$	Calcium carbonate
CCM	CO_2-concentrating mechanism
Chl *a*	Chlorophyll *a*
C_i	Inorganic carbon (species)
CO_2	Carbon dioxide
$[CO_2]$	CO_2 concentration(s)
CO_3^{2-}	Carbonate ion(s)
$[CO_3^{2-}]$	CO_3^{2-} concentration(s)
DBS	Dextrane-bound sulfonamide
DIC	Sum of the dissolved inorganic carbon species
ETC	Electron transfer chain
fCO_2	Fraction of net CO_2 uptake relative to overall net C_i uptake
H^+	Proton(s)
$[H^+]$	H^+ concentration(s)
H_2CO_3	Carbonic acid
HCO_3^-	Bicarbonate
$[HCO_3^-]$	HCO_3^- concentration(s)
K_m	Half-saturation (Michaelis) constant
$K_{1/2}$	Half-saturation constant
MIMS	Membrane-inlet mass spectrometry
1N	Haploid life-cycle stage
2N	Diploid life-cycle stage
OA	Ocean acidification
O_2	Oxygen
pCO_2	Partial pressure of CO_2
PIC	Particulate inorganic carbon
POC	Particulate organic carbon
PON	Particulate organic nitrogen
RubisCO	Ribulose-1,5-bisphosphate-carboxylase/oxygenase
TA	Total alkalinity
TPC	Total particulate carbon
Ω	Carbonate saturation state of seawater
μ	Specific growth constant

II. Summary

Summary

Coccolithophores are unicellular, calcareous microalgae that are amongst the most important marine primary producers and responsible for roughly half of the oceanic calcium carbonate ($CaCO_3$) precipitation. Due to their important biogeochemical role, they have been in the focus of ocean acidification (OA) research in the last decades. *Emiliania huxleyi*, the most abundant coccolithophore in the modern ocean, has been found to be very sensitive towards OA: Under increased partial pressures of carbon dioxide (pCO_2), the species' photosynthesis is stimulated, whereas its calcification and growth are impaired. The relative decrease in calcification over photosynthesis has been shown to become more pronounced with lower irradiances.

Ocean acidification involves two components: carbonation, i.e., increased levels of carbon dioxide (CO_2) and bicarbonate (HCO_3^-), as well as acidification, i.e., increased levels of free protons (H^+) or decreased pH. Most studies investigating OA effects on coccolithophores simulate "natural" OA by exposing the cells to increased pCO_2 over several generations in order to allow the cells to acclimate, i.e., to change their gene expression according to the altered conditions. After acclimation, *integrated* responses in cellular growth and elemental composition, e.g., cellular quotas of biomass (particulate organic carbon; POC) and $CaCO_3$ (particulate inorganic carbon; PIC) are measured. This approach provides information about the consequences of OA. In order to understand the cellular processes governing the integrated responses, *real-time* measurements of cellular oxygen (O_2), CO_2 and HCO_3^- fluxes need to be applied. The aim of this thesis was therefore to investigate the carbonate-chemistry dependent flux regulations in *E. huxleyi* using different *real-time* measurements.

The aim of the first study was to investigate whether OA has an effect on the inorganic carbon (C_i) species that *E. huxleyi* takes up for photosynthesis. In a first step, *E. huxleyi* was acclimated to present-day and future OA scenarios, and the integrated responses in growth and elemental composition (e.g., cellular POC and PIC quotas) were measured. In the second step, C_i fluxes underlying these observed responses were characterized. In order to differentiate between the cellular uptake of CO_2 and HCO_3^-, the ^{14}C disequilibrium method was applied to the present-day and OA-acclimated cells, each at five ecologically relevant pH values (pH 7.9 - 8.7). The study revealed increased POC and decreased PIC production rates under OA. Independent of the acclimation history of the cells, a strong increase in the fraction of CO_2 uptake under decreasing pH values and the concomitantly increasing $[CO_2]$ was measured. The pH-dependent increase in CO_2 uptake can explain why OA has a stimulatory effect on POC production. The strong pH-dependence of in cellular C_i fluxes showed that, when identifying physiological processes causing the integrated OA responses, cellular fluxes should be measured at the same carbonate chemistry conditions as having been applied during acclimation, rather than at pH-standardized conditions as it is often the case.

The aim of the second study was to identify the chemical drivers causing the short-term responses in *E. huxleyi* that were observed in the first study. Membrane-inlet mass

spectrometry (MIMS) was used to measure O_2, CO_2 as well as HCO_3^- fluxes associated with photosynthesis and respiration under these conditions. Cells were acclimated to present-day conditions and, in order to differentiate the effects of carbonation and acidification, cellular fluxes were measured under artificially decoupled carbonate chemistry. To address how energization modulates the C_i fluxes, cells were also acclimated to different light intensities. The study revealed a pronounced H^+ sensitivity of the investigated processes: under all irradiances, HCO_3^- uptake was significantly decreased under high [H^+], but was relatively unaffected by carbonation. In low-light acclimated cells, CO_2 uptake was strongly increased under high [H^+], and overcompensated the inhibition in HCO_3^- uptake. Photosynthesis was consequently increased under acidification. In high-light acclimated cells, however, CO_2 uptake was not affected by [H^+]. As a consequence of the impaired HCO_3^- uptake, photosynthesis became C_i-limited and decreased relative to non-acidified conditions. These responses indicate that typical OA responses of *E. huxleyi* are mainly driven by [H^+]. Furthermore, photosynthetic performance in low-light grown cells seems to benefit from OA, while high-light grown cells face the risk of being C_i-limited in the future ocean.

The aim of the third study was to investigate whether C_i fluxes in high-light acclimated cells are regulated similarly when cells are allowed to acclimate to the modulated conditions. *E. huxleyi* was grown under high irradiance and acclimated either to carbonation, to acidification, or to a combination of the two. Subsequently, the integrated responses (e.g., PIC and POC quotas) were measured. MIMS was then used to quantify the *real-time* fluxes under the same carbonate chemistry as had been applied during acclimation. By measuring PIC:POC ratios, it was furthermore possible to calculate the proportion of C_i flux used for calcification. Carbonation had a stimulatory effect on HCO_3^- uptake for photosynthesis and calcification, but led to decreased CO_2 uptake. However, as HCO_3^- levels are expected to increase only slightly, these stimulatory effects do not explain typical OA responses. H^+ dependent flux regulations were similar as were observed on short time scales: cellular HCO_3^- uptake (for photosynthesis and calcification) was decreased under high [H^+], whereas photosynthetic CO_2 uptake was concomitantly increased. Because calcification could not access CO_2 as an alternative Ci source, it decreased relative to photosynthesis. The opposing H^+ dependent regulations in HCO_3^- and CO_2 uptake can explain the typical decrease in PIC:POC ratios often observed in *E. huxleyi* and other coccolithophores acclimated to OA.

Next to the investigation of carbonate chemistry and light effects on cellular processes, the focus of this thesis was the comparison of the diploid, calcifying and the haploid, non-calcifying life-cycle stage. Physiological key characteristics of both stages could be identified, which permitted conclusions to be drawn about the function of calcification. By measuring OA responses using different commonly applied methods, methodological strengths and weaknesses could be detected.

III. Zusammenfassung

Zusammenfassung

Coccolithophoriden sind einzellige, kalzifizierende Algen, die zu den wichtigsten marinen Primärproduzenten zählen und für etwa die Hälfte der Kalziumkarbonatproduktion ($CaCO_3$) im Ozean verantwortlich sind. Aufgrund ihrer besonderen biogeochemischen Bedeutung wurde in den letzten Jahrzehnten intensiv an der Frage geforscht, ob Coccolithophoriden von anthropogener Ozeanversauerung betroffen sind. Dabei zeigte sich, dass der häufigste Vertreter der Coccolithophoriden, *Emiliania huxleyi*, üblicherweise mit gesteigerten Photosyntheseraten und reduzierten Kalzifizierungsraten auf die veränderte Karbonatchemie reagieren. Die Auswirkungen sind hierbei stärker, wenn die Zellen unter niedrigen Lichtintensitäten wachsen.

Ozeanversauerung beinhaltet zwei chemische Komponenten: die Karbonisierung, d.h. erhöhte Konzentrationen an Kohlenstoffdioxid (CO_2) und Hydrogenkarbonat (HCO_3^-), und die Versauerung, d.h. eine erhöhte Konzentration freier Protonen (H^+) bzw. einen niedrigeren pH-Wert. In den meisten Ozeanversauerungs-Studien an Coccolithophoriden werden „natürliche" Szenarien simuliert, in denen Zellen einem erhöhten CO_2-Partialdruck über mehrere Generationen hinweg aussetzt werden, so dass sie sich an die veränderten Bedingungen akklimieren, d.h. ihre Genexpression anpassen können. Nach ausreichender Akklimierungszeit werden oftmals die integrierten zellulären Veränderungen im Wachstum oder der elementaren Zusammensetzung gemessen, z.B. im zellulären Biomasse-Anteil (partikulärer organischer Kohlenstoff, POC) und im $CaCO_3$-Anteil (partikulärer anorganischer Kohlenstoff, PIC). Dieser Ansatz ermöglicht es, Konsequenzen der Ozeanversauerung abzuschätzen. Aber nur physiologisch Echtzeitmessungen der Sauerstoff (O_2)-, CO_2- und HCO_3^- -Flüsse können über die den integrierten Antworten zugrundeliegenden Prozesse Auskunft geben. In dieser Doktorarbeit werden daher Echtzeitmessungen verwendet, um Karbonatchemie-abhängige Regulationen in den zellulären Flüssen zu untersuchen und die typischen Ozeanversauerungsreaktionen von *E. huxleyi* zu erklären.

Das Ziel der ersten Studie war es herauszufinden, ob Ozeanversauerung einen Einfluss auf die externen anorganischen Kohlenstoffquellen (C) hat, welche *E. huxleyi* für die Photosynthese aufnimmt. Hierzu wurden Zellen zunächst an heutige sowie an Ozeanversauerungs-Szenarien akklimiert und die integrierten Reaktionen im Wachstum und der Elementarzusammensetzung (z.B. zelluläre PIC- und POC-Anteile) gemessen. Anschließend wurde untersucht, welche C-Flüsse den gemessenen Reaktionen zugrunde liegen. Dazu wurde die sogenannte ^{14}C-Disequlibriums-Methode, die zwischen der zellulären Aufnahme von CO_2 und HCO_3^- unterscheiden kann, bei fünf ökologisch relevanten pH-Werten (zwischen pH 7,9 und pH 8,7) in den unterschiedlich akklimierten Zellen angewandt. Die Ergebnisse zeigten, dass die POC-Produktion unter Ozeanversauerung deutlich stimuliert wird, während die PIC-Produktion abnimmt. Zudem wurde ein starker Anstieg in der CO_2-Aufnahme gemessen, nachdem die Zellen in ein Medium mit niedrigeren pH-Wert und gleichzeitig höherer CO_2 -Konzentration überführt wurden. Diese gesteigerte CO_2-Nutzung unter erhöhten [H^+] und [CO_2] trat

unabhängig davon auf, wie die Zellen zuvor akklimiert waren und könnte die gesteigerte POC-Produktion unter Ozeanversauerung erklären. Aus der starken pH-Anhängigkeit in der C-Aufnahme konnte geschlussfolgert werden, dass die zelluläre Prozesse, welche die integrierten Ozeanversauerungsantworten verursachen, bei der gleichen Karbonatchemie, die auch während der Akklimierung angewandt wurde, gemessen werden sollten.

Das Ziel der zweiten Studie war es, den chemischen Treiber hinter der erhöhten CO_2-Nutzung in der ersten Studie zu identifizieren. Dazu wurde die Methode der sogenannten „Membrane-inlet mass spectrometry“ (MIMS) angewandt, mit derer die zellulären O_2-, CO_2- und HCO_3^--Flüsse während Photosynthese und Respiration unterschieden werden können. Die Zellen wurden an heutige Bedingungen akklimiert. Anschließend wurden die zellulären Flüsse unter künstlich entkoppelten Karbonatchemie-Bedingungen gemessen, um zwischen dem Einfluss von Karbonisierung und Versauerung zu differenzieren. Um den Effekt von Licht-Energetisierung auf die C-Flüsse zu untersuchen, wurden die Zellen zudem an unterschiedliche Lichtintensitäten akklimiert. In der Studie wurden ausgeprägte H^+-Sensitivitäten aufgezeigt: In allen Licht-Akklimierungen wurde die photosynthetische HCO_3^--Aufnahme durch hohe H^+-Konzentrationen deutlich gehemmt, wohingegen dieser Prozess durch Karbonisierung kaum beeinflusst wurde. In Niedriglicht-akklimierten Zellen wurde die Hemmung in der HCO_3^--Aufnahme überkompensiert, in dem die Zellen die die CO_2-Aufnahme gleichzeitig stark erhöhten. In Hochlicht-akklimierten Zellen war die CO_2-Aufnahme hingegen unbeeinflusst, weshalb die herabgesetzten HCO_3^--Aufnahme unter Versauerung zu einer C-Limitierung in der Photosynthese führte. Folglich werden typische Ozeanversauerungs-Reaktionen nicht primär von erhöhten CO_2-Konzentrationen, sondern vor allem durch erhöhte H^+-Konzentrationen hervorgerufen. Es wurde außerdem deutlich, dass Photosynthese in Niedriglicht-akklimierten Zellen aufgrund der gesteigerten CO_2-Aufnahme eher von Ozeanversauerung profitiert, während Hochlicht-akklimierte Zellen unter Ozeanversauerung C-limitiert werden könnten.

Das Ziel der dritten Studie war es herauszufinden, ob C-Flüsse in Hochlicht-akklimierten Zellen ähnlich reguliert werden, wenn sie veränderter Karbonatchemie nicht nur kurzfristig sondern über Akklimierungs-Zeiträume ausgesetzt werden. Zu diesem Zweck wurde *E. huxleyi* bei Hochlicht an reine Karbonisierungs- und Versauerungs-Szenarien sowie eine Kombination der beiden (Ozeanversauerung) akklimiert. Anschließend wurden die integrierten zellulären Veränderungen gemessen und die Echtzeit-Flüsse unter derselben Karbonatchemie, die auch während der Akklimierung vorlag, mittels MIMS-Technik gemessen. Zusätzlich konnten mithilfe der in dieser Studie gemessenen zelluären PIC:POC-Ratios auch die C-Flüsse der Kalzifizierung berechnet werden. Karbonisierung führte zu einer gesteigerten HCO_3^--Aufnahme für Photosynthese und Kalzifizierung, aber auch zu einer verringerten CO_2-Aufnahme. Diese Effekte können typische Ozeanversauerungseffekte jedoch nicht erklären, da sich die HCO_3^--Konzentration unter natürlichen Ozeanversauerungs-Bedingungen nur geringfügig erhöht ist. Die Regulationen der zellulären Flüsse unter Versauerung waren den Beobachtungen während Kurzzeit-Versauerung sehr ähnlich: Die

HCO_3^--Aufnahme für Photosynthese und Kalzifizierung war herabgesetzt, während die CO_2-Aufnahme für Photosynthese kompensatorisch heraufgesetzt wurde. Insgesamt blieb die C-Aufnahme für Photosynthese somit gleich hoch und die Zellen konnten ihre Photosyntheseraten aufrechterhalten. Kalzifizierung konnte jedoch auf keine alternative C-Quelle zugreifen, was die typischen, gegenläufigen Trends in Photosynthese- und Kalzifizierungsraten unter Ozeanversauerung erklärt.

Die beobachteten Regulierungen können nicht nur für eine mechanistische Erklärung der typischen Reaktion von *E. huxleyi* auf Ozeanversauerung genutzt werden, sondern zeigen auch, wie diese durch Licht-Energetisierung beeinflusst wird. Zum ersten Mal wurde aufgezeigt, dass die erhöhte Photosynthese und die herabgesetzte Kalzifizierung unter Ozeanversauerung keine Reaktionen auf Karbonisierung sind, sondern durch hohe H^+-Konzentrationen ausgelöst werden. Im Rahmen dieser Doktorarbeit wurden zudem die zellulären Flüsse des haploiden, nicht-kalzifizierten und des diploiden, kalzifizierenden Lebensstadiums von *E. huxleyi* verglichen. Das haploide Stadium zeigte kaum Reaktionen auf Ozeanversauerung. Durch die Unterschiede in den Flüssen konnten Rückschlüsse auf mögliche physiologische Funktionen der Kalzifizierung gezogen werden. Durch den Vergleich der ^{14}C- und des MIMS-Messungen wurden außerdem Stärken und Schwächen der beiden Methoden aufgezeigt.

Chapter 1
General Introduction

Preface

Two and a half centuries ago, humankind started to "carry out a large-scale geophysical experiment of a kind that could not happened in the past nor be reproduced in the future" in which "organic carbon stored in sedimentary rocks over hundreds of millions of years is returned to atmosphere and oceans" (Revelle and Suess 1957). This "geophysical experiment", as Revelle and Suess called it, refers to the increasing combustion of fossil fuels since the beginning of the industrial age that, since then, has led to the successive increase in the atmospheric carbon dioxide (CO_2) levels, and a significant uptake of anthropogenic CO_2 in the ocean. These effects, nowadays referred to as "climate change", caused the earth's atmosphere to continuously warm and the oceans to acidify. Both effects have turned out to have severe environmental and social consequences (IPCC, 2013). In order for humans to find solutions and to finally stop "the experiment", scientists currently face the challenge of understanding how these environmental changes affect chemical and biological processes; and improving predictions of future consequences of global change.

1.1 Human perturbation of the global carbon cycle

The earth's carbon is transported between large terrestrial, atmospheric and oceanic reservoirs and thereby undergoes changes in its chemical form (Post *et al.*, 1990). A huge part of the carbon is stored in geological pools with very high residence times of >10,000 yrs. The exchange of carbon between "slow turnover" (geological pools) and "fast turnover" reservoirs (e.g., the atmosphere, the ocean, surface oceans sediments and on-land vegetation) is relatively sparse (<0.3 Pg carbon yr^{-1}) and was restricted to emissions of CO_2 by volcanic activity, erosion, sediment formation and chemical weathering for a majority of the earth's history (Sundquist, 1990; Archer & Maier-Reimer, 1994). However, since the industrial revolution in the 18th century increasing amounts of fossil fuels have been extracted from geological reservoirs and their combustion resulted in a significant transfer of fossil carbon from the slow to fast turnover reservoirs (Le Quéré *et al.*, 2014). Combined with the strong increase in deforestation, these combustion emissions caused a strong disequilibrium in the global carbon cycle and have led to a significant increase in the atmospheric CO_2 levels over the last centuries. While the atmospheric partial pressure of CO_2 (pCO_2) fluctuated between ~180 μatm and 290 μatm for at least 800,000 years, it has increased to ~390 μatm and is currently higher than at any time over the least 2.1 million years (Fig. 1.1; Petit *et al.*, 1999; Luthi *et al.*, 2008; Keeling *et al.*, 2009). Climate projections by the Intergovernmental Panel on Climate Change (IPCC) predict that the atmospheric pCO_2 will continuously rise and reach levels between ~670 μatm and ~930 μatm by the end of the century (Fig. 1.1; Ciais *et al.*, 2013). On time scales of decades, the oceans will have absorbed roughly a third of the anthropogenic CO_2 and have shifted from a source of CO_2 in preindustrial times to a sink for CO_2 (Sabine *et al.*, 2004).

The increase in pCO_2 will have strong impacts on the earth's climate, not only because atmospheric CO_2 connects the carbon pools of land and ocean, but especially because CO_2 is one of the most important greenhouse gas after water vapor (Fourier, 1822; Arrhenius, 1896). The elevated pCO_2 has already induced a rise in the global average temperature by ~0.85°C since 1951 and is expected to increase further by up to 4.8°C by the end of the century (Ciais *et al.*, 2013). This will, amongst others, lead to more frequent extreme weather and climate events, e.g., heat waves, heavy precipitation, droughts, floods, cyclones and wildfires. The melting of Greenland and Antarctic ice sheets and the worldwide shrinking of glaciers are expected to continue (Ciais *et al.*, 2013). Increased temperature and water input from ice sheets lead to a continuous rise in the sea level. The oceans, absorbing ~90% of the earth´s additional heat and ~30% of the anthropogenic CO_2, are also affected with respect to physical properties, such as temperature, salinity and water mass circulation (Fig 1.1), and with respect to the chemical properties (see chapter 1.2; Rhein *et al.*, 2013). These changes will not only have severe impacts on marine ecosystems, but ultimately impact humans. Since almost one billion people live at the coasts, the oceans do not only play an important economic role, but currently provide ~10% of proteins eaten by humans. Humans nowadays face climate-change induced risks of pollution, health problems, hunger crises and poverty (Pörtner *et al.*, 2014).

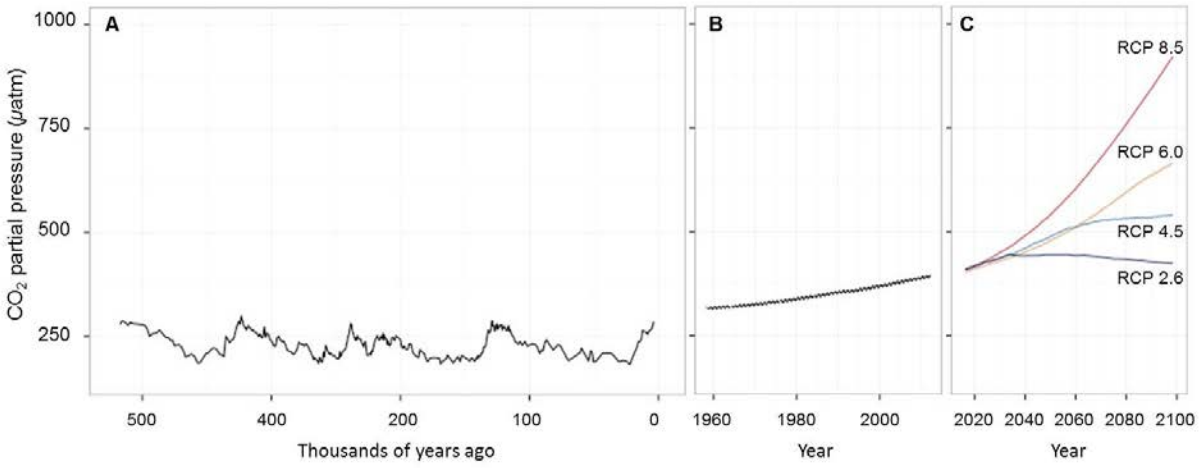

Figure 1.1: Fluctuations in atmospheric pCO_2. A Changes over the past 400,000 years (Vostok ice cores; Barnola *et al.*, 2003), **B** between 1960 and 2015 from atmospheric measurements (Mauna Loa; Keeling *et al.*, 2009) and **C** as predicted by the different IPCC emission scenarios (Ciais *et al.*, 2013). Representative concentration pathways (RCPs) and respective numbers refer to the potential radiative forcing values in 2100 relative to pre-industrial values (+2.6, 4.5, 6.0 and 8.5 W m^{-2})

1.2 Carbon in the ocean

Carbonate chemistry

Atmospheric CO_2 exchange with the surface ocean is driven by differences in pCO_2 between air and sea (Zeebe & Wolf-Gladrow, 2001). At equilibrium, the surface concentration of dissolved CO_2 ($[CO_2]_{aq}$, L^{-1}) is proportional to pCO_2 (atm). The relation is expressed by Henry's law:

$$[CO_2]_{aq} = pCO_{2_{atm}} K_0 \qquad (1.1)$$

where K_0 is the temperature-, pressure- and salinity-dependent Henry's constant (mol L^{-1} atm^{-1}) as defined by Weiss (1974).

In seawater, dissolved CO_2 does not only exist in the free form, but also is in equilibrium with the three other inorganic carbon (C_i) species; carbonic acid (H_2CO_3), bicarbonate (HCO_3^-) and carbonate ion (CO_3^{2-}; Eq. 1.2). As the concentration of H_2CO_3 is <0.3% of the overall CO_2 and chemically not separable from CO_2, both species are often subsumed in the term CO_2.

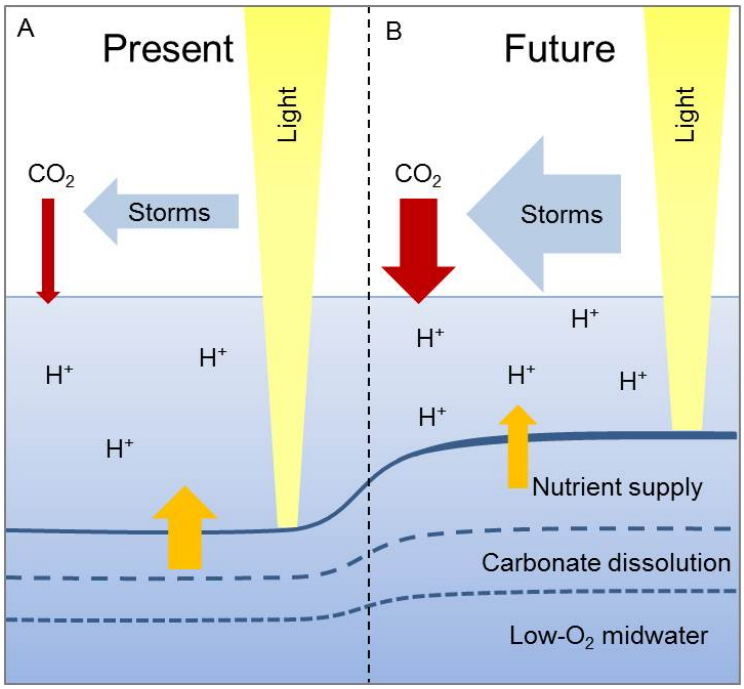

Figure 1.2: Consequences of increased anthropogenic CO_2 emissions on marine systems. Increased surface temperatures lead to an increased density stratification (thickness of solid horizontal line) and to a shallower mixed layer (solid horizontal line), resulting in higher mean irradiances, reduced winter mixing and nutrient supply for photosynthesizing organisms. The increased pCO_2 is associated with shifts in the carbonate chemistry towards increased proton (H^+) levels (discussed in more details below). Acidification causes a rise of the lysocline, i.e., the depth below which $CaCO_3$ dissolves (long-dashed line). Further changes that may indirectly affect ecosystems are rising of low-O_2 midwaters (short-dashed line) and increased storm frequencies. Modified after Reusch and Boyd (2013).

The sum of the dissolved forms of C_i is usually referred to as dissolved inorganic carbon (DIC; Zeebe & Wolf-Gladrow, 2001). The equilibrium between the different C_i species can be expressed as:

$$CO_2 + H_2O \overset{K_1^*}{\rightleftharpoons} HCO_3^- + H^+ \overset{K_2^*}{\rightleftharpoons} CO_3^{2-} + 2\,H^+ \qquad (1.2)$$

K_1^* and K_2^* are the first and second T-, p-, S-dependent stoichiometric equilibrium constants of carbonic acid, respectively:

$$K_1^* = \frac{[HCO_3^-]\,[H^+]}{[CO_2]} \qquad (1.3)$$

$$K_2^* = \frac{[CO_3^{2-}]\,[H^+]}{[HCO_3^-]} \qquad (1.4)$$

During the dissociation of H_2CO_3 into HCO_3^- and CO_3^{2-}, protons (H^+) are set free. Consequently, the pH value decreases with increasing CO_2 dissolution. The relation between carbon speciation and pH is commonly illustrated in the so-called "Bjerrum plot" (Fig. 1.3). Under typical present-day ocean conditions with a pCO_2 of ~390 μatm (T = 15°C, DIC = ~2100, pH_{NBS} = ~8.1), ~ 90% of DIC is in the form of HCO_3^-, 10% in the form of CO_2^{3-}, and less than 1% is in the form of CO_2. This is paralleled with a surface pH_{NBS} of ~8.1.

The hydration of CO_2, i.e., the reaction of CO_2 with H_2O to HCO_3^- and H^+ is a very slow reaction and the time-determining step in the equilibration of the seawater surface with the

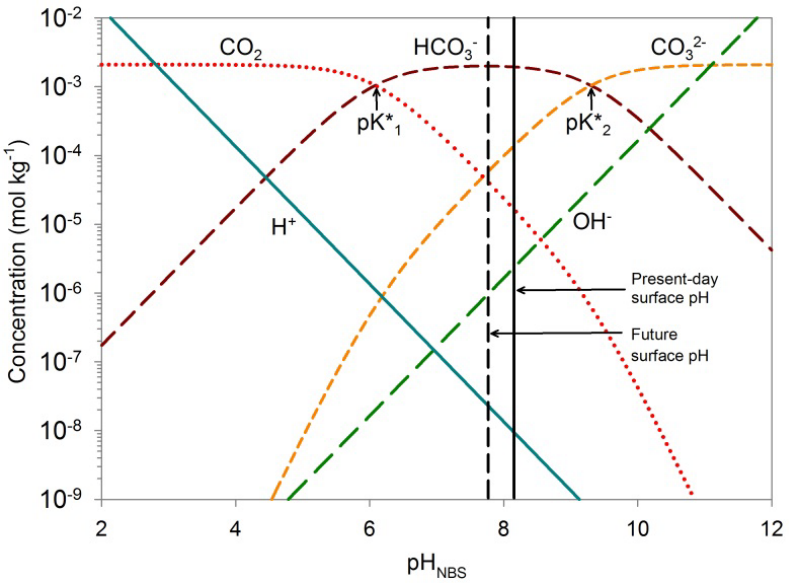

Figure 1.3: Carbon speciation in seawater. Bjerrum plot for conditions of DIC = 2100 μmol kg^{-1}, temperature = 15°C, salinity = 30, pressure = 1 dbar. Black lines indicate present-day (solid) and future (dashed) pH values. Vertical arrows indicate pK^*_1 and pK^*_2 values of carbonic acid, i.e., the pH at which $[CO_2]$ and $[HCO_3^-]$ or $[CO_3^{2-}]$ and $[HCO_3^-]$ are equal. Modified after Zeebe and Wolf-Gladrow (2001).

atmosphere (Eq. 1.2). It can occur via different pathways, each following their own reaction kinetics being defined by the rate constants (Fig. 1.4). So called "effective rate constants" (s^{-1}) describe the temperature and salinity-dependent kinetics of the sum of these reactions:

$$k_{-} = k_{-1}[H^{+}] + k_{-4} \quad (1.5)$$

$$k_{+} = k_{+1} + k_{+4}[OH^{-}] \quad (1.6)$$

where k_{-1} and k_{-4} (s^{-1}; calculated) as well as k_{+1} and k_{+4} (kg mol^{-1} s^{-1}; after Johnson 1982) are the rate constants describing the hydration reaction between CO_2 and HCO_3^- (Fig. 1.4; Zeebe & Wolf-Gladrow, 2001). The protolysis and hydrolysis reaction involved in the interconversion of HCO_3^- and CO_3^{2-} are, in contrast to the hydration step, basically instantaneous (Fig. 1.4).

The overall equilibrium situation of the carbonate systems can be calculated based on four equations accounting for [CO_2], [HCO_3^-], [CO_3^{2-}], DIC, pH and a further quantity of the seawater, the so-called total alkalinity (TA). When two of the six quantities are known, the other four can be calculated (Zeebe & Wolf-Gladrow, 2001). Total alkalinity can be defined as the excess of chemical compounds that serve as H^+ acceptors over the compounds being H^+ donors with respect to zero level of H^+ (Dickson, 1981) and is associated with the ocean's buffer capacity, i.e., the alkalinity within the carbonate system acts as a natural buffer for the seawater pH. For example, when strong acid (<3 mmol L^{-1}) is added to seawater, HCO_3^- and CO_3^{2-} ions are transformed to CO_2 and the pH remains between 8 and 6. Alkaline properties of seawater mainly originate from continental weathering and, to a smaller fraction, from

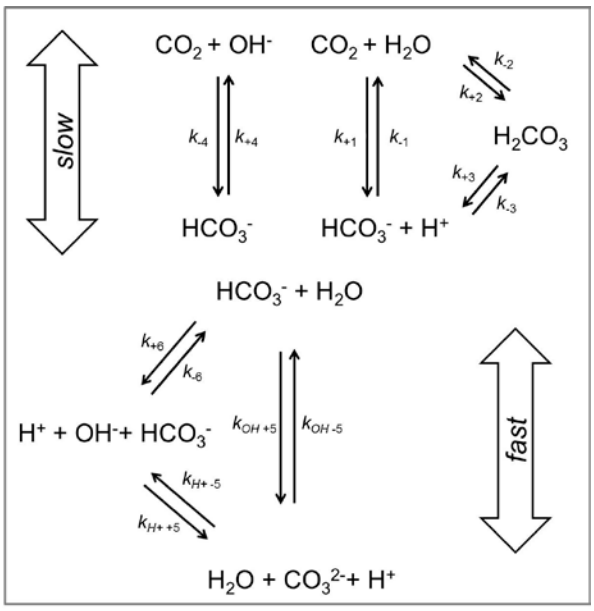

Figure 1.4: Reactions and rate constants of the carbonate system. The hydration CO_2 is a relatively slow reaction, while the protolysis and hydrolysis of HCO_3^- are very fast. After Zeebe and Wolf-Gladrow (2001).

hydrothermal vents. The buffer capacity does not only relate to the carbonate alkalinity (CA), but furthermore includes other compounds, such as borate and water alkalinity. The traditional definition by Dickson reads:

$$\mathrm{TA} = [\mathrm{HCO_3^-}] + 2[\mathrm{CO_3^{2-}}] + [\mathrm{B(OH)_4^-}] + [\mathrm{OH^-}] + [\mathrm{HPO_4^{2-}}] + 2[\mathrm{PO_4^{3-}}] + [\mathrm{H_3SiO_4^-}] + [\mathrm{NH_3}] + [\mathrm{HS^-}] - [\mathrm{H^+}] - [\mathrm{HSO_4^-}] - [\mathrm{HF}] - [\mathrm{H_3PO_4}] + \ldots \quad (1.7)$$

where H^+ acceptors are weak acids with pK ≥4.5. (e.g., HCO_3^-), H^+ donors are acids with pK <4.5 (e.g., H_3PO_4) and ellipses are additional yet undefined acid-base species. A complementary definition of TA takes into account the concentrations of major ions of seawater, a conservative quantity, rather than the level of H^+ donors and acceptors, which depend on temperature and pressure (Wolf-Gladrow *et al.*, 2007). Therefore, this definition is referred to as the explicit conservative for of TA (TA_{EC}):

$$\mathrm{TA_{EC}} = [\mathrm{Na^+}] + 2[\mathrm{Mg^{2+}}] + 2[\mathrm{Ca^{2+}}] + 2[\mathrm{Sr^{2+}}] + \cdots - [\mathrm{Cl^-}] - [\mathrm{Br^-}] - [\mathrm{NO_3^-}] \ldots - \mathrm{TPO_4} + \mathrm{TNH_3} - 2\mathrm{TSO_4} - \mathrm{THF} - \mathrm{THNO_2} \quad (1.8)$$

with $TPO_4 = [H_3PO_4] + [H_2PO_4^-] + [HPO_4^{2-}] + [PO_4^{3-}]$, $TNH_3 = [NH_3] + [NH_4^+]$, $TSO_4 = [SO_4^{2-}] + [HSO_4^-]$, $THF = [F^-] + [HF]$, and $THNO_2 = [NO_2^-] + [HNO_2]$ being the total phosphate, ammonia, sulfate, fluoride and nitrite concentrations, respectively.

The effect of biological processes on carbonate chemistry

Biological processes, especially marine primary production, strongly influence carbonate chemistry and therewith significantly contribute to the CO_2 fluxes between atmosphere and ocean. Primary production in the ocean is mainly carried out by phytoplankton (greek: phyton = plant and plankton = wanderer), a phylogenetically diverse group of mostly single-celled photosynthetic organisms that contribute to ~50% of the global primary production, even though its biomass is only 1% of the terrestrial biomass (Behrenfeld & Falkowski, 1997; Field *et al.*, 1998; Falkowski *et al.*, 2004). In the process of photosynthesis, light energy is captured and stored in organic matter, so-called particulate organic carbon (POC). Carbon dioxide is therefore extracted from the system, leading to decreased DIC levels, while TA remains unaffected by this process:

$$6\,\mathrm{CO_2} + 6\,\mathrm{H_2O} \leftrightarrow \mathrm{C_6H_{12}O_6} + 6\,\mathrm{O_2} \quad (1.9)$$

Next to CO_2, phytoplankton takes up other nutrients in the course of its growth. Under optimal growth conditions, the uptake of NO_3^- approximately follows a stoichiometry of C:N = 106:16 = ~6.6:1 (Redfield, 1958). During the uptake of nitrate (NO_3^-), DIC is unaffected, but TA increases due to the removal of the negative charge of NO_3^- (Eq. 1.8). Hence, during organic matter production, one unit of DIC is reduced while TA increases by 0.06 units (Fig. 1.5; Brewer & Goldman, 1980; Zeebe & Wolf-Gladrow, 2001). This can, however,

change when phytoplankton uses alternative N-sources: Uptake of ammonium (NH_4^+), for example, affects TA adversely (Eq. 1.8).

Pelagic and benthic calcifiers (e.g., coccolithophores, foraminifera or corals) are organisms that form skeletons from calcium carbonate ($CaCO_3$). During the process of calcite formation:

$$Ca^{2+} + CO_3^{2-} \leftrightarrow CaCO_3 \qquad (1.10)$$

DIC is reduced by one unit, and TA decreases by two units due to the removal of two negative charges (Eq. 1.8, Fig. 1.5; Zeebe & Wolf-Gladrow, 2001). As a result, the system shifts to higher CO_2 concentrations (Fig. 1.5) and to a lower pH value. Please note that alternative chemical reaction pathways of $CaCO_3$ formation are generally possible, e.g., with HCO_3^- as substrate (Rost & Riebesell, 2004). However, these would affect the carbonate chemistry equally.

Consequences of ocean acidification on biological processes

The invasion of anthropogenic CO_2 into the surface seawater not only induces shifts in the equilibrium between the different C_i species towards higher concentrations of CO_2, HCO_3^- and decreased concentrations of CO_3^{2-}, but also towards higher levels of H^+ (Fig. 1.3, 1.5, 1.6). This is why the sum of these changes is referred to as ocean acidification (OA; Wolf-Gladrow *et al.*, 1999; Caldeira & Wickett, 2003). As most of the CO_2 taken up by the oceans

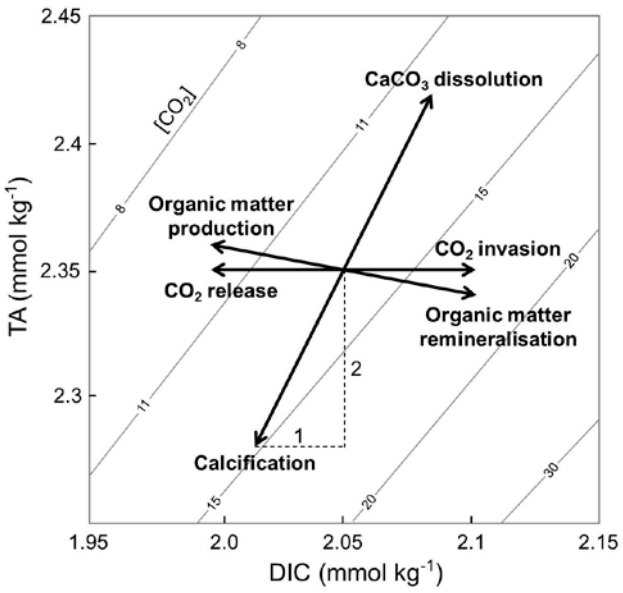

Figure 1.5: Effects of various processes on DIC and TA. Solid lines indicate constant $[CO_2]_{aq}$ as a function of DIC and TA. During organic matter production, DIC is decreased by one unit, and, in the example of NO_3^- uptake, TA is increased by 0.06 units, while remineralisation has the opposite effect. During calcification, DIC is decreased by one and TA by two units, while $CaCO_3$ dissolution shifts the carbonate system in the other direction. The invasion of atmospheric CO_2 increases DIC, while CO_2 release into the atmosphere decreases DIC by one unit. In these cases, TA is unaffected. Modified after Zeebe and Wolf-Gladrow (2001).

is converted to HCO_3^-, the OA-related absolute increase in DIC levels is higher than the absolute increase in CO_2 levels. In terms of relative changes, however, CO_2 levels increase much more than DIC levels (Fig. 1.3, 1.6). Since the beginning of the industrial era, pH has already dropped from 8.2 to 8.1, which corresponds to an increase in H^+ levels by ~30%. The current pH is lower than at any time during the last 50 million years (Ciais *et al.*, 2013). Estimates based on projected future pCO_2 indicate that under continuous combustion of fossil fuels, pH might even drop by another 0.2 to 0.4 units (Fig. 1.6; Rhein *et al.*, 2013). The acidification varies locally and is more pronounced in areas with lower buffer capacities (i.e., low TA) and cold temperatures, such as polar and subpolar regions.

Ocean acidification has been shown to affect marine biota in many ways, ranging from alterations in physiology, behavior and ultimately survival and population dynamics of the species (Howes *et al.*, 2015; Mackey *et al.*, 2015). Hence, biogeography and phenology change, which has severe consequences for ecosystems and biogeochemical cycling (Pörtner *et al.*, 2014; Gaylord *et al.*, 2015). Regarding primary producers, elevated CO_2 levels were hypothesized to have a fertilizing effect on primary production (Riebesell *et al.*, 1993; Wolf-Gladrow *et al.*, 1999b) and, indeed, some taxa of phytoplankton and macroalgae exhibit increased growth and photosynthetic rates under elevated pCO_2 (Rost *et al.*, 2008; Kroeker *et al.*, 2013; Mackey *et al.*, 2015). Such beneficial effects are usually attributed to an increased CO_2 accumulation at the highly conserved CO_2-fixing enzyme Ribulose-1,5-bisphosphate-carboxylase/oxygenase (RubisCO) that evolved at times of very high CO_2 concentrations and low O_2 concentrations (Falkowski & Raven, 2007). The enzyme is relatively low-affine and

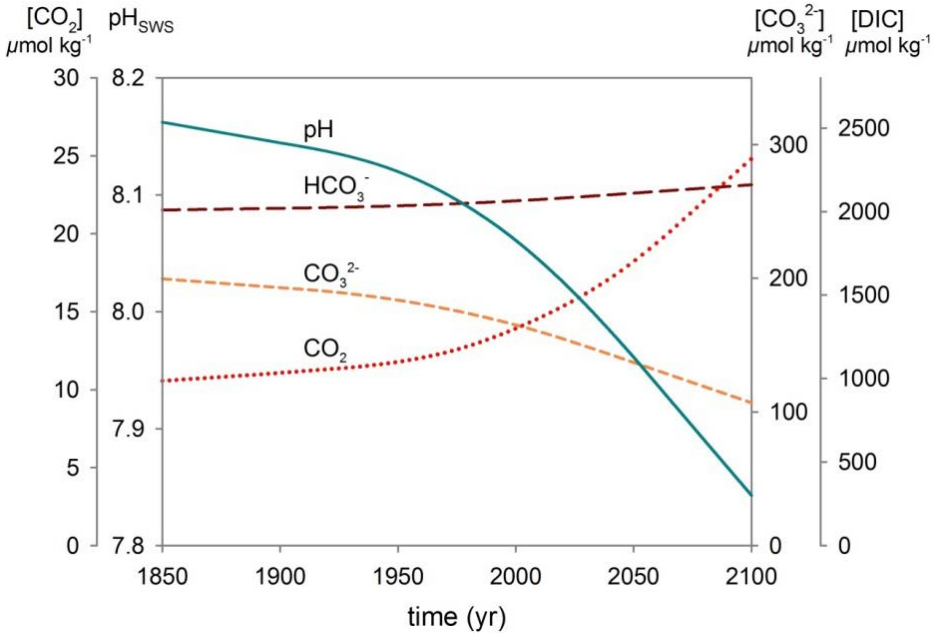

Figure 1.6: Predicted changes of the marine seawater carbonate chemistry. Data is based on the RCP 6.0 scenario (IPCC 2014). Illustrated scenarios are calculated for TA = 2300 μmol kg^{-1}, S = 35 and T = 15°C and smoothed for illustration.

therefore not substrate-saturated at present-day [CO_2] (cf., section 1.4; Badger *et al.*, 1998; Rost *et al.*, 2003). Increased photosynthesis would give a "negative feedback" on climate, as it leads to an increased removal of CO_2 uptake from seawater and atmosphere and an improved biological carbon pump (cf., section 1.3; Rost & Riebesell 2004).

Lowered CO_3^{2-} levels are accompanied by a decreased carbonate saturation state (Ω), a factor that reflects the thermodynamic stability of the $CaCO_3$ structures. The calcite saturation state of seawater is defined as the ion product of [Ca^{2+}] and [CO_3^{2-}]:

$$\Omega = \frac{[Ca^{2+}]\,[CO_3^{2-}]}{K^*_{sp}} \qquad (1.11)$$

with K^*_{sp} being the temperature-, salinity, and pressure-dependent solubility product. Because formation of $CaCO_3$ only occurs at $\Omega > 1.0$ and dissolution usually occurs at $\Omega < 1.0$, lowered Ω and the OA-dependent shoaling of saturation horizons can have severe consequences for calcifying organisms (Zeebe & Westbroek, 2003; Orr *et al.*, 2005). Corals, coccolithophores, and mollusks often show reduced calcification and weakened $CaCO_3$ structures under OA, while survival is affected in corals, mollusks and echinoderms (Kroeker *et al.*, 2013). Many biogenic $CaCO_3$ shells are covered with organic layers that protect them from spontaneous dissolution. This is one reason why the degree to which calcifying organisms are affected by the decrease in Ω depends on taxa and species. Recent findings for corals and coccolithophores suggest that rather high seawater H^+ concentrations are the reason for the lowered $CaCO_3$ production (Allemand *et al.*, 2011; Taylor *et al.*, 2011; Cyronak *et al.*, 2015). From the biogeochemical point of view, decreased calcification would give a "positive feedback" on climate, because this would cause TA levels to remain high and allow for a higher CO_2 uptake of the seawater (cf., section 1.3; Gehlen *et al.*, 2012).

Ocean acidification effects on biota can be driven by the different carbonate chemistry parameters (e.g., CO_2 and H^+) that are simultaneously changing with increasing pCO_2. Thus, when assessing OA effects under "coupled" changes in carbonate chemistry, i.e., when seawater pCO_2/[CO_2] is increased while the TA is kept constant, the effects of CO_2 and H^+ cannot be distinguished. In order to investigate CO_2 and H^+ effects in isolation, the carbonate chemistry can be "decoupled" by changing TA and DIC concomitantly, e.g., by adding hydrochloric acid (HCl) and/or sodium hydroxide (NaOH) (Gatusso *et al.*, 2010). When increasing TA and DIC while maintaining constant pH/[H^+], the "isolated" effect of carbonation, i.e., a combined increase in [CO_2] and [HCO_3^-], can be investigated. When decreasing TA and DIC concomitantly while maintaining pCO_2/[CO_2] constant, the "isolated" effect of acidification, i.e., an increase in [H^+], can be investigated. Yet, it needs to be considered that [HCO_3^-] concomitantly decreases under this condition. As parameters of the carbonate chemistry are always interconnected, also when CO_2 and H^+ are decoupled, experiments on the identification of drivers are therefore also of correlative nature.

1.3 Coccolithophores and their role in biogeochemical cycles

Coccolithophores are unicellular algae forming tiny calcite exoskeletons (coccospheres) that are composed of multiple intracellularly produced coccolith plates. The group of calcifying phytoplankton appeared in the late Triassic ~220 million years ago (Bown *et al.*, 2004; Falkowski *et al.*, 2004), at a time when the pCO_2 was roughly six times higher than today (Royer *et al.*, 2007). However, at that time, high pCO_2 did not involve acidification (i.e., increased $[H^+]$), as the oceans were buffered through higher alkalinity that derived from the efficient weathering and the associated entry of cations to the seawater (Stanley & Hardie, 1998; Kump *et al.*, 2000). Today, coccolithophores belong to the most important marine primary producers next to diatoms and dinoflagellates. Being the most important pelagic calcifiers, they are estimated to be responsible for half the oceanic $CaCO_3$ precipitation (Milliman, 1993). Coccolithophores are distributed across the oceans and play a major role in the global carbon cycle due to their significant contribution to the biological carbon pumps.

The organic carbon pump represents the biologically driven sequestration of POC in the deep sea that is driven by photosynthetic carbon fixation of a relatively small number of phytoplankton species (Rost & Riebesell, 2004). While the large-scale transport of DIC takes place by the solution of CO_2 in cold and saline water masses at high latitudes, and the subsequent sinking of the DIC-rich, dense water masses into the ocean's interior (Falkowski *et al.*, 2000), the marine primary producers have a significant role in establishing a CO_2 gradient across the oceans that leads to an increased CO_2 uptake from the atmosphere (Maier-Reimer & Hasselmann, 1987). During photosynthesis in the upper layers of the oceans, light energy is captured and stored in chemical energy in biomass (e.g., in sugars, $C(H)_2O$; Fig. 1.7). The produced biomass is then either cycled through the food web or directly sinks into deeper waters, where the carbon is released to the ocean by dissolution and microbial decomposition (Fig. 1.7). Due to this biological "pump", surface DIC levels are ~15% lower than in the deep ocean. Model runs showed that these gradients are responsible for ~50% of the oceanic CO_2 uptake (Sarmiento, 2013).

Coccolithophores have an exceptional role in DIC distribution, because in the process of calcification they also contribute to the so-called carbonate counter pump. This pump is driven by the precipitation of $CaCO_3$ in the surface ocean during which alkalinity is reduced. When $CaCO_3$ sinks to depths below the lysocline (with Ω is <1) and $CaCO_3$ dissolves, alkalinity increases (Ridgwell & Zeebe, 2005). Coccolithophores are thus able to "pump" alkalinity from upper to deeper layers (Fig. 1.7). They are, next to foraminifers, the main contributors to an alkalinity gradient of ~5% and can thus, despite their contribution to the organic pump, increase surface CO_2 levels (Sarmiento, 2013).

The relative strength of the two biological carbon pumps is represented by the so-called "rain ratio", i.e., the ratio of PIC to POC of the transported material, which determines whether surface pCO_2 increases or decreases (Rost & Riebesell, 2004; Lam *et al.*, 2011). Due to its high density, biogenic $CaCO_3$ also constitutes an ideal material for ballast aggregates of

biomass and thus enhance the sedimentation (Fig. 1.7; Armstrong *et al.*, 2002). The hypothesized ballasting role is supported by the strong correlation of sinking organic and mineral fluxes (Klaas & Archer, 2002). Over geological time scales, a relatively small fraction of biomass (~0.1%) reaches the sea floor without being decomposed. A larger fraction (≤10%) of $CaCO_3$ is deposited in the sediment, yet this critically depends on the depth of the seafloor in relation to the lysocline. Coccoliths are the main component of limestone and other chalk sediments. In the present-day oceans, coccoliths are a major constituent of the calcareous oozes that cover up to 35% of the ocean floor (de Vargas *et al.*, 2004). While the $CaCO_3$ export lowers the surface TA and therefore the DIC storage capacity of the ocean on time scales of decades, changes in the rate of $CaCO_3$ sedimentation can modulate the steady-state with the $CaCO_3$ supply from terrestrial weathering on time scales of thousands of years (Broecker & Peng, 1987; Archer & Maier-Reimer, 1994). Variations in coccolithophores abundances are often associated with glacial-interglacial transitions.

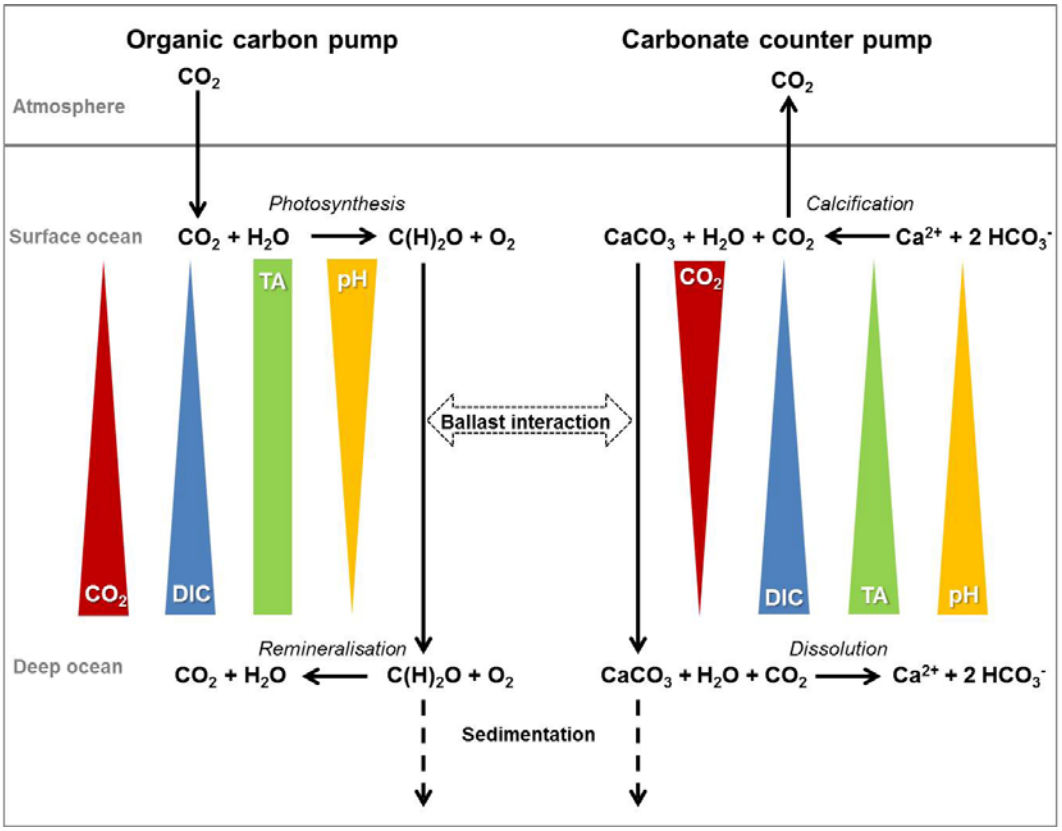

Figure 1.7: The biological carbon pumps. The organic carbon pump produces gradients of lowered [CO_2] and DIC at the surface and elevated [CO_2] and DIC in the depth. It also causes a gradient of increased pH at the surface and decreased pH in the depth. Total alkalinity is thereby relatively unaffected. The carbonate counter pump affects CO_2 concentrations in the opposite direction; it leads to increased [CO_2] at the surface and decreased [CO_2] in the depth. The pH is decreased at the surface and increased in the depth. Dissolved inorganic carbon and TA are transported downwards. The relative strength of both pumps, i.e., the ratio of biomass production to calcification sinking out of the surface layer can determine CO_2 fluxes between ocean and atmosphere. Please note that illustrated gradients between the C_i species are not equal in magnitude.

Coccolithophores predominated during interglacial periods (McIntyre et al. 1972). The smaller abundance of coccolithophores during glacial times may have contributed to the higher alkalinity and thus lower pCO_2 during these periods (Archer & Maier-Reimer, 1994; Ridgwell & Zeebe, 2005). Thus, changes in the rates of $CaCO_3$ production and dissolution do not only affect the marine ecosystems in the coming decades, but can give strong feedbacks on biogeochemistry and the climate (Lovelock, 1979; Rost & Riebesell, 2004; Doney *et al.*, 2009). In order to predict the potential feedback induced by coccolithophores, we therefore require an understanding of their ecophysiology, in particular how these microalgae are affected by environmental change.

1.4 *Emiliania huxleyi* - the most prominent coccolithophore

Ecophysiology

Within the group of coccolithophores, the species *Emiliania huxleyi* and *Gephyrocapsa oceanica* are able to form intense blooms over large areas of the ocean (Tyrrell & Merico, 2004). *Emiliania huxleyi* is relatively young and arose from the older *G. oceanica* ~270.000 years ago (Thierstein *et al.*, 1977). Nowadays, it is the most abundant coccolithophore species in the ocean (Paasche, 2001). It occurs in all latitudes except the polar oceans, but has been shown to even successively expand polewards (Bauerfeind *et al.*, 2009; Winter *et al.*, 2013). Blooms of *E. huxleyi* can be >250,000 km^2 in size and exhibit cell concentrations of up to 10 million cells L^{-1} (Holligan *et al.*, 1983; Brown & Yoder, 1994; Tyrrell & Merico, 2004). They often occur under stratified conditions with relatively high irradiances and low nutrient conditions in late spring/early summer (Nanninga & Tyrrell, 1996; Raitsos *et al.*, 2006; Sadeghi *et al.*, 2012). Its high growth under these conditions is possible because *E. huxleyi* tolerates very high irradiances, apparently without becoming photoinhibited (Paasche, 1964; Nielsen, 1995; Suggett *et al.*, 2007; Loebl *et al.*, 2010). The species also performs well under oligotrophic conditions (van der Wal *et al.*, 1994; Egge & Heimdal, 1994; Rouco *et al.*, 2013; Rokitta *et al.*, 2014), which can be explained by their high affinities for phosphate (Riegman *et al.*, 2000) and their effective nitrogen budgeting (Rokitta *et al.*, 2014).

Emiliania huxleyi undergoes a heteromorphic life-cycle, in which it alternates between a non-calcifying, flagellated haploid stage (1N) and a coccolith-bearing, non-motile diploid stage (2N; Fig. 1.8; Paasche, 2001; Young & Henriksen, 2003; Billard & Inoye, 2004). Both stages are able to independently reproduce and are connected by meiosis and syngamy (Klaveness, 1972; Green *et al.*, 1996; von Dassow *et al.*, 2015). Haplo-diplontic life cycling might facilitate the adaptation to heterogeneous environments through niche partitioning (Hughes & Otto, 1999; Coelho *et al.*, 2007; von Dassow *et al.*, 2015). Ecological and functional differences between the haploid and diploid stage were also indicated by their physiology and gene expression (Houdan *et al.*, 2005; von Dassow *et al.*, 2009; Rokitta *et al.*, 2011; Rokitta *et al.*, 2012; von Dassow *et al.*, 2015). Sexual reproduction may provide genetic advantages for adaptation to new environments and ensure survival during periods under non-favourable

conditions (Paasche, 2001; Kaltz & Bell, 2002; Becks & Agrawal, 2010). For example, meiosis was discussed to provide an escape mechanism for the *E. huxleyi* (Frada *et al.*, 2008) because blooms of the diploid stage are controlled by *E. huxleyi*-specific lytic viruses (Brussaard *et al.*, 1996; Wilson *et al.*, 2002; Coolen, 2011; von Dassow *et al.*, 2015). The virus-resistance of the haploid stage allows genes to be passed on to the next generation in a virus-free environment (Frada *et al.*, 2008).

The mechanism of calcification

Diploid cells of *E. huxleyi* are ~4-5 μm in size and contain typical eukaryote plant cell organelles, i.e., nucleus, chloroplasts, mitochondria, Golgi apparatus, and the endoplasmic reticulum. In addition to these, they possess the Golgi-derived coccolith vesicle and the Reticular body (Paasche, 2001). The coccolith vesicle is the organelle in which coccoliths are synthesized. The Reticular body constitutes a labyrinthine membrane system that is connected to the coccolith vesicle and is involved in coccolith synthesis and movements, i.e., it has been suggested to be involved in Ca^{2+} supply for calcification (Westbroek *et al.*, 1984; Marsh, 2003; Mackinder *et al.*, 2011; Holtz *et al.*, 2013a). The biomineralization of calcite takes place under stringently controlled conditions, leading to a product that strongly differs from abiotically produced calcite (Taylor & Brownlee, 2005; Mackinder *et al.*, 2010). Coccoliths consist of different crystal units arrayed in a radial symmetry (Billard & Inoye, 2004). The coccolith synthesis is initiated by precipitation of simple calcite crystals around the rim of the organic base-plates and is sequentially continued in distinct directions to form the final coccolith structure (Fig. 1.9; Young *et al.*, 1999; Young & Henriksen, 2003). The precipitation is guided along a matrix, probably consisting of acidic polysaccharides and

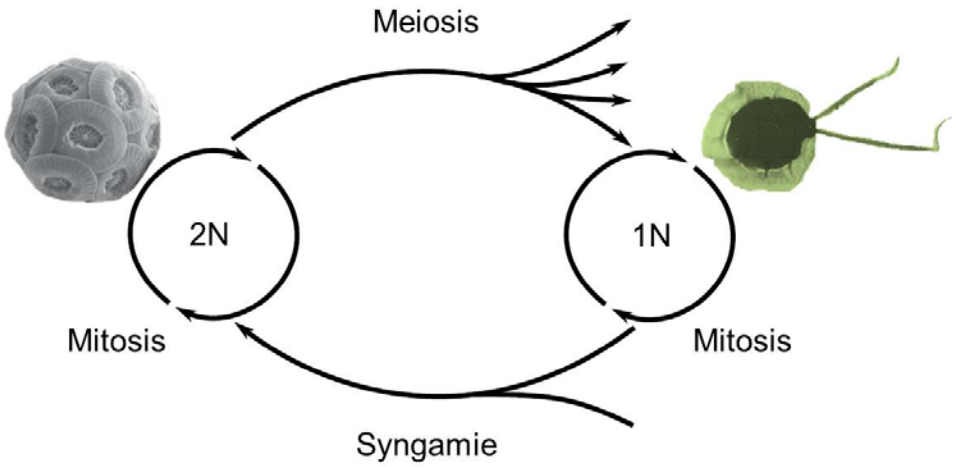

Figure 1.8: The haplo-diplontic life-cycle of *E. huxleyi*. The species alternates between a coccolith-bearing, non-motile diploid stage (2N) and a non-calcifying, flagellated haploid stage (1N) stage through meiosis and syngamie. Modified after Young and Henriksen (2003)

glutamic acid, proline- and alanine-rich protein GPA (Westbroek *et al.*, 1984; Marsh, 2003). When being completed, coccolith vesicles are exocytosed and positioned into the extracellular coccosphere (Taylor & Brownlee, 2005).

Calcification involves transport of Ca^{2+} and C_i from the extracellular medium into the Golgi-derived CV. Several modes of Ca^{2+} supply have been suggested, but the exact molecular mechanisms have yet to be resolved (Mackinder *et al.*, 2010; Holtz *et al.*, 2013b). The uptake of Ca^{2+} probably involves Ca^{2+}-binding proteins, calreticulin, calnexin and calmodulin (Corstjens *et al.*, 1998; Wahlund *et al.*, 2004; von Dassow *et al.*, 2009). Furthermore voltage-gated H^+ channels (HVCN1), Ca^{2+}/H^+ antiporters (VCX, CAX3), Na^+/Ca^{2+} exchangers (NCKX), and vacuolar as well as sarcoplasmic/endoplasmic reticulum calcium (SERCA-type) ATPases have been suggested to be involved in calcification (Araki & Gonzalez, 1998; von Dassow *et al.*, 2009; Mackinder *et al.*, 2011; Rokitta *et al.*, 2011; Taylor *et al.*, 2011). Holtz et al. (2013, 2015a) investigated substrate supply for calcification by means of numerical cell models and found that coupled Ca^{2+} and HCO_3^- uptake in antiport with H^+ would be kinetically and energetically the most feasible strategy. *E. huxleyi* is known to express HCO_3^- transporters of the solute carrier (SLC) 4 family that have been proposed to be involved in the uptake of HCO_3^- for calcification (von Dassow *et al.*, 2009; Mackinder *et al.*, 2011; Rokitta *et al.*, 2011; von Dassow *et al.*, 2015), but also other, yet unknown C_i transporters and channels are likely to play a role. High contributions of HCO_3^- uptake for calcification were indicated by the $\delta^{13}C$ signature of the coccoliths (Sikes & Wilbur, 1980; Rost *et al.*, 2002). Also the high correlation of calcification rates with external HCO_3^- concentrations indicated that calcification uses HCO_3^- as external C_i source (Paasche, 1964; Herfort *et al.*, 2002, Bach *et al.*, 2013).

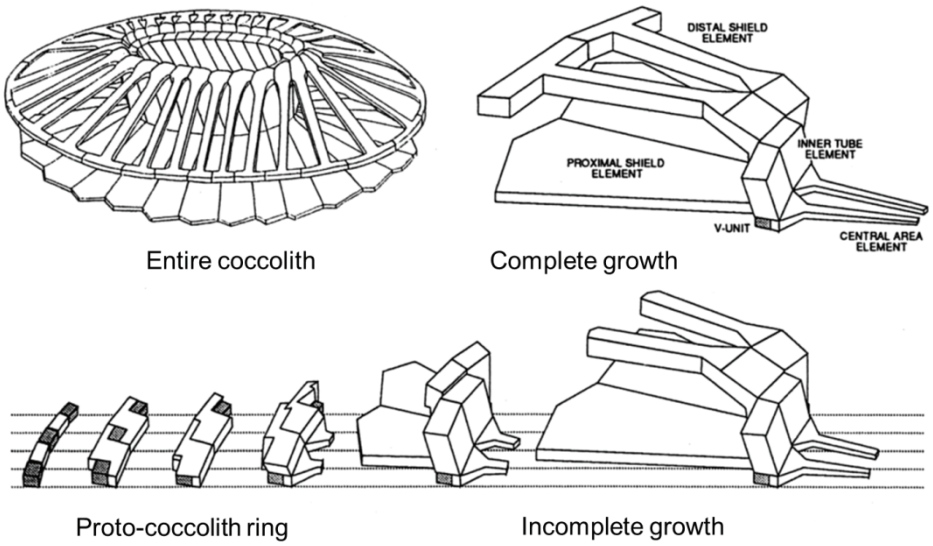

Figure 1.9: Structure of an *E. huxleyi* coccolith and its development. Modified after Marsh (2003).

Photosynthesis and the supply of inorganic carbon

In the light reactions of photosynthesis, taking place at the thylakoid membranes, photons are captured by photosynthetic pigments. The absorption leads to the formation of excitons (i.e., electrons in a higher energetic state) that are successively transferred to the reaction center of photosystem II, where they are carried forward to a primary electron acceptor of the linear electron transfer chain (ETC; Fig. 1.10). In the ETC, electrons create a chain of redox reactions that produce reductive power (NADPH) and a H^+ gradient across the thylakoid membrane. This H^+ gradient is used to generate the energy carrier ATP (Fig. 1.10). The dominant proportion of NADPH and ATP, which are typically produced in a ratio of ~1:1, is successively used for the C_i fixation in the Calvin cycle. As the Calvin cycle consumes ATP and NADPH in a ratio of ~3:2 (Falkowski & Raven, 2007), several alternative pathways exist that use the captured energy for additional ATP production (Halsey & Jones, 2015). One way to increase the proportion of ATP generation is the so-called cyclic electron chain that transports electron in a cyclic manner around photosystem I and thereby produces ATP only (Asada, 1999; Behrenfeld *et al.*, 2008).

Photosynthetic C_i fixation via the Calvin cycle in *E. huxleyi* takes place in the pyrenoid, a dense, protein structure of the thylakoid stroma that consists of up to 90% of RubisCO and is often located in the center of the chloroplast stroma (Fig. 1.10; Vaughn *et al.*, 1990; Borkhsenious *et al.*, 1998; Stojkovic *et al.*, 2013). The Calvin cycle is a chain of redox reactions, which uses the ATP and NADPH produced in the light reaction to convert CO_2 to organic compounds. The primary and rate-limiting enzyme of the Calvin cycle is RubisCO, which catalyzes the carboxylation of ribulose-1,5-bisphosphate (RuBP), forming two molecules of 3-phosphoglycerate. Roughly one third is used in the subsequent regeneration of RuBP, and the other part is used for the buildup of other compounds. RubisCO has a relatively poor affinity to its substrate CO_2, with its half-saturation constant K_m (20-70 μmol L^{-1}; Badger *et al.*, 1998; Shiraiwa, 2003; Boller *et al.*, 2011) being higher than the current [CO_2] in seawater (~10-20 μmol L^{-1}). As O_2 is a competing substrate at RubisCO, the carboxylation reaction can be inhibited by the oxygenation reaction at low [CO_2]/[O_2] (Spreitzer & Salvucci, 2002; Moroney *et al.*, 2013). To avoid substrate-limitation of RubisCO, most phytoplankton taxa employ so-called CO_2-concentrating mechanisms (CCMs) that increase the concentration of CO_2 at the enzyme's catalytic site (Giordano *et al.*, 2005; Raven *et al.*, 2008; Reinfelder, 2011).

The C_i affinity of *E. huxleyi* is relatively low compared to other phytoplankton taxa (Raven & Johnston, 1991; Rost *et al.*, 2003), but the species is nevertheless able to actively accumulate CO_2 at RubisCO. This is, for example, indicated by the fact that the half-saturating concentration ($K_{1/2}$) of the cells is lower than the K_m value of RubisCO (e.g., Boller *et al.* 2011; Badger *et al.*, 1998). Furthermore, the C_i affinity of *E. huxleyi* decreases when the cells are acclimated to elevated pCO_2 (Rost *et al.*, 2003). Also the relative RubisCO content (Losh *et al.*, 2013; Raven, 2013), the abundance of pyrenoids (Stojkovic *et al.*, 2013) and the upre-

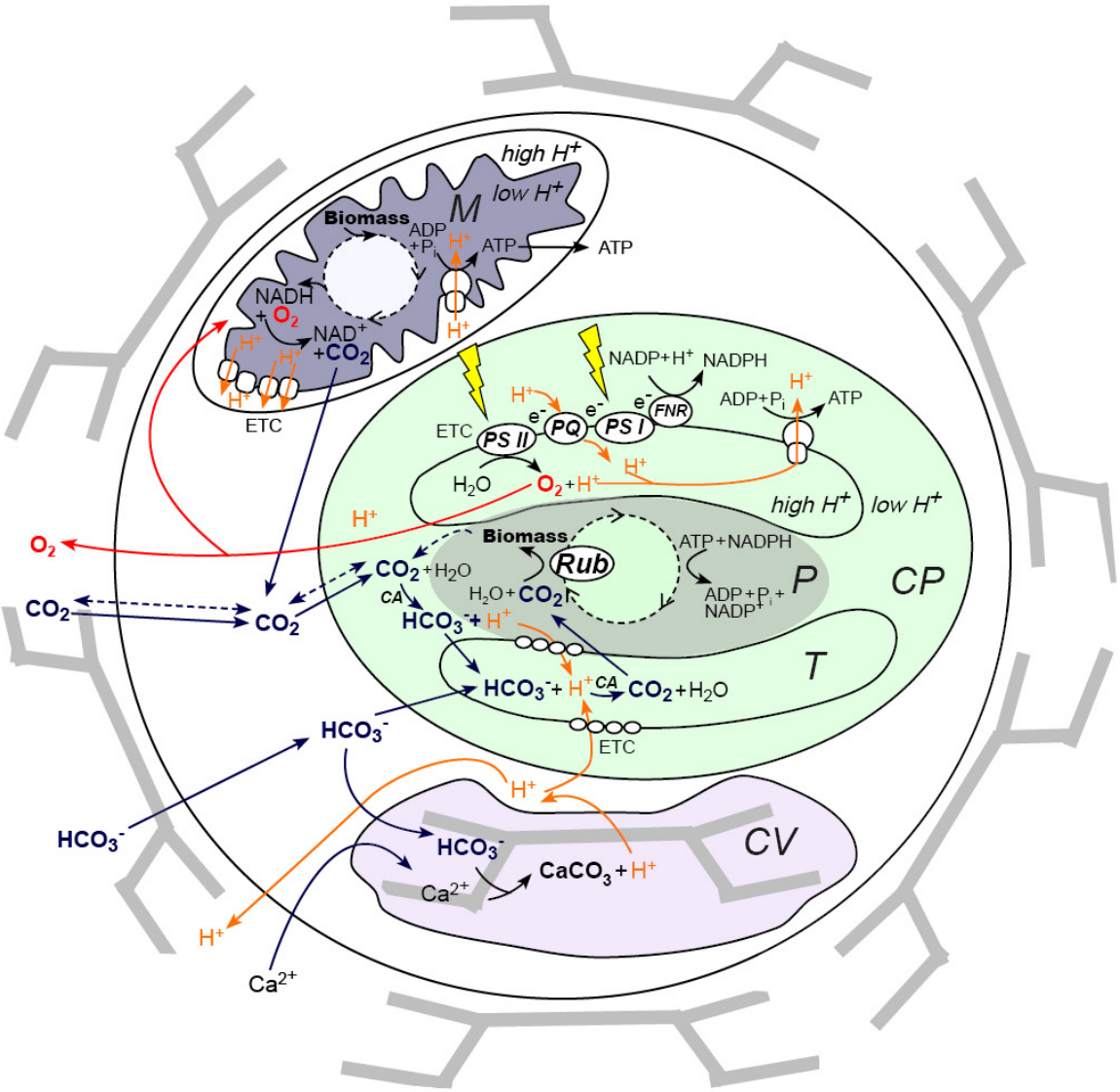

Figure 1.10: Schematic illustration cellular C_i, O_2 and H^+ fluxes in *E. huxleyi* as conceivable from current state of knowledge. Solid blue arrows: CO_2 and HCO_3^- net fluxes supplying calcification (taking place in the coccolith vesicle, CV) and photosynthetic C_i fixation (taking place in the pyrenoid, P); Enrichment of C_i is thought to take place inside the thylakoid (T) lumen. In the process of mitochondrial respiration, CO_2 is released. C_i fixation rates at RubisCO (gross C_i fixation) are therefore higher than the sum of the net CO_2 uptake and HCO_3^- uptake (net C_i uptake) that can be measured outside the cell. Dashed blue lines: Additional in- and outward CO_2 fluxes. The sum of the inward CO_2 fluxes (dashed and solid arrow) constitutes the gross CO_2 uptake. The outward flux (dashed) represents the constant loss of CO_2 that cell experience simultaneously (i.e., the efflux). The ratio of efflux over gross influx is termed "leakage". Red arrows: O_2 fluxes; the production of O_2 takes place as part of the linear electron transfer chain (ETC) of the light reaction (gross O_2 evolution). Part of the O_2 is consumed in the mitochondrial respiration. Fluxes of O_2 that can be measured outside the cells reflect the sum of O_2 production and consumption, i.e., the net O_2 evolution. In orange: H^+ fluxes do not only play a role in the CCM of *E. huxleyi*, but are required in the chemiosmotic synthesis of the energy carrier ATP. Abbreviations: Mitochondrion (M), PS I & PSII (Photosystems I & II), plastoquinone (PQ), ferredoxin-NADP reductase (FNR), chloroplast (CP).

gulation of CCM-related genes under DIC-limiting conditions (Bach *et al.*, 2013; Beardall & Raven, 2013) give evidence for active CCMs. *Emiliania huxleyi* is known to use both, CO_2 and HCO_3^- as external C_i sources for photosynthesis, but the estimated proportions of CO_2 uptake differ between studies and depend on the applied methods and assay conditions (e.g., Sikes et al., 1980; Raven & Johnston, 1991; Buitenhuis et al., 1999; Herfort *et al.*, 2002; Rost *et al.*, 2007; Schulz *et al.*, 2007; Trimborn *et al.*, 2007). The species´ CCM also involves differently located carbonic anhydrases (CA; e.g., Soto *et al.*, 2006; Mackinder *et al.*, 2011; Richier *et al.*, 2011; Bach *et al.*, 2013), which accelerate the otherwise slow conversion between CO_2 and HCO_3^- (Fig. 1.10). The activity of external CA was, however, shown to be very low in *E. huxleyi* (Nimer *et al.*, 1994; Herfort *et al.*, 2002; Trimborn *et al.*, 2007; Stojkovic *et al.*, 2013). CCMs usually comprise also features that allow for the reduction of diffusive losses of CO_2. It is likely that the same also accounts for *E. huxleyi*.

Photosynthetic C_i uptake is commonly assumed to take place diffusively in the case of CO_2 and actively in the case of HCO_3^-. The details of the uptake mechanisms and routes are, however, not yet resolved and differ between phytoplankton taxa. The uptake of HCO_3^- likely occurs via the same transport route as also taken by the HCO_3^- used for calcification (Fig. 1.10). Uptake proteins may involve anion exchangers (e.g., SLC 4 transporters) and other yet undefined transporters or HCO_3^- channels (e.g., Mackinder *et al.*, 2010). Holtz *et al.* (2015a) modelled a kinetically feasible CCM of *E. huxleyi*, in which CO_2 and/or HCO_3^- are get into the chloroplast stroma by passing the plasma membrane and the chloroplast envelope. Inside the alkaline chloroplast stroma, the CA-catalyzed conversion of any CO_2 leads to an accumulation of HCO_3^- (Fig. 1.10). Active pumping of HCO_3^- into the acidic thylakoid lumen, and the expression of a CA leads to an accumulation of CO_2, which can diffuse to the close-by RubisCO inside the pyrenoid (Fig. 1.10; Holtz *et al.*, 2013b; Holtz *et al.*, 2015 a, b). Calcification has earlier been hypothesized to constitute a component of *E. huxleyi's* CCM. It was suggested that the use HCO_3^- for calcification and the concomitant production of H^+ shifts the intracellular carbonate chemistry towards higher levels of CO_2, which is subsequently used for photosynthesis (Sikes *et al.*, 1980; Anning *et al.*, 1996; Nimer & Merrett, 1996; Brownlee & Taylor, 2004). Indeed, there are indications that calcification and photosynthesis share the same intracellular C_i pool and that the processes therefore closely interact or even compete for C_i (Rokitta & Rost, 2012). However, photosynthesis was shown to work independently of calcification and is thus not involved in the operation of the CCM (Rost *et al.*, 2002; Herfort *et al.*, 2004; Trimborn *et al.*, 2007; Leonardos *et al.*, 2009).

The response of *Emiliania huxleyi* to ocean acidification

Emiliania huxleyi appears to be very vulnerable to OA (see Raven, 2011; Meyer & Riebesell, 2015 for overview). A large number of laboratory and field studies found unaffected or stimulated biomass production under OA, and typically impaired calcification and growth in this species (e.g., Riebesell *et al.*, 2000; Langer *et al.*, 2009; De Bodt *et al.*, 2010; Beaufort *et al.*, 2011; Hoppe *et al.*, 2011; Ziveri *et al.*, 2014). Ocean acidification responses were shown

to strongly depend on genetic predisposition and other environmental factors such as irradiance, temperature or nutrients (Iglesias-Rodriguez *et al.*, 2008; Langer *et al.*, 2009; Lefebvre *et al.*, 2012; Rokitta & Rost, 2012; Sett *et al.*, 2014). Rokitta and Rost (2012), for example, showed that OA responses are very pronounced in *E. huxleyi* grown under low irradiances, but become much smaller under high irradiances. Surprisingly, the haploid life-cycle stage of *E. huxleyi*, which carries the exact same set of genes as the diploid stage, was shown to be relatively insensitive towards OA.

Most of the studies investigating OA effects on *E. huxleyi* are *acclimation* studies, i.e., cells are exposed to different pCO_2 levels (and/or other environmental changes) over several generations in order to *acclimate* or, in other words, adjust their gene expression and metabolism to the altered conditions. After this acclimation step, most experimenters measure the changes in integrated responses (e.g., in growth or cellular PIC and POC quotas) or, in other words, the responses that result from the sum of several processes taking place over the course of the time (e.g., photosynthesis, respiration, calcification and cell division). From the integrated results, estimations about the efficiency of the individual processes can be made. For example, photosynthetic C_i acquisition is often assessed as POC production that is the product of the cellular POC quota (pg $cell^{-1}$) and the specific growth constant μ (d^{-1}). This estimate of photosynthesis may constitute a good approximation, but in order to investigate the regulation of individual mechanisms, the underlying *real-time* fluxes should be measured.

Two established methods measuring C_i (and O_2) fluxes associated with photosynthesis are the ^{14}C disequilibrium method (Espie & Colman, 1986) and the membrane-inlet mass spectrometry (MIMS) technique (Badger *et al.*, 1994). Both techniques can measure rates of photosynthesis and distinguish between external C_i sources for photosynthesis (i.e., CO_2 and HCO_3^-). While the first technique is technically less costly, the second method allows resolving O_2, CO_2 and HCO_3^- in more detail. Both methods have been shown to deliver comparable results earlier (Rost *et al.*, 2007), even though traditionally being applied at very different pH values. Methods detecting cellular *real-time* fluxes are often deployed at standardized (buffered) pH value, in order to see how the metabolic capacities differ. However, measured C_i fluxes at standardized pH values can be very different from the fluxes under *acclimation* or rather *in situ* conditions. In order to understand OA responses, flux measurements should therefore be performed at *in situ* carbonate chemistry.

1.5 Aims of this thesis

The aim of this thesis is to explain typical OA responses in *E. huxleyi* by measuring cellular *real-time* O_2 and C_i fluxes and their dependence on the external carbonate chemistry and light. Three experiments were performed in which the species was acclimated to different coupled and uncoupled carbonate chemistry settings. To describe the integrated cellular responses to these conditions, cellular growth and elemental compositions were measured. In order to identify the regulation mechanisms underlying these responses, the species' flux regulations were assessed by applying a ^{14}C disequilibrium method (Espie & Colman, 1986) and a MIMS method (Badger *et al.*, 1994).

Publication I: Strong shift from HCO_3^- to CO_2 uptake in *Emiliania huxleyi* with acidification: new approach unravels acclimation versus short-term pH effects

The focus of the first study was to investigate whether *E. huxleyi* undergoes a shift in its external C_i source for photosynthesis in response to OA. To this end, a ^{14}C disequilibrium method was applied and the photosynthetic C_i sources of present-day and OA acclimated *E. huxleyi* cells were measured each at five different pH values (pH 7.9 - 8.7 at constant DIC). Instantaneous responses to pH were compared with acclimation responses in order to understand if measurements of cellular fluxes at standardized pH conditions are able to mask flux regulations. Differences in flux regulation of the diploid and haploid cells were assessed by performing the experiment with both life-cycle stages.

Publication II: Acidification, not carbonation, is the major regulator of carbon fluxes in the coccolithophore *Emiliania huxleyi*

On the basis of the strong and direct flux regulations observed in the first study, the aim of the second study was to resolve the drivers behind these flux regulations; i.e., to investigate whether carbonation or acidification caused photosynthetic CO_2 uptake to be stimulated under OA. Present-day acclimated diploid and haploid cells were confronted to a matrix of two DIC levels (1400, 2800 μmol kg^{-1}) and two pH (8.15, 7.85) at which the resulting fluxes were assessed by MIMS. While the ^{14}C disequilibrium technique was only able to resolve the relative usage of CO_2 and HCO_3^-, the MIMS approach was able to quantify the CO_2 and HCO_3^- fluxes individually and to measure concurrent regulations in the photosynthetic O_2 evolution and respiratory O_2 consumption. In order to address the question why acclimation to different irradiances modulates OA responses, flux regulations in low- and high-light grown cells were measured at low and high irradiances. By comparing C_i acquisition of the diploid and the haploid stage, physiological functions of calcification could be derived.

Publication III: H^+-driven impairment of HCO_3^- uptake manifests after acclimation and explains declined calcification in coccolithophores

In order to assess whether flux regulation in cells being exposed to OA over longer time scales are similar to short-term regulations, diploid *E. huxleyi* was acclimated to a matrix of two CO_2 (15 and 30 µmol kg^{-1}) and two pH levels (8.15 and 7.85) under irradiances of 400 μmol photons m^{-2} s^{-1}. After acclimation, integrated responses in the cellular composition and the gas fluxes associated with photosynthesis and calcification were measured under *in situ* conditions. By decoupling the effects of carbonation and acidification, the drivers causing typical integrated acclimation responses were derived. By applying measured cellular PIC:POC ratios onto the measured fluxes, C_i fluxes into calcification were characterized as well. From the differences in the short-term and long-term responses, conclusions about acclimation processes could be drawn. By comparing integrated responses with *real-time* measurements, methodical differences were assessed.

1.6 List of publications

Publications

I. **Strong shift from HCO_3^- to CO_2 uptake in *Emiliania huxleyi* with acidification: new approach unravels acclimation versus short-term pH effects**

Dorothee M. Kottmeier, Sebastian D. Rokitta, Philippe D. Tortell, Björn Rost

Published in **Photosynthesis Research**

II. **Acidification, not carbonation, is the major regulator of carbon fluxes in the coccolithophore *Emiliania huxleyi***

Dorothee M. Kottmeier, Sebastian D. Rokitta, Björn Rost

Published in **New Phytologist**

III. **H^+-driven impairment of HCO_3^- uptake manifests after acclimation and explains declined calcification in coccolithophores**

Dorothee M. Kottmeier, Sebastian D. Rokitta, Björn Rost

submitted to Journal of Experimental Botany

The first author´s contribution to the publications

For all publications, the experimental concepts and approaches were developed together with the coauthors. The first author conducted experiments, performed the analyses, and evaluated the data. The manuscript was drafted by the first author and adapted and discussed with the coauthors.

Chapter 2
Publication I

Strong shift from HCO_3^- to CO_2 uptake in *Emiliania huxleyi* with acidification: new approach unravels acclimation versus short-term pH effects

Dorothee M. Kottmeier, Sebastian D. Rokitta, Philippe D. Tortell, Björn Rost

Photosynthesis Research

Photosynth Res (2014) 121:265–275
DOI 10.1007/s11120-014-9984-9

REGULAR PAPER

Strong shift from HCO_3^- to CO_2 uptake in *Emiliania huxleyi* with acidification: new approach unravels acclimation versus short-term pH effects

Dorothee M. Kottmeier · Sebastian D. Rokitta · Philippe D. Tortell · Björn Rost

Received: 7 October 2013 / Accepted: 10 February 2014 / Published online: 23 February 2014

Abstract Effects of ocean acidification on *Emiliania huxleyi* strain RCC 1216 (calcifying, diploid life-cycle stage) and RCC 1217 (non-calcifying, haploid life-cycle stage) were investigated by measuring growth, elemental composition, and production rates under different pCO_2 levels (380 and 950 µatm). In these differently acclimated cells, the photosynthetic carbon source was assessed by a ^{14}C disequilibrium assay, conducted over a range of ecologically relevant pH values (7.9–8.7). In agreement with previous studies, we observed decreased calcification and stimulated biomass production in diploid cells under high pCO_2, but no CO_2-dependent changes in biomass production for haploid cells. In both life-cycle stages, the relative contributions of CO_2 and HCO_3^- uptake depended strongly on the assay pH. At pH values $\leq$ 8.1, cells preferentially used CO_2 ($\geq$ 90 % CO_2), whereas at pH values $\geq$ 8.3, cells progressively increased the fraction of HCO_3^- uptake ($\sim$45 % CO_2 at pH 8.7 in diploid cells; $\sim$55 % CO_2 at pH 8.5 in haploid cells). In contrast to the short-term effect of the assay pH, the pCO_2 acclimation history had no significant effect on the carbon uptake behavior. A numerical sensitivity study confirmed that the pH-modification in the ^{14}C disequilibrium method yields reliable results, provided that model parameters (e.g., pH, temperature) are kept within typical measurement uncertainties. Our results demonstrate a high plasticity of *E. huxleyi* to rapidly adjust carbon acquisition to the external carbon supply and/or pH, and provide an explanation for the paradoxical observation of high CO_2 sensitivity despite the apparently high HCO_3^- usage seen in previous studies.

Keywords CO_2 concentrating mechanism · pH · Inorganic carbon source · Coccolithophore · Ocean acidification · Isotopic disequilibrium · Photosynthesis

Introduction

Marine phytoplankton account for $\sim$50 % of global primary production and are the main drivers of the marine "particulate organic carbon" (POC) pump (Falkowski et al. 1998; Field et al. 1998). Calcifying phytoplankton species also contribute to the "particulate inorganic carbon" (PIC) pump and thereby play a dual role in regulating marine biogeochemical cycling of carbon through their effects on surface ocean alkalinity (Broecker and Peng 1982; Zeebe and Wolf-Gladrow 2007). One key species of calcifying phytoplankton is the cosmopolitan and bloom-forming coccolithophore *Emiliania huxleyi*, which has been established as a model organism over the recent decades (Paasche 2002; Raven and Crawfurd 2012; Read et al. 2013; Westbroek et al. 1993). While the calcifying diploid life-cycle stage of this species has been intensively studied in field and laboratory experiments, the non-calcifying haploid stage has only recently gained attention due to its important ecological role. In blooms of diploid *E. huxleyi*, which are usually terminated by viruses, the haploid life-

Electronic supplementary material The online version of this article (doi:10.1007/s11120-014-9984-9) contains supplementary material, which is available to authorized users.

Guest Editor: James Moroney.

D. M. Kottmeier (✉) · S. D. Rokitta · B. Rost
Alfred Wegener Institute Helmholtz Centre for Polar and Marine Research, Am Handelshafen 12, 27570 Bremerhaven, Germany
e-mail: Dorothee.Kottmeier@awi.de

P. D. Tortell
Department of Earth Ocean and Atmospheric Sciences, and Deparment of Botany, University of British Columbia, Vancouver, BC V6TZ4, Canada

cycle stage functions as a virus-resistant backup population (Frada et al. 2012). Furthermore, the presence and absence of calcification in the differing life-cycle stages of *E. huxleyi* make them ideal candidates to investigate the cellular mechanisms of calcification and their interaction with photosynthesis under increasing oceanic CO_2 concentrations (Mackinder et al. 2010; Rokitta and Rost 2012).

Increasing pCO_2 in oceanic surface water directly affects carbonate chemistry by elevating the concentration of dissolved inorganic carbon (DIC) and shifting the carbon speciation toward higher CO_2 and H^+ concentrations, a phenomenon often referred to as ocean acidification (OA; Caldeira and Wickett 2003; Wolf-Gladrow et al. 1999). Compared to preindustrial values, pH is expected to drop by 0.4–0.5 units until the end of this century. In several studies testing the effects of OA on *E. huxleyi*, diploid strains were found to exhibit strong, yet opposing responses in terms of biomass and calcite production. While biomass production was either unaffected or stimulated by increased pCO_2, calcification typically decreased and malformations of coccoliths increased (e.g., Hoppe et al. 2011; Langer et al. 2009; Riebesell et al. 2000). Bach et al. (2011) suggested that biomass production is stimulated by increasing CO_2 concentration at sub-saturating conditions, whereas calcification is specifically responsive to the associated decrease in pH. Such differential CO_2 and pH effects on biomass and calcite production are supported by the observation that OA distorts ion homeostasis and shifts the metabolism from oxidative to reductive pathways (Rokitta et al. 2012; Taylor et al. 2011). In a number of studies, the sensitivity of *E. huxleyi* toward OA has been attributed to its mode of inorganic carbon (C_i) acquisition, which is intrinsically responsive to changes in carbonate chemistry. Thus, for understanding the differential responses to OA, one needs to look at this crucial process of C_i assimilation.

Like most phytoplankton, *E. huxleyi* operates a CO_2 concentrating mechanism (CCM), which utilizes CO_2 and/or HCO_3^- uptake systems to accumulate CO_2 in the vicinity of RubisCO, and employs the enzyme carbonic anhydrase (CA) to accelerate the inter-conversion between these C_i species (see Reinfelder 2011 for review). For a long time, the CCM in *E. huxleyi* was assumed to rely on the CO_2 delivery by calcification (Anning et al. 1996; Sikes et al. 1980). More recently, however, studies have demonstrated that C_i fluxes for photosynthesis and calcification are independent (Herfort et al. 2004; Rost et al. 2002; Trimborn et al. 2007), and that these two processes may even compete for C_i substrates (Rokitta and Rost 2012). Most studies performed on the CCM of *E. huxleyi* to date yielded moderately high substrate affinities for C_i, which decreased slightly under OA scenarios (e.g., Rokitta and Rost 2012; Rost et al. 2003, Stojkovic et al. 2013). Moreover, low activity for extracellular CA and high contribution of HCO_3^- uptake for photosynthesis have been reported (e.g., Herfort et al. 2002; Rokitta and Rost 2012; Stojkovic et al. 2013; Trimborn et al. 2007). This high apparent HCO_3^- usage is puzzling, however, as it suggests biomass production to be rather insensitive to OA-related changes in CO_2 supply, which is in contrast to what studies usually have observed.

Most physiological methods characterizing the CCM and its functional elements are performed under standardized assay conditions, including a fixed pH value, and thus differing from treatment conditions. The pH and the concominant C_i speciation can, however, influence the cell's physiology, in particular its C_i acquisition. When identifying the cause-effect relationship in OA responses, it is difficult to separate the effects of changes in C_i speciation from concomitant changes in H^+ concentrations. Changes in external pH have been shown to directly drive changes in cytosolic pH in *E. huxleyi*, which, in turn, affected H^+ gradients and membrane potentials (Suffrian et al. 2011; Taylor et al. 2011). This effect could indirectly impact secondary active transporters, e.g., the Cl^-/HCO_3^- antiporter (Herfort et al. 2002; Rokitta et al. 2011). Moreover, the protonation of amino acid side chains can affect activity, specificity, and kinetics of enzymes and transporters involved in cellular processes (Badger 2003; Raven 2006). Hence, aside from altered concentrations of C_i species, pH itself could directly impact the mode of CCM (Raven 1990). These possible effects of the assay pH on C_i acquisition should be accounted for when performing experiments to characterize the CCM.

One common approach to determine the C_i source for photosynthesis is the application of the ^{14}C disequilibrium method (Espie and Colman 1986), which has proven suitable for the study of marine phytoplankton in laboratory cultures (e.g., Elzenga et al. 2000; Rost et al. 2006a) and in natural field assemblages (e.g., Cassar et al. 2004; Martin and Tortell 2006; Tortell and Morel 2002; Tortell et al. 2008). The method makes use of the relatively slow chemical conversion between the CO_2 and HCO_3^- in the absence of CA (Johnson 1982), allowing for a differential labeling of these C_i species with ^{14}C. This method is typically performed at pH of 8.5 ("assay pH"), deviating strongly from most natural in situ values and even more from the pH values applied in OA-experiments ("acclimation pH"). In this study, we aimed to disentangle the short-term effect of assay pH from the long-term effect of acclimation history on the photosynthetic C_i source of *E. huxleyi*. To this end, we grew haploid and diploid life-cycle stages at present-day (380 µatm) and elevated pCO_2 (950 µatm), and measured the responses in growth, elemental composition, and production rates. These low and high pCO_2-acclimated cells were then tested for their preferred C_i source by applying the ^{14}C disequilibrium

method, with assay conditions set to a range of ecologically relevant pH values (pH 7.9–8.7). The reliability of this new approach was tested by performing sensitivity studies.

Methods

pCO_2 acclimations

Haploid and diploid cells of *E. huxleyi* (strains RCC 1217 and RCC 1216, obtained from the Roscoff culture collection) were grown at 15 °C as dilute batch incubations. North Sea seawater medium (salinity 32.4) was sterile-filtered (0.2 µm) and enriched with vitamins and trace metals according to F/2 (Guillard and Ryther 1962), as well as phosphate and nitrate (100 and 6.25 µmol L^{-1}). Cells were exposed to a light:dark cycle (16:8 h) and saturating light (300 µmol photons m^{-2} s^{-1}) provided by daylight lamps (FQ 54W/965HO, OSRAM, Munich, Germany). Light intensity was monitored with the LI-6252 datalogger (LI-COR, Lincoln, NE, USA) using a 4π-sensor (US-SQS/L, Walz, Effeltrich, Germany). Culturing was carried out in sterilized 2.4 L borosilicate bottles (Duran Group, Mainz, Germany) on roller tables to avoid sedimentation.

Prior to experiments, cells were acclimated to the respective pCO_2 and light conditions for at least 7 days (i.e., more than 10 generations). Prior to initiating cultures, medium was pre-aerated for at least 36 h with humidified, 0.2 µm-filtered air comprising pCO_2 values of 380 or 950 µatm (equivalent to 38.5 and 96.3 Pa, or ~15 and ~35 µmol kg^{-1}, respectively). Gas mixtures were created by a gas flow controller (CGM 2000 MCZ Umwelttechnik, Bad Nauheim, Germany) using pure CO_2 (Air Liquide Deutschland, Düsseldorf, Germany) and CO_2-free air (CO2RP280, Dominick Hunter, Willich, Germany). Sampling and measurements were done 4–8 h after the beginning of the light period (i.e., at midday) in exponential growth at densities of 40,000–60,000 cells mL^{-1}. Cultures showing a pH drift of > 0.05 were excluded from further analyses.

The carbonate system (Table 1) during the acclimations was assessed based on measurements of pH and total alkalinity (TA). The pH_{NBS} of the cultures was measured potentiometrically and corrected for temperature (pH-meter 3110; WTW, Weilheim, Germany). The electrode (A157, Schott Instruments, Mainz, Germany) was three-point calibrated with NBS certified standard buffers and the measurement uncertainty was 0.03 pH units. TA was determined by potentiometric titration (Dickson 1981; TitroLine alpha plus, Schott Instruments). Measurements were accuracy-corrected with certified reference materials (CRMs) supplied by A. Dickson (Scripps Institution of Oceanography, USA). Calculation of the carbonate system was performed using CO2sys (Pierrot et al. 2006). Input parameters were pH_{NBS} and TA, as well as temperature (15 °C), salinity (32.4), and pressure (1 dbar, according to 1 m depth; Hoppe et al. 2012). For all calculations, phosphate and silicate concentrations were assumed to be 7 and 17 µmol kg^{-1}, respectively, based on assessments of the media. Equilibrium constants for carbonic acid, K_1 and K_2 given by Mehrbach et al. (1973) and refit by Dickson and Millero (1987) were used. For the dissociation of sulfuric acid, the constants reported by Dickson (1990) were employed.

Cell growth was assessed by daily cell counting with a Multisizer III hemocytometer (Beckman-Coulter, Fullerton, CA, USA) and the specific growth rates (μ) were calculated from daily increments (cf., Rokitta and Rost 2012). For the determination of total particulate carbon (TPC), POC and particulate organic nitrogen (PON), cell suspensions were vacuum-filtered (-200 mbar relative to atmosphere) onto pre-combusted (12 h, 500 °C) GF/F filters (1.2 µm; Whatman, Maidstone, UK), which were dried at 65 °C and analyzed with a EuroVector CHNS-O elemental analyzer (EuroEA, Milano, Italy). Before quantification of POC, filters were HCl-soaked (200 µL, 0.2 M) and dried to remove calcite. PIC was assessed as the difference between TPC and POC. By multiplying the POC and PIC cell quotas with μ, the respective production rates were derived (cf., Rokitta and Rost 2012). For Chl *a* measurements, cells were filtered onto cellulose nitrate filters (0.45 µm; Sartorius, Göttingen, Germany) and instantly frozen in liquid nitrogen. Chl *a* was extracted in 90 % acetone (v/v, Sigma, Munich, Germany) and determined fluorometrically (TD-700 fluorometer, Turner Designs, Sunnyvale, USA) following the protocol by Holm-Hansen and Riemann (1978). The calibration of the fluorometer was carried out with a commercially available Chl *a* standard (*Anacystis nidulans*, Sigma, Steinheim, Germany).

^{14}C disequilibrium method

The C_i source for photosynthesis was determined by applying the ^{14}C disequilibrium method (Elzenga et al. 2000; Espie and Colman 1986; Tortell and Morel 2002). In this method, a transient isotopic disequilibrium is induced by adding a small volume of a $^{14}C_i$ "spike" solution with a relatively low pH (typically 7.0) into larger volume of buffered cell suspension with a relatively high pH (typically 8.5). The cell suspension contains dextran-bound sulfonamide (DBS) to eliminate possible external CA activity. Due to the pH-dependent speciation of DIC, the relative CO_2 concentration of the spike is high (~19 % of DIC at pH 7.0), compared to the cell suspension (~0.3 % of DIC at pH 8.5). When adding the spike to the cell suspension, the majority of the CO_2 added with the spike

Table 1 Carbonate chemistry of the pCO_2 acclimations at the time of harvesting and in cell-free media (reference); Attained pCO_2, DIC, HCO_3^-, CO_3^{2-}, and $\Omega_{calcite}$ are calculated based on measured pH_{NBS} and TA using CO2sys (Pierrot et al. 2006)

Strain, ploidy	Treatment pCO_2 (μatm)	Attained pCO_2 (μatm)	pH_{NBS}	TA (μmol kg^{-1})	DIC (μmol kg^{-1})	CO_2 (μmol kg^{-1})	HCO_3^- (μmol kg^{-1})	CO_3^{2-} (μmol kg^{-1})	$\Omega_{calcite}$
RCC 1216, 2N	Low, 380	353 ± 8	8.19 ± 0.02	2,259 ± 19	2,023 ± 15	13 ± 0	1,857 ± 13	161 ± 3	3.9 ± 0.1
	High, 950	847 ± 55	7.86 ± 0.04	2,278 ± 20	2,156 ± 2	32 ± 2	2,060 ± 28	84 ± 4	2.0 ± 0.1
RCC 1217, 1N	Low, 380	345 ± 4	8.23 ± 0.00	2,317 ± 12	2,068 ± 10	13 ± 0	1,885 ± 10	170 ± 1	4.1 ± 0.0
	High, 950	837 ± 25	7.89 ± 0.01	2,317 ± 3	2,210 ± 5	32 ± 1	2,092 ± 5	86 ± 3	2.1 ± 0.1
Cell-free medium	Low, 380	405 ± 3	8.17 ± 0.00	2,304 ± 5	2,092 ± 5	15 ± 0	1,926 ± 5	151 ± 1	3.7 ± 0.0
	High, 950	997 ± 17	7.82 ± 0.01	2,305 ± 7	2,214 ± 12	38 ± 1	2,128 ± 11	75 ± 1	1.8 ± 0.0

Results are reported for 15 °C ($n \geq 3$; ± SD)

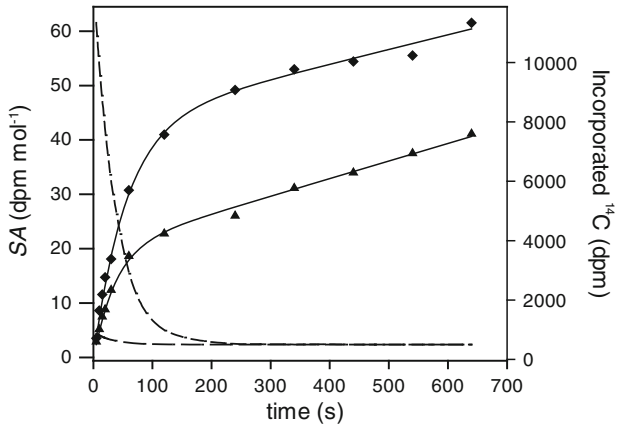

Fig. 1 Time-course of specific activities of CO_2 and HCO_3^- (medium and long dashed lines, respectively, here calculated for assay pH 8.5) in the isotopic disequilibrium method and examples for the ^{14}C incorporation of the diploid life-cycle stage for predominant CO_2 usage ($f_{CO_2} = 1.00$, *squares*) and considerable HCO_3^- usage ($f_{CO_2} = 0.60$, *triangles*)

converts into HCO_3^- until equilibrium is achieved (Johnson 1982; Millero and Roy 1997). Consequently, the specific activity of CO_2 (SA_{CO_2}, dpm (mol CO_2)$^{-1}$) is initially high and exponentially decays over time (Fig. 1). The slope of the ^{14}C incorporation curve of a "CO_2 user" is, therefore, initially much steeper than during final linear ^{14}C uptake, when isotopic equilibrium is achieved. In contrast, the slope of ^{14}C incorporation for "HCO_3^- users" changes only marginally over time because $SA_{HCO_3^-}$ stays more or less constant during the assay.

Quantification of the relative proportion of CO_2 or HCO_3^- usage was done by fitting data with the integral function of the ^{14}C fixation rate (Elzenga et al. 2000; Espie and Colman 1986; Martin and Tortell 2006). The function includes terms representing the instantaneous fixation rate of $DI^{14}C$, the fractional contribution of CO_2 (f_{CO_2}) or HCO_3^- usage ($1 - f_{CO_2}$) to the overall C_i fixation and the specific activity (SA, dpm mol^{-1}) of these substrates at any given time (Eq. 1; Espie and Colman 1986; Elzenga et al. 2000; Tortell and Morel 2002). Strictly speaking, as HCO_3^- and CO_3^{2-} cannot be differentially labeled, $1 - f_{CO_2}$ also comprises the potential fraction of CO_3^{2-} used.

$$\begin{aligned} \text{dpm} = & V_{DI14C}(f_{CO_2})(\alpha_1 t + (\Delta SA_{CO_2}/SA_{DIC})(1 - e^{-\alpha_1 t}))/\alpha_1 \\ & + V_{DI14C}(1 - f_{CO_2})(\alpha_2 t + (\Delta SA_{HCO_3}/SA_{DIC})(1 - e^{-\alpha_2 t}))/\alpha_2 \end{aligned} \quad (1)$$

In this equation, V_{DI14C} is the total rate of ^{14}C uptake; f_{CO_2} is the fraction of uptake attributable to CO_2; α_1 and α_2 are the temperature-, salinity-, and pH-dependent first-order rate constants for CO_2 and HCO_3^- hydration and dehydration, respectively; t is the time (s); ΔSA_{CO_2} and ΔSA_{HCO_3} are the differences between the initial and equilibrium values of the specific activities of CO_2 and HCO_3^-, respectively; and SA_{DIC} is the specific activity of DIC. During steady-state photosynthesis, V_{DI14C} and f_{CO_2} are assumed to be constant so that changes in the instantaneous ^{14}C uptake rate reflect only changes in the specific activity of CO_2 and HCO_3^-.

In the present study, the ^{14}C disequilibrium method was modified to enable measurements over a range of ecologically relevant pH values (7.90–8.70). In order to maintain a suitably large initial isotopic disequilibrium ($\Delta SA_{CO_2}/SA_{DIC}$), the pH of the ^{14}C spike solutions needs to be adjusted in conjunction with the pH of the assay buffer. We, thus, used either MES or HEPES buffers to set the pH of spike solutions over the range of 5.75–7.30 (see Table 2 for exact pH values of assay and spike buffers). For the assays, 10–30 × 10^6 cells were concentrated via gentle filtration over a polycarbonate filter (2 μm; Millipore, Billerica, MA, USA) to a final volume of 15 mL. During this filtration procedure, cells were kept in suspension, while the medium was gradually exchanged with buffered assay medium of the appropriate pH value. Assay media and spike buffers were prepared at least 1 day prior

Table 2 Chemical characteristics of ^{14}C disequilibrium assay media and spike buffers, and the associated parameter values for model fits (Eq. 1)

Assay medium			Spike solution			Conditions for RCC 1216, 2N						Conditions for RCC 1217, 1N					
pH	Buffer chemical	CO_2 (%)	pH	Buffer chemical	CO_2 (%)	DIC (μM)	CO_2 (μM)	α_1	α_2	$\frac{\Delta SA_{CO_2}}{SA_{DIC}}$	$\frac{\Delta SA_{HCO_3^-}}{SA_{DIC}}$	DIC (μM)	CO_2 (μM)	α_1	α_2	$\frac{\Delta SA_{CO_2}}{SA_{DIC}}$	$\frac{\Delta SA_{HCO_3^-}}{SA_{DIC}}$
7.90	BICINE	1.1	5.75	MES	80.4	2,210	23.4	0.0186	0.0197	29.09	−0.786	2,490	26.7	0.0176	0.0186	28.44	−0.786
8.10	BICINE	0.7	6.35	MES	50.7	2,250	14.6	0.0205	0.0225	30.08	−0.451	2,680	17.6	0.0194	0.0212	30.09	−0.454
8.30	BICINE	0.4	6.70	MES	31.5	2,290	8.9	0.0236	0.0272	30.46	−0.204	2,590	10.3	0.0223	0.0256	29.83	−0.206
8.50	BICINE	0.2	7.00	HEPES	18.7	2,380	5.4	0.0285	0.0355	31.37	−0.012	2,310	5.4	0.0270	0.0334	27.87	0.008
8.70	BICINE	0.1	7.30	HEPES	10.3	2,150	2.8	0.0364	0.0504	29.16	−0.237	–	–	–	–	–	–

Assays with the diploid cells (2N) were conducted at an assay temperature of 15.5 °C, a spike temperature of 23 °C, an added radioactivity of 315 kBq and a salinity of 32.4. Assays with the haploid cells (1N) were conducted at an assay temperature of 15.0 °C, a spike temperature of 23 °C, a spike radioactivity of 370 kBq and a salinity of 32.4

to the assay and stored in closed containers to avoid CO_2 exchange and pH drift. The pH value and temperatures of all buffers were measured immediately prior to assay runs. DIC concentration of the assay buffers was determined colorimetrically according to Stoll et al. (2001) using a TRAACS CS800 autoanalyzer (Seal Analytical, Norderstedt, Germany), and measurements were accuracy-corrected with CRMs supplied by A. Dickson (Scripps Institution of Oceanography, USA).

To initiate the assays, a volume of 4 mL buffered concentrated cell suspension was transferred into a temperature-controlled, illuminated glass cuvette (15 °C; 300 μmol photons m^{-2} s^{-1}) to which 50 μM DBS was added (Ramidus, Lund, Sweden). Cells were continuously stirred in the light for at least 5 min prior to spike addition to reach steady-state photosynthesis. Spike solutions were prepared by adding $NaH^{14}CO_3$ solution (1.88 GBq (mmol DIC)$^{-1}$; GE Healthcare, Amersham, UK) into a final volume of 200 μL of pH-buffered MilliQ water (various buffers at 20 mM; Table 2), yielding activities of ~370 kBq (10 μCi). Following the spike addition, 200 μL subsamples of the cell suspension were transferred into 2 mL HCl (6 M) at time points between 5 s and 12 min. Addition of these aliquots to the strong acid caused instant cell death and converted all DIC and PIC to CO_2. $DI^{14}C$ background was degassed in a custom-built desiccator for several days until samples were dry. Deionized water (1 mL) was then added to re-suspend samples prior to addition of 10 mL of scintillation cocktail (Ultima Gold AB, GMI, Ramsey, MN, USA), and the sample was vortexed thoroughly.

Acid-stable (i.e., organic) ^{14}C activity in samples was counted with a Packard Tri-Carb Liquid Scintillation Counter (GMI). Blank samples, consisting of cell-free medium, were treated alongside the other samples. In the few cases where no blanks were available, time zero values were approximated by extrapolating the y-axis intercept from linear fitting of the first three data points of the ^{14}C incorporation curves. Total radioactivity of the $NaH^{14}CO_3$ stock solution was regularly quantified and compared to expected values to estimate loss of radioactivity or changes in counting efficiency. In all spike solutions, measured radioactivity ranged between 80 and 100 % of the theoretical values, and the actual radioactivity levels were used in the calculation of the specific activities. Blank-corrected data were fitted (Eq. 1), using a least-squares-fitting procedure. Applied fit parameters are given in Table 2. Furthermore, a detailed Excel spread sheet for calculating the fit parameters in dependence of the applied conditions (e.g., pH, temperature and DIC concentrations) is provided as Supplementary Material. Please note that in the calculation of initial and final specific activities, we accounted not only for changes in concentrations of $^{14}C_i$ species but also for

Table 3 Growth rates, elemental quotas and production rates, elemental ratios, as well as pigment composition of haploid (1N) and diploid (2N) cells of *E. huxleyi*, cultured at low (380 µatm) and elevated pCO_2 (950 µatm): μ (day^{-1}), POC quota (pg $cell^{-1}$), POC production (pg $cell^{-1}$ day^{-1}), PIC quota (pg $cell^{-1}$), PIC production (pg $cell^{-1}$ day^{-1}), TPC quota (pg $cell^{-1}$), TPC production (pg $cell^{-1}$ day^{-1}), PON quota (pg $cell^{-1}$), PON production (pg $cell^{-1}$ day^{-1}), PIC:POC ratio (mol:mol), POC:PON ratio (mol:mol), Chl *a* quotas (pg $cell^{-1}$), and Chl *a*:POC ratios (pg:pg)

Parameter	1N low pCO_2	1 N high pCO_2	p	2N low pCO_2	2N high pCO_2	p
μ	1.12 ± 0.04	1.08 ± 0.06	†	1.08 ± 0.05	1.04 ± 0.04	†
POC quota	10.76 ± 0.23	11.08 ± 1.19	†	8.35 ± 0.84	14.78 ± 1.91	**
POC production	12.09 ± 0.25	12.81 ± 0.44	†	9.02 ± 0.91	13.97 ± 0.63	*
PIC quota	0.48 ± 0.43	−0.18 ± 0.21	†	11.78 ± 0.78	10.90 ± 0.60	†
PIC production	–	–	†	12.71 ± 0.29	11.35 ± 0.90	**
TPC quota	11.23 ± 0.66	12.01 ± 1.27	†	20.13 ± 1.34	25.68 ± 2.00	*
TPC production	12.63 ± 0.70	12.51 ± 0.52	†	21.73 ± 1.05	26.77 ± 3.10	≤ 0.06
PON quota	1.39 ± 0.06	1.45 ± 0.09	†	1.54 ± 0.12	1.95 ± 0.22	*
PON production	1.56 ± 0.06	1.56 ± 0.08	†	1.66 ± 0.10	2.03 ± 0.30	†
PIC:POC	–	–	†	1.42 ± 0.14	0.75 ± 0.11	**
POC:PON	9.03 ± 0.19	8.90 ± 0.69	†	6.31 ± 0.30	8.83 ± 0.17	***
Chl *a* quota	0.10 ± 0.01	0.12 ± 0.01	†	0.18 ± 0.01	0.17 ± 0.01	†
Chl *a* :POC	0.009 ± 0.001	0.012 ± 0.001	†	0.022 ± 0.001	0.012 ± 0.001	***

For the haploid cells, PIC production and PIC:POC ratios were not calculated. Stars indicate statistical significance levels in differences between low and high pCO_2 treatments with * $p \leq 0.05$, ** $p \leq 0.01$ and *** $p \leq 0.001$. No significant difference ($p > 0.05$) is indicated by †

changes in concentrations of $DI^{12}C$, $^{12}CO_2$, and $H^{12}CO_3^-$ upon spike addition. If these changes are neglected, $\Delta SA_{CO_2}/SA_{DIC}$ will be significantly overestimated, leading to an underestimation of f_{CO_2} (Eq. 1, Table 2, Supplementary material).

We used a numerical sensitivity study to examine how offsets in parameters such as pH, DIC concentrations, radioactivity, temperature, or blank values influence the derived estimates of f_{CO_2}. First, theoretical ^{14}C incorporation curves for "HCO_3^- users" ($f_{CO_2} = 0.25$) and "CO_2 users" ($f_{CO_2} = 0.80$) were generated for two assay pH values (7.90 and 8.50) and used as a reference, assuming fixed values of DIC concentrations of 2,300 µmol kg^{-1}, assay temperature of 15 °C, spike solution temperature of 23 °C and spike radioactivity of 370 kBq. In a second step, model fits were obtained using slight offsets in these parameters (e.g., pH 7.95 and 7.85 instead of 7.90) to obtain the effect of parameter variability on f_{CO_2} estimates. Sensitivity toward over- and underestimation of pH, temperature, DIC concentration, and radioactivity was tested. We further assessed the effects of blank values (±100 dpm) on f_{CO_2} estimates as a function of different final ^{14}C incorporation rates.

Statistics

All experiments were performed using at least biological triplicates (i.e., three independent, but equally treated cultures). When data were normally distributed (Shapiro-Wilk test) and showed equal variance (Equal-Variance Test), significance in difference between pCO_2 treatments was tested by performing student′s t-tests. When samples were not normally distributed or did not show equal variance, a rank sum test was performed instead. Null hypotheses were rejected when $p \leq 0.05$, unless otherwise indicated.

Results

In diploid cells of *E. huxleyi*, the specific growth rate μ and PIC quotas did not change significantly in response to elevated pCO_2 (Table 3). While there was a small decrease in PIC production rates (−11 %), POC quotas and production rates increased strongly under elevated pCO_2 (+77 and +55 %, respectively). In conjunction with these changes, the quotas and production rates of TPC also increased (+28 and +23 %, respectively). The PIC:POC ratios of diploid cells decreased from 1.4 to 0.7 under elevated pCO_2, while the POC:PON ratios increased from 6.3 to 8.8. Chl *a* quotas were largely unaffected by the pCO_2 treatments, although Chl *a*:POC ratios decreased significantly from 0.022 to 0.012 pg pg^{-1} under elevated pCO_2, owing to the change in POC quotas. In haploid cells, neither μ, elemental quotas or the respective production rates showed any significant response to elevated pCO_2

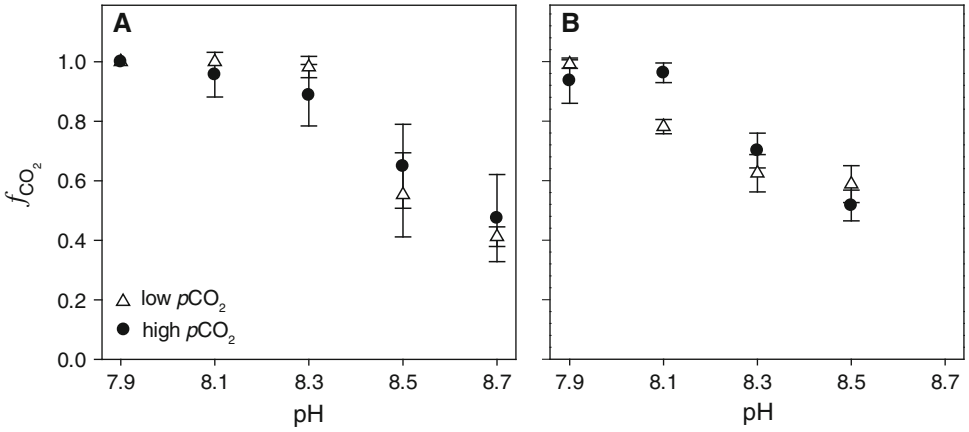

Fig. 2 Fraction of CO_2 usage (f_{CO_2}) as a function of the assay pH in **A** the diploid *E. huxleyi* RCC 1216 and **B** the haploid RCC 1217 being acclimated to low pCO_2 (380 µatm, *white triangles*) and high pCO_2 (950 µatm, *black circles*)

(Table 3). Similarly, Chl *a* quotas, Chl *a*:POC, and POC:PON ratios were all unaffected by the experimental CO_2 manipulations in the haploid strain.

Under both pCO_2 acclimations, diploid cells were shown to be predominant "CO_2 users" under low assay pH ($f_{CO_2} \sim 1.0$ at pH 7.9; Fig. 2a). With increasing assay pH, however, we observed a significant increase in relative HCO_3^- utilization. HCO_3^- uptake was induced at assay pH $\geq$ 8.3 (equivalent to CO_2 concentrations $\leq$ 9 µmol L^{-1}), reaching considerable contribution at high assay pH ($f_{CO_2} \sim 0.44$ at pH 8.7). In contrast to the strong effect of the assay pH, the tested pCO_2 acclimations had no effect on the pH-dependent C_i uptake behavior (Fig. 2a). In other words, both low and high pCO_2-acclimated cells showed the same short-term response of f_{CO_2} to assay pH. Like the diploid stage, haploid cells progressively changed from high CO_2 usage at low assay pH ($f_{CO_2} \sim 0.96$ at pH 7.9) to substantial HCO_3^- contributions when assays were conducted in high pH assay buffers ($f_{CO_2} \sim 0.55$ at pH 8.5; Fig. 2b). HCO_3^- uptake became relevant at pH $\geq$ 8.1 (equivalent to CO_2 concentrations $\leq$ 14 µmol L^{-1}), particularly in low pCO_2-acclimated cells. Except for haploid cells measured at pH 8.1, no significant differences in f_{CO_2} were observed between the low and high pCO_2 acclimations (Fig. 2b).

The sensitivity analysis showed that an offset in the input pH of the buffered assay cell suspension (± 0.05 pH units) led to deviations in f_{CO_2} of $\leq$ 0.09 (i.e., 9 percentage points) in "CO_2 users" and $\leq$ 0.02 in "HCO_3^- users" (Fig. 3a). An offset in the input temperature of the assay buffer (± 2 °C) led to a deviation in f_{CO_2} of $\leq$ 0.09 in "CO_2 users" and $\leq$ 0.03 in "HCO_3^- users" (Fig. 3a). An offset in the input pH of the spike (± 0.05 pH units) changed the f_{CO_2} estimates by $\leq$ 0.08 in "CO_2 users" and $\leq$ 0.03 in "HCO_3^- users" (Fig. 3a). Applying an offset in the input temperature of the spike (± 2 °C) caused a deviation in f_{CO_2} by $\leq$ 0.06 in "CO_2 users" and had practically no effect on f_{CO_2} in "HCO_3^- users" ($\leq$ 0.01; Fig. 3a). An offset in the input DIC concentration of the buffer (± 100 µmol kg^{-1}) affected f_{CO_2} by $\leq$ 0.08 in "CO_2 users" and $\leq$ 0.03 in "HCO_3^- users". Regarding the radioactivity of the spike (± 37 kBq), deviations in f_{CO_2} were $\leq$ 0.12 in "CO_2 users" and $\leq$ 0.04 in "HCO_3^- users." Irrespective of CO_2 or HCO_3^- usage, offsets in blank estimations (± 100 dpm) led to deviating f_{CO_2} by $\leq$ 0.27, but only when equilibrium ^{14}C fixation rates were $\leq$ 1 dpm s^{-1} (Fig. 3b). When steady-state ^{14}C incorporation rates were $\geq$ 2 dpm s^{-1} (i.e., average rate in diploid cells) and $\geq$ 4 dpm s^{-1} (i.e., average rate in haploid cells), the deviations in f_{CO_2} due to offsets in the blanks were $\leq$ 0.17 and $\leq$ 0.11, respectively.

Discussion

Acclimation responses

This study corroborates previous findings on the general sensitivity of the diploid life-cycle stage of *E. huxleyi* toward OA (e.g., Feng et al. 2008; Langer et al. 2009; Riebesell et al. 2000). While growth rate was unaffected, OA reduced PIC production and stimulated POC production (Table 3). Consequently, the PIC:POC ratio was strongly decreased under OA, indicating a redirection of C_i fluxes between these two processes. Transcriptomics have previously attributed this redirection to an inhibition of calcification in response to impaired signal-transduction and ion-transport, as well as to stimulation in the production of glycoconjugates and lipids (Rokitta et al. 2012). In our study, also the TPC production increased significantly under OA (Table 3), indicating that not only C_i is allocated differently, but also the overall C_i uptake increases with the increasing pCO_2. Our data further suggest that less energy is required for the C_i acquisition under OA as more POC and TPC could be produced even though the Chl *a* quota

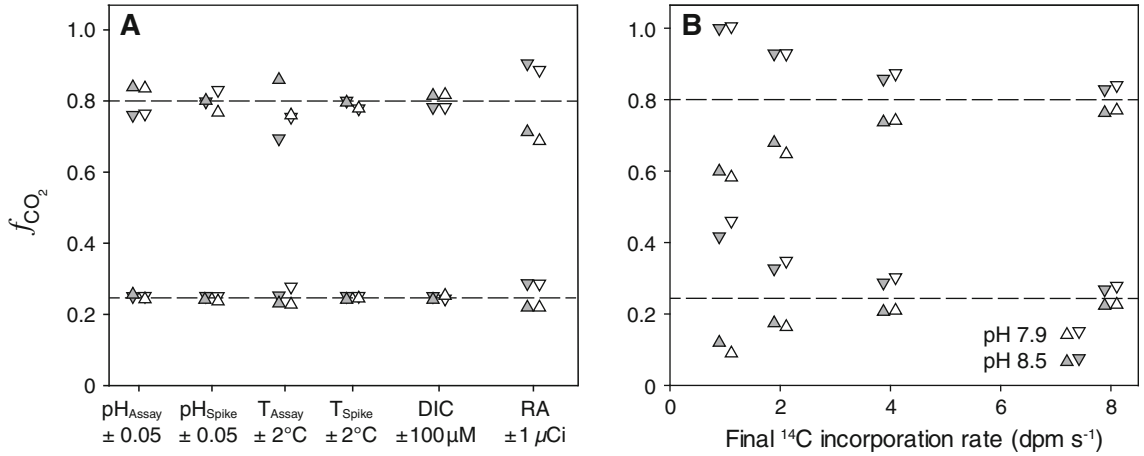

Fig. 3 Sensitivity in f_{CO_2} estimates for "CO_2 users" ($f_{CO_2} = 0.80$) and "HCO_3^- users" ($f_{CO_2} = 0.25$) at low pH (7.9, *in gray*) and high pH (8.5, *in white*) **A** toward negative (*inverted filled triangle*) and positive (*filled triangle*) offsets in the pH, temperature, and DIC concentration of the assay buffer (pH_{Assay}, T_{Assay}, and [DIC]), as well as toward offsets pH, temperature, and radioactivity of the spike (pH_{Spike}, T_{Spike}, and RA), and **B** toward negative (*inverted filled triangle*) and positive (*filled triangle*) offsets in blank measurements (±100 dpm) in dependence of the final ^{14}C incorporation rates. Sensitivity was assessed based on theoretical curves with constraints of a $[DIC]_{Assay} = 2{,}300$ µM, $T_{Assay} = 15$ °C, $T_{Spike} = 23$ °C, and $RA_{Spike} = 37$ kBq. *Dashed lines* indicate f_{CO_2} values as expected for optimal experimental conditions

remained unaffected by the pCO_2 treatment (Table 3). Improved energy-use efficiencies under OA have previously been proposed for the diploid life-cycle stage of *E. huxleyi* (Rokitta and Rost 2012).

In strong contrast to the diploid strain, the haploid life-cycle stage of *E. huxleyi* was insensitive toward OA with respect to growth rate and elemental composition (Table 3). The ability of the haploid cells to maintain homeostasis under OA has also been observed by Rokitta and Rost (2012). Even though the haploid cells appeared non-responsive toward OA on the phenomenological level (i.e., growth, elemental composition), transcriptomics have revealed significant changes at the subcellular level, such as an upregulation of catabolic pathways under OA (Rokitta et al. 2012). Based on the comparison of the life-cycle stages, Rokitta and co-workers concluded that the OA sensitivity in diploid cells originates from calcification, differences in C_i acquisition or both.

A number of studies have shown that *E. huxleyi* has moderately high C_i affinities and uses HCO_3^- as the primary C_i source (e.g., Herfort et al. 2002; Rokitta and Rost 2012; Rost et al. 2006b; Stojkovic et al. 2013), irrespective of the degree of calcification (Trimborn et al. 2007; Rokitta and Rost 2012). These characteristics would suggest *E. huxleyi* to be rather insensitive toward OA and the associated rise in CO_2 concentration, contrary to most results obtained for the diplont. As discussed below, this apparent discrepancy could originate from differences in conditions applied during short-term physiological measurements and those conditions cells experience in the long-term acclimation.

Modes of C_i acquisition

Our results demonstrate that the C_i source of both life-cycle stages of *E. huxleyi* is significantly influenced by the pH of the assay medium and the resulting carbonate chemistry (Fig. 2). With increasing pH in assay buffers, cells progressively changed from predominant CO_2 usage at lower pH values (≤ 8.1) to significant HCO_3^- contribution at higher pH (≥ 8.3). Surprisingly, this change occurred irrespectively of the pCO_2 conditions in the acclimation. To our knowledge, such a strong short-term pH-dependence in C_i acquisition has not been previously reported, which is most likely due to the fact that assays are typically performed under standardized pH values. Measuring physiological responses under one reference condition have the advantage that consequences of different acclimations can readily be compared in terms of altered capacities of certain processes, e.g., enzyme activities or transport rates. However, determination of the C_i source at one standard pH appears to impose a methodological bias, and our results, therefore, bear direct relevance to the interpretation of previous laboratory observations.

In view of the short-term pH effect on C_i acquisition, the contribution of HCO_3^- as a photosynthetic C_i source in *E. huxleyi* may have possibly been overestimated in previous studies. This overestimation is likely to be the most significant in those studies when ^{14}C disequilibrium assays were conducted at pH 8.5 (e.g., Rokitta and Rost 2012; Rost et al. 2007). By looking at the C_i source determined at an assay pH mimicking the acclimation condition, we can now re-evaluate and in fact explain the responses of

E. huxleyi toward elevated pCO_2. When assessing f_{CO_2} using assay buffers of pH 7.9 and 8.1 (equivalent to the acclimation pH of high and low pCO_2 treatments), we observed predominant CO_2 uptake under both conditions (Fig. 2). Being "CO_2 user", cells were thus able to directly benefit from changes in the CO_2 concentrations in our acclimations ($\sim$15 µmol kg^{-1} at 380 µatm and $\sim$38 µmol kg^{-1} at 950 µatm). For a "HCO_3^- user", however, it would be difficult to argue for a beneficial OA-effect as HCO_3^- concentrations do not differ much between treatments ($\sim$1,930 µmol kg^{-1} at 380 µatm and $\sim$2,130 µmol kg^{-1} at 950 µatm). Our results thus suggest that biomass production in diploid cells not only profits from the declined calcification at high pCO_2, as suggested by Rokitta and Rost (2012) but also from the higher CO_2 supply under OA. As CO_2 usage is considered to be less costly than HCO_3^- uptake (Raven 1990), this could also explain the higher energy-use efficiency observed for *E. huxleyi* (Rokitta and Rost 2012).

Although the haploid life-cycle stage of *E. huxleyi* exhibited a pH-dependent C_i uptake behavior that was similar to the diploid (Fig. 2), the haploid cells did not show any CO_2-dependent stimulation in biomass production (Table 3). This could partly be related to the fact that the biomass production cannot profit from a down-scaling of calcification, simply because this process is absent in the haploid life-cycle stage. The lack of significantly stimulated biomass buildup under OA could also be attributed to the concomitant upregulation of catabolic pathways, such as higher lipid consumption, which is a specific feature of the haploid cells (Rokitta et al. 2012). After all, the similar C_i uptake behavior of both life-cycle stages confirms that photosynthetic HCO_3^- usage is not tied to calcification (Herfort et al. 2004; Trimborn et al. 2007; Bach et al. 2013) and that the preference for CO_2 or HCO_3^- is predominantly controlled by carbonate chemistry.

Our findings clearly demonstrate that the acclimation history, in both life-cycle stages, has little or no effect on the C_i usage of the cells (Fig. 2). In other words, the instantaneous effect of the assay conditions dominates over acclimation effects. We cannot preclude, however, that cells acclimated to higher pH values, where CO_2 supply becomes limiting, may increase their capacity for HCO_3^- uptake and acclimations effects would then be evident. Notwithstanding the potential for some acclimation effects, the extent to which short-term pH and/or CO_2 levels in the assay medium directly control cellular C_i usage is striking. This implies that even though *E. huxleyi* did not use significant amounts of HCO_3^- for photosynthesis, it must constitutively express a HCO_3^- transporter in all acclimations. Without the presence of a functional HCO_3^- transport system we could otherwise not explain the capacity for significant HCO_3^- uptake under short-term exposure to high pH (even in high pCO_2-acclimated cells).

In the diploid life-cycle stage, HCO_3^- transporter may be constitutively expressed to fuel calcification, as HCO_3^- was identified as the main C_i source for this process (Paasche 1964; Rost et al. 2002; Sikes et al. 1980). If CO_2 supply for photosynthesis becomes limiting, HCO_3^- transport could then also fuel photosynthesis. In the haploid cells, which do not calcify, we nonetheless observed the same capacity for HCO_3^- uptake, which suggests that HCO_3^- uptake capacity represents a fundamental component of the CCM of both life-cycle stages of *E. huxleyi*. Whether levels of protons or CO_2 concentrations are the main trigger for the shift between CO_2 and HCO_3^- uptake remains unclear, even though there is strong evidence that CO_2 supply is the main driver for the responses in photosynthesis (Bach et al. 2011).

Sensitivity analyses

In our sensitivity study, the applied offsets in pH (± 0.05 pH units), temperature (± 2 °C), DIC of the assay buffer (± 100 µM), and spike radioactivity (± 37 kBq) were larger than typical measurement errors to represent "worst-case scenarios". None of these offsets caused f_{CO_2} estimates to deviate by more 0.12 in any of the pH treatments (Fig. 3a). When adequate efforts are taken to control these parameters (e.g., using reference buffers, thermostats), methodological uncertainties are thus negligible. DIC concentrations and radioactivity, however, are often not measured and in view of the potential drift over time, offsets can easily exceed typical measurement errors and lead to severe deviations in f_{CO_2}. For instance, $^{14}CO_2$ out-gassing causes the spike solution to progressively lose radioactivity. This loss of ^{14}C can easily be > 20 % over the course of weeks or months, despite the high pH values of the stock solution and small headspace in the storage vial (Gattuso et al. 2010).

The average final ^{14}C fixation rates, which depend on the biomass and radioactivity used, were 2.1 ± 0.8 dpm s^{-1} in the runs with diploid and 6.6 ± 2.2 dpm s^{-1} in those with haploid cells (Fig. 3b). In these ranges, offsets in blank values (± 100 dpm) can lead to biases in the estimated f_{CO_2} by up to 0.20 (Fig. 3b). This strong sensitivity highlights the need to thoroughly determine blank values, but also to work with sufficiently high biomass and/or radioactivity to maximize ^{14}C incorporation rates. When working with dense cell suspensions, however, self-shading or significant drawdown of DIC during the assay might bias results. Higher label addition generally increases the resolution of the assay and lowers the consequences of offsets in the blank value. It should be noted, however, that high concentrations of ^{14}C in

spike solutions can affect not only the isotopic but also the chemical conditions in the cuvette (e.g., pH and DIC).

Overall, our sensitivity study revealed that the ^{14}C disequilibrium method is a straightforward and robust assay, which is very useful for resolving the C_i source of phytoplankton over a range of different pH values. It is important to realize, however, the pH of assay buffers has the potential to significantly affect the C_i uptake behavior of cells.

Conclusions

Our data clearly demonstrate that both life-cycle stages of *E. huxleyi* predominantly use CO_2 as C_i source for photosynthesis under typical present-day and future CO_2 levels, but constitutively express HCO_3^- transporters allowing them to directly use HCO_3^- when CO_2 becomes limiting. Under bloom conditions, where pH values can easily increase to 8.5 or higher, cells might, therefore, be able to maintain efficient C_i acquisition. Future research needs to investigate whether and how the assay pH governs the mode of C_i acquisition also in other coccolithophores species or phytoplankton taxa and how this may alter the energy budget of cells. Results from previous studies may need re-consideration in the light of our data showing strong short-term pH effects on C_i uptake of phytoplankton.

Acknowledgments We thank Silke Thoms and Lena Holtz for the discussion of our data and their constructive feedback on this manuscript. This work was supported by the European Community's Seventh Framework Programme/ERC grant agreement #205150, and by an Alexander Von Humboldt fellowship to PDT.

References

Anning T, Nimer N, Merrett M, Brownlee C (1996) Costs and benefits of calcification in coccolithophorids. J Mar Syst 9:45–56

Bach LT, Riebesell U, Schulz KG (2011) Distinguishing between the effects of ocean acidification and ocean carbonation in the coccolithophore *Emiliania huxleyi*. Limnol Oceanogr 56:2040–2050

Bach LT, Mackinder LCM, Schulz KG, Wheeler G, Schroeder DC, Brownlee C, Riebesell U (2013) Dissecting the impact of CO_2 and pH on the mechanisms of photosynthesis and calcification in the coccolithophore *Emiliania huxleyi*. New Phytol 199:121–134

Badger MR (2003) The roles of carbonic anhydrases in photosynthetic CO_2 concentrating mechanisms. Photosynth Res 77:83–94

Broecker WS, Peng T-H (1982) Tracers in the Sea. EldigioPress, New York

Caldeira K, Wickett ME (2003) Anthropogenic carbon and ocean pH—the coming centuries may see more oceanic acidification than the past 300 million years. Nature 425:365

Cassar N, Laws EA, Bidigare RR, Popp BN (2004) Bicarbonate uptake by Southern Ocean phytoplankton. Glob Biogeochem Cy 18:GB2003. doi:10.1029/2003GB002116

Dickson AG (1981) An exact definition of total alkalinity and a procedure for the estimation of alkalinity and total inorganic carbon from titration data. Deep Sea Res 28A:609–623

Dickson AG (1990) Standard potential of the reaction: $AgCl(s) + ½ H_2(g) = Ag(s) + HCl(aq)$, and the standard acidity constant of the ion HSO_4^- in synthetic seawater from 273.15 to 318.15 K. J Chem Thermodyn 22:113–127

Dickson AG, Millero FJ (1987) A comparison of the equilibrium constants for the dissociation of carbonic acid in seawater media. Deep Sea Res 34:1733–1743

Elzenga JTM, Prins HBA, Stefels J (2000) The role of extracellular carbonic anhydrase activity in inorganic carbon utilization of *Phaeocystis globosa* (Prymnesiophyceae): a comparison with other marine algae using the isotopic disequilibrium technique. Limnol Oceanogr 45:372–380

Espie GS, Colman B (1986) Inorganic carbon uptake during photosynthesis—a theoretical analysis using the isotopic disequilibrium technique. Plant Physiol 80:863–869

Falkowski PG, Barber RT, Smetacek V (1998) Biogeochemical controls and feedbacks on ocean primary production. Science 281:200–206

Feng Y, Warner ME, Zhang Y, Sun J, Fu FX, Rose JM, Hutchins DA (2008) Interactive effects of increased pCO_2, temperature and irradiance on the marine coccolithophore *Emiliania huxleyi* (Prymnesiophyceae). Eur J Phycol 43:87–98

Field CB, Behrenfeld MJ, Randerson JT, Falkowski P (1998) Primary production of the biosphere—integrating terrestrial and oceanic components. Science 281:237–240

Frada MJ, Bidle KD, Probert I, de Vargas C (2012) *In situ* survey of life cycle phases of the coccolithophore *Emiliania huxleyi* (Haptophyta). Environ Microbiol 14(6):1558–1569

Gattuso J-P, Gao K, Lee K, Rost B, Schulz K (2010). Approaches and tools to manipulate the carbonate chemistry, In: Riebesell U, Fabry VJ, Hansson L, Gattuso J-P (eds) Guide for best practices in ocean acidification research and data reporting. European Commission, pp 41–52

Guillard RRL, Ryther JH (1962) Studies of marine planktonic diatoms. Can J Microbiol 8:229–239

Herfort L, Thake B, Roberts J (2002) Acquisition and use of bicarbonate by *Emiliania huxleyi*. New Phytol 156:427–436

Herfort L, Loste E, Meldrum F, Thake B (2004) Structural and physiological effects of calcium and magnesium in *Emiliania huxleyi* (Lohmann) Hay and Mohler. J Struct Biol 148:307–314

Holm-Hansen O, Riemann B (1978) Chlorophyll a determination: improvements in methodology. Oikos 30:438–447

Hoppe CJM, Langer G, Rost B (2011) *Emiliania huxleyi* shows identical responses to elevated pCO_2 in TA and DIC manipulations. J Exp Mar Biol Ecol 406:54–62

Hoppe CJM, Langer G, Rokitta SD, Wolf-Gladrow DA, Rost B (2012) Implications of observed inconsistencies in carbonate chemistry measurements for ocean acidification studies. Biogeosciences 9:2401–2405

Johnson KS (1982) Carbon dioxide hydration and dehydration kinetics in seawater. Limnol Oceanogr 27:849–855

Langer G, Nehrke G, Probert I, Ly J, Ziveri P (2009) Strain-specific responses of *Emiliania huxleyi* to changing seawater carbonate chemistry. Biogeosciences 6:2637–2646

Mackinder L, Wheeler G, Schroeder D, Riebesell U, Brownlee C (2010) Molecular mechanisms underlying calcification in coccolithophores. Geomicrobiol J 27:585–595

Martin CL, Tortell PD (2006) Bicarbonate transport and extracellular carbonate anhydrase in Bering Sea phytoplankton assemblages:

results from isotopic disequilibrium experiments. Limnol Oceanogr 51:2111–2121
Mehrbach C, Culberson CH, Hawley JE, Pytkowicz RM (1973) Measurement of the apparent dissociation constants of carbonic acid in seawater at atmospheric pressure. Limnol Oceanogr 18:897–907
Millero FJ, Roy RN (1997) A chemical equilibrium model for the carbonate system in natural waters. Croat Chem Acta 70:1–38
Paasche E (1964) A tracer study of the inorganic carbon uptake during coccolith formation and photosynthesis in the coccolithophorid *Coccolithus huxleyi*. Physiol Plant 18:138–145
Paasche E (2002) A review of the coccolithophorid *Emiliania huxleyi* (Prymnesiophyceae), with particular reference to growth, coccolith formation, and calcification-photosynthesis interactions. Phycologia 40:503–529
Pierrot D, Lewis E, Wallace D (2006) MS Excel program developed for CO_2 system calculations. ORNL/CDIAC-105 Carbon Dioxide Information Analysis Center, Oak Ridge National Laboratory, U.S. Department of Energy, Oak Ridge
Raven JA (1990) Sensing pH? Plant Cell Environ 13:721–729
Raven JA (2006) Sensing inorganic carbon: CO_2 and HCO_3^-. Biochem J 396:e5–e7. doi:10.1042/BJ20060574
Raven JA, Crawfurd K (2012) Environmental controls on coccolithophore calcification. Mar Ecol Prog Ser 470:137–166
Read BA, Kegel J, Klute MJ, Kuo A, Lefebvre SC, Maumus F, Mayer C, Miller J, Monier A, Salamov A et al (2013) Pan genome of the phytoplankton *Emiliania* underpins its global distribution. Nature 499:209–213
Reinfelder JR (2011) Carbon concentrating mechanisms in eukaryotic marine phytoplankton. Annu Rev Mar Sci 3:291–315
Riebesell U, Zondervan I, Rost B, Tortell PD, Zeebe E, Morel FMM (2000) Reduced calcification in marine plankton in response to increased atmospheric CO_2. Nature 407:364–367
Rokitta SD, Rost B (2012) Effects of CO_2 and their modulation by light in the life-cycle stages of the coccolithophore *Emiliania huxleyi*. Limnol Oceanogr 57(2):607–618
Rokitta SD, De Nooijer LJ, Trimborn S, De Vargas C, Rost B, John U (2011) Transcriptome analyses reveal differential gene expression patterns between lifecycle stages of *Emiliania huxleyi* (Haptophyta) and reflect specialization to different ecological niches. J Phycol 47:829–838
Rokitta SD, John U, Rost B (2012) Ocean acidification affects redox-balance and ion-homeostasis in the life-cycle stages of *Emiliania huxleyi*. PLoS One 7(12):e52212. doi:10.1371/journal.pone.0052212
Rost B, Zondervan I, Riebesell U (2002) Light-dependent carbon isotope fractionation in the coccolithophorid *Emiliania huxleyi*. Limnol Oceanogr 47:120–128
Rost B, Riebesell U, Burkhardt S, Sültemeyer D (2003) Carbon acquisition of bloom-forming marine phytoplankton. Limnol Oceanogr 48:55–67
Rost B, Richter K-U, Riebesell U, Hansen PJ (2006a) Inorganic carbon acquisition in red tide dinoflagellates. Plant Cell Environ 29:810–822
Rost B, Riebesell U, Sültemeyer D (2006b) Carbon acquisition of marine phytoplankton: effect of photoperiod length. Limnol Oceanogr 51:12–20
Rost B, Kranz SA, Richter KU, Tortell PD (2007) Isotope disequilibrium and mass spectrometric studies of inorganic carbon acquisition by phytoplankton. Limnol Oceanogr Methods 5:328–337
Sikes CS, Roer RD, Wilbur KM (1980) Photosynthesis and coccolith formation: inorganic carbon sources and net inorganic reaction of deposition. Limnol Oceanogr 25:248–261
Stojkovic S, Beardall J, Matear R (2013) CO_2-concentrating mechanisms in three southern hemisphere strains of *Emiliania huxleyi*. J Phycol 49:670–679
Stoll MHC, Bakker K, Nobbe GH, Haese AR (2001) Continuous-flow analysis of dissolved inorganic carbon content in seawater. Anal Chem 73:4111–4116
Suffrian K, Schulz KG, Gutowska MA, Riebesell U, Bleich M (2011) Cellular pH measurements in *Emiliania huxleyi* reveal pronounced membrane proton permeability. New Phytol 190:595–608
Taylor AR, Chrachi A, Wheeler G, Goddard H, Brownlee C (2011) A voltage-gated H^+ channel underlying pH homeostasis in calcifying coccolithophores. PLoS Biol 9(6):14–16
Tortell PD, Morel FMM (2002) Sources of inorganic carbon for phytoplankton in the eastern Subtropical and Equatorial Pacific Ocean. Limnol Oceanogr 47:1012–1022
Tortell PD, Payne CD, Li Y, Trimborn S, Rost B, Smith WO, Riesselman C, Dunbar R, Sedwick P, DiTullio G (2008) The CO_2 response of Southern Ocean phytoplankton. Geophys Res Lett 35:L04605
Trimborn S, Langer G, Rost B (2007) Effect of varying calcium concentrations and light intensities on calcification and photosynthesis in *Emiliania huxleyi*. Limnol Oceanogr 52:2285–2293
Westbroek P, Brown CW, Van Bleijswijk J, Brownlee C, Brummer GJ, Conte M, Egge J, Fernandez E, Jordan R, Knappertsbusch M, Stefels J, Veldhuis M, Van Der Wal P, Young J (1993) A model system approach to biological climate forcing—the example of *Emiliania huxleyi*. Glob Planet Change 8:27–46
Wolf-Gladrow DA, Riebesell U, Burkhardt S, Bijma J (1999) Direct effects of CO_2 concentration on growth and isotopic composition of marine plankton. Tellus 51:461–476
Zeebe RE, Wolf-Gladrow DA (2007) CO_2 in seawater: equilibrium, kinetics, isotopes. Elsevier Science B.V, Amsterdam

Chapter 3
Publication II

Acidification, not carbonation, is the major driver of carbon fluxes in the coccolithophore *Emiliania huxleyi*

Dorothee M. Kottmeier, Sebastian D. Rokitta, Björn Rost

New Phytologist

New Phytologist

Research

Acidification, not carbonation, is the major regulator of carbon fluxes in the coccolithophore *Emiliania huxleyi*

Dorothee M. Kottmeier, Sebastian D. Rokitta and Björn Rost

Alfred Wegener Institute, Helmholtz Centre for Polar and Marine Research, Am Handelshafen 12, 27570 Bremerhaven, Germany

Author for correspondence:
Dorothee M. Kottmeier
Tel: +49 471 48311450
Email: Dorothee.Kottmeier@awi.de

Received: *13 October 2015*
Accepted: *6 January 2016*

New Phytologist (2016)
doi: 10.1111/nph.13885

Key words: calcification, CO_2-concentrating mechanism, life-cycle stages, membrane-inlet mass spectrometry, ocean acidification, pH, photosynthesis.

Summary

- A combined increase in seawater [CO_2] and [H^+] was recently shown to induce a shift from photosynthetic HCO_3^- to CO_2 uptake in *Emiliania huxleyi*. This shift occurred within minutes, whereas acclimation to ocean acidification (OA) did not affect the carbon source.
- To identify the driver of this shift, we exposed low- and high-light acclimated *E. huxleyi* to a matrix of two levels of dissolved inorganic carbon (1400, 2800 μmol kg^{-1}) and pH (8.15, 7.85) and directly measured cellular O_2, CO_2 and HCO_3^- fluxes under these conditions.
- Exposure to increased [CO_2] had little effect on the photosynthetic fluxes, whereas increased [H^+] led to a significant decline in HCO_3^- uptake. Low-light acclimated cells overcompensated for the inhibition of HCO_3^- uptake by increasing CO_2 uptake. High-light acclimated cells, relying on higher proportions of HCO_3^- uptake, could not increase CO_2 uptake and photosynthetic O_2 evolution consequently became carbon-limited.
- These regulations indicate that OA responses in photosynthesis are caused by [H^+] rather than by [CO_2]. The impaired HCO_3^- uptake also provides a mechanistic explanation for lowered calcification under OA. Moreover, it explains the OA-dependent decrease in photosynthesis observed in high-light grown phytoplankton.

Introduction

Coccolithophores are unicellular calcareous algae that take a dual role in global carbon cycling. During photosynthesis, carbon dioxide (CO_2) is fixed into organic matter, leading to a net decrease in dissolved inorganic carbon (DIC) and CO_2 from seawater. In the process of calcification, calcium carbonate ($CaCO_3$) is precipitated, which results in lowered DIC and alkalinity, thus elevated CO_2 levels. *Emiliania huxleyi* is the most abundant coccolithophore in the present-day ocean with a distribution from tropical to subpolar waters (Winter *et al.*, 2013). The species is able to form extensive blooms (Brown & Yoder, 1994; Sadeghi *et al.*, 2012), which are often associated with a shallow mixed-layer depth and high irradiances (Nanninga & Tyrrell, 1996; Raitsos *et al.*, 2006). As one of the most important pelagic calcifiers, *E. huxleyi* has been a major focus of oceanographic research over the last decades, in particular with respect to ocean acidification (OA; e.g. Rost & Riebesell, 2004; Raven & Crawfurd, 2012).

As the ocean takes up anthropogenic CO_2, levels of HCO_3^- and CO_2 increase, whereas pH and levels of CO_3^{2-} decrease (Wolf-Gladrow *et al.*, 1999). These changes in carbonate chemistry are often summarized as OA, but strictly speaking this phenomenon comprises carbonation (i.e. increased [CO_2] and [HCO_3^-]) as well as acidification (i.e. increased [H^+]/lowered pH). With a few exceptions, investigations of OA effects on *E. huxleyi* and other coccolithophores showed stimulated or unaffected production rates of particulate organic carbon (POC, i.e. biomass), with concomitantly impaired or unaffected production rates of particulate inorganic carbon (PIC, i.e. $CaCO_3$; see Raven & Crawfurd, 2012, for overview). Some of the observed diversity in the OA responses could be attributed to genetic variability; but more importantly environmental factors such as irradiance were shown to modulate OA effects (Nielsen, 1997; Zondervan *et al.*, 2002; van de Poll *et al.*, 2007; Feng *et al.*, 2008; Rokitta & Rost, 2012; Sett *et al.*, 2014; Xu & Gao, 2015). OA responses are typically measured after acclimation to altered conditions over several generations, allowing cells to adjust their metabolism. A study by Barcelos e Ramos *et al.* (2010) demonstrated that the OA-induced changes in cellular POC and PIC production are already evident after a few hours, indicating that OA effects are relatively immediate. In order to identify the drivers causing the OA responses in *E. huxleyi*, Bach and co-workers disentangled the effects of carbonation and acidification by acclimating cells to artificial carbonate chemistry conditions (Bach *et al.*, 2011, 2013). In these experiments, POC and PIC production were shown to be stimulated by carbonation, but inhibited by acidification.

In order to improve our understanding of *E. huxleyi*'s response to OA, it is important to assess which cellular processes are affected by carbonation, acidification or the combination of both. *Emiliania huxleyi* is known to use CO_2 and HCO_3^- as external inorganic carbon (C_i) sources of photosynthesis, but the estimated proportions of CO_2 uptake differ between studies and depend on the applied methods and assay conditions (e.g. Sikes

et al., 1980; Herfort *et al.*, 2002; Trimborn *et al.*, 2007; Kottmeier *et al.*, 2014). The increase in POC production after acclimation to OA is often attributed to the higher aqueous CO_2 levels, which are thought to directly increase the diffusive CO_2 supply at the CO_2-fixing enzyme Ribulose-1,5-bisphosphate-carboxylase/-oxygenase (RubisCO; Raven & Johnston, 1991; Rokitta & Rost, 2012; Stojkovic *et al.*, 2013). A recent study demonstrated that the fraction of photosynthetic CO_2 uptake relative to active HCO_3^- uptake is indeed strongly increased under high $[CO_2]$/low pH (Kottmeier *et al.*, 2014). This switch in the C_i source occurred at short timescales of seconds to minutes, whereas the acclimation to OA did not significantly affect the C_i source. Thus, the beneficial OA effect seems to be directly caused by the changing carbonate chemistry rather than by changes in the expression of genes related to the CO_2-concentrating mechanism (CCM). The inhibitory effect of OA on PIC production is often attributed to changes in electrochemical gradients under high $[H^+]$ and the associated costs of H^+ removal (Anning *et al.*, 1996; Berry *et al.*, 2002; Suffrian *et al.*, 2011; Taylor *et al.*, 2011). Tracer studies found HCO_3^- to be the major external C_i source for calcification (Paasche, 1964; Sikes *et al.*, 1980; Buitenhuis *et al.*, 1999; Herfort *et al.*, 2002; Rost *et al.*, 2002), and it was suggested that increased H^+ levels also affect HCO_3^- uptake mechanisms (Fukuda *et al.*, 2014). Despite the gained knowledge on cellular processes, relatively little is known about the differential effects of carbonation and acidification on photosynthesis, calcification and their underlying C_i supply.

In order to investigate the drivers causing the immediate shifts in the photosynthetic C_i source under high $[CO_2]$/low pH (Kottmeier *et al.*, 2014), here we measured the photosynthetic oxygen (O_2) and C_i fluxes in direct response to carbonation, acidification and the combination of both. To this end, we acclimated both life-cycle stages of *E. huxleyi* to present-day carbonate chemistry and exposed them to a matrix of two DIC levels (1400 and 2800 µmol kg^{-1}) and two pH values (8.15 and 7.85), yielding three different CO_2 concentrations (~10, 20 and 40 µmol kg^{-1}; Fig. 1). To further address the effect of energization, cells were acclimated to low and high photon flux densities (PFD; 50 and 400 µmol photons m^{-2} s^{-1}), and fluxes were measured at two different PFD (180 and 700 µmol photons m^{-2} s^{-1}).

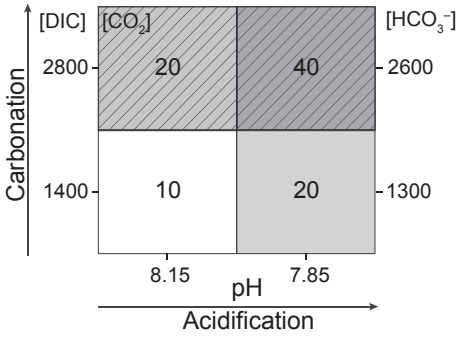

Fig. 1 Decoupled carbonate chemistry during mass spectrometric measurements of cellular O_2 and external inorganic carbon (C_i) fluxes in *Emiliania huxleyi*. Applied conditions were: low dissolved inorganic carbon (DIC)/high pH ($L_{DIC}H_{pH}$; white); high DIC/high pH ($H_{DIC}H_{pH}$; dashed, light grey); low DIC/low pH ($L_{DIC}L_{pH}$; light grey); high DIC/low pH ($H_{DIC}L_{pH}$; dashed, dark grey). All concentrations are given in µmol kg^{-1}.

Materials and Methods

Culture conditions

The calcifying diplont (diploid life-cycle stage) *Emiliania huxleyi* (Lohmann) Hay and Mohler, strain RCC 1216, and its noncalcifying haplont, RCC 1217, were acclimated to low and high light levels (LL, 50 ± 30 µmol photons s^{-1} m^{-2}; HL, 400 ± 30 µmol photons s^{-1} m^{-2}) under present-day carbonate chemistry and a 16 h : 8 h, light : dark-cycle. Light was provided by daylight lamps (FQ 54W/965HO; OSRAM, Munich, Germany) and adjusted by measuring photon flux densities (PFD) inside water-containing culturing bottles with a Walz Universal Light meter (ULM 500; Walz, Effeltrich, Germany) using a 4π-sensor (US-SQS/L).

Cells were grown as dilute-batch cultures in sterile-filtered North Sea seawater (0.2 µm, Sartobran 300; Sartorius AG, Gottingen, Germany) enriched with phosphate and nitrate (~7 and ~100 µmol kg^{-1}, respectively) as well as vitamins and trace metals according to F/2 (Guillard and Ryther, 1962). Culturing was performed in sterilized, gas-tight 2-l borosilicate bottles (Duran Group, Mainz, Germany), which were placed on roller tables to enable an homogenous cell suspension. Growth temperature was 15 ±1°C and was monitored by an Almemo 28–90 data logger (Ahlborn, Holzkirchen, Germany).

In all treatments, acclimations were performed under a CO_2 partial pressure (pCO_2) of 380 µatm (38.5 Pa), representing near-present-day conditions. The pCO_2 was adjusted by pre-aerating culture media with humidified, 0.2-µm-filtered air (Midisart 2000, PTFE; Sartorius AG), containing the desired pCO_2. The gas mixture was created by a gas flow controller (CGM 2000; MCZ Umwelttechnik, Bad Nauheim, Germany) using pure CO_2 (Air Liquide, Dusseldorf, Germany) and CO_2-free air (Air purification system; Parker, Kaarst, Germany). During the acclimation, head space inside the culture bottles was minimized to avoid outgassing effects. Carbonate chemistry was monitored based on total alkalinity (TA) measurements by potentiometric titration (Dickson, 1981; TitroLine alpha plus, measurement reproducibility ± 7 µmol kg^{-1}; Schott Instruments, Mainz, Germany) and colorimetric DIC measurements with a QuAAtro autoanalyzer (measurement reproducibility ± 5 µmol kg^{-1}; Seal Analytical, Norderstedt, Germany) in sterile-filtered samples with the method of Stoll *et al.* (2001). Calculations of the carbonate system (CO2sys; Pierrot *et al.*, 2006) were based on TA and DIC (Supporting Information Table S1). To monitor potential drifts of the carbonate chemistry on a daily basis, potentiometric measurements of pH_{NBS} were performed with a Metrohm pH meter (826 pH mobile; Metrohm, Filderstadt, Germany) with an electrode containing an integrated temperature sensor (Aquatrode Plus with Pt 1000, measurement reproducibility ± 0.01 pH units).

Cell growth was monitored by daily cell counting with a Coulter Counter (Beckman-Coulter, Fullerton, CA, USA) and specific

growth constants μ (d^{-1}) were determined as $\mu = (\log_e c_1 - \log_e c_0)\ \Delta t^{-1}$ (c_1 and c_0, cell concentrations (cells ml^{-1}); Δt, time interval (d)). In both life-cycle stages, μ was more or less equal and significantly reduced in the low-light acclimations (~0.7 d^{-1}), confirming a light limitation in this treatment (Table S1). In the high-light treatment, μ (~1.1 d^{-1}) was at the upper range of previously reported growth constants for the same strain (Langer *et al.*, 2009; Rokitta & Rost, 2012).

Mass spectrometric flux measurements

Photosynthetic and respiratory O_2 and C_i fluxes were measured with a mass spectrometer (Isoprime, GV Instruments, Manchester, UK) that was coupled to a cuvette via a gas-permeable PTFE membrane (0.01 mm). This membrane-inlet mass spectrometry (MIMS) technique uses the chemical disequilibrium between CO_2 and HCO_3^- during steady-state photosynthesis to distinguish CO_2 and HCO_3^- uptake across the plasmalemma. Estimates of these fluxes were made following the equations of Badger *et al.* (1994). To include the process of calcification, we followed modifications introduced by Schulz *et al.* (2007).

The MIMS signals were calibrated for [CO_2] by known additions of $NaHCO_3$ into phosphoric acid (0.2 N), ensuring that all added DIC was quantitatively converted to CO_2. Baseline values were obtained by adding sodium hydroxide (0.25 mmol l^{-1}) into DIC-free media, ensuring that any residual DIC was converted CO_3^{2-}. Calibration for [O_2] was obtained by equilibrating medium with air (21% O_2), followed by the addition of sufficient amounts of sodium dithionite (Merck) to quantitatively scavenge O_2 (0% O_2). MIMS signals were translated into [O_2] by applying the O_2 solubility constants of seawater (Weiss, 1970). All O_2 signals were furthermore corrected for the machine-inherent consumption.

Experiments were performed with cells in their exponential growth phase with maximal cell concentrations of 5×10^4 cells ml^{-1} within 6–10 h after the start of the light period. Before the measurements, cells were concentrated to 4–10 $\times 10^6$ cells ml^{-1} at acclimation temperature by gentle vacuum filtration over polycarbonate filters (Isopore TSTP, 3 μm or RTTP, 1.2 μm; Isopore membranes, Merck, Darmstadt, Germany). In this process, the medium was successively exchanged with pH-buffered DIC-free culture medium (50 mM N,N-bis(2-hydroxyethyl)-glycine, BICINE; pH_{NBS} of 7.85 or 8.15), and 8 ml were placed into an temperature-controlled MIMS cuvette in the dark. Subsequently, 25 μmol kg^{-1} membrane-impermeable dextrane-bound sulfonamide (DBS; Synthelec, Lund, Sweden) was added, inhibiting any external carbonic anhydrase. Samples were continuously stirred to keep the cell suspension homogeneously mixed. To disentangle carbonate chemistry in the cuvette, inorganic carbon was added as ~1400 or ~2800 μmol kg^{-1} $NaHCO_3$ to the DIC-free medium, buffered at a pH of 8.15 or 7.85, yielding four different carbonate chemistry conditions (Fig. 1; Table 1): 'Low DIC/High pH' ($L_{DIC}H_{pH}$), 'High DIC/High pH' ($H_{DIC}H_{pH}$), 'Low DIC/Low pH '($L_{DIC}L_{pH}$) and 'High DIC/Low pH' ($H_{DIC}L_{pH}$). For each carbonate chemistry condition, photosynthetic and respiratory O_2 and C_i fluxes were measured in consecutive light-dark intervals (6 min per step), at two different light levels (180 and 700 μmol photons m^{-2} s^{-1}).

Calculations of oxygen and carbon fluxes

Oxygen fluxes Net photosynthesis (Phot, μmol kg^{-1} min^{-1}) and respiration (Resp, μmol kg^{-1} min^{-1}) were deduced from steady-state O_2 fluxes in the light and dark, respectively (Badger *et al.*, 1994):

$$\text{Phot} = \frac{dO_2}{dt}_{\text{light}} \qquad \text{Eqn 1}$$

$$\text{Resp} = -\frac{dO_2}{dt}_{\text{dark}} \qquad \text{Eqn 2}$$

Carbonate chemistry before light (BL) For the calculation of the C_i fluxes, carbonate chemistry before and after the light phase

Table 1 Carbonate chemistry during mass measurements of O_2 and inorganic carbon (C_i) fluxes in *Emiliania huxleyi*

Acclimation	Carbonate chemistry	$L_{DIC}H_{pH}$	$H_{DIC}H_{pH}$	$L_{DIC}L_{pH}$	$H_{DIC}L_{pH}$
2N LL	[CO_2]	12.4 ± 0.6	22.0 ± 0.8	24.0 ± 1.5	43.7 ± 1.8
	[HCO_3^-]	1370 ± 70	2500 ± 90	1420 ± 80	2590 ± 110
	[H^+]	9.5 ± 0.2	9.5 ± 0.2	18.4 ± 0.3	18.4 ± 0.3
2N HL	[CO_2]	13.6 ± 0.9	22.7 ± 1.0	nd	47.4 ± 2.0
	[HCO_3^-]	1560 ± 110	2730 ± 130	nd	2730 ± 110
	[H^+]	9.1 ± 0.3	8.9 ± 0.3	nd	18.8 ± 0.3
1N LL	[CO_2]	10.6 ± 0.5	20.5 ± 0.3	17.1 ± 0.5	40.9 ± 2.8
	[HCO_3^-]	1200 ± 50	2400 ± 30	1050 ± 30	2460 ± 160
	[H^+]	9.2 ± 0.1	9.2 ± 0.1	17.4 ± 0.5	18.1 ± 0.0
1N HL	[CO_2]	10.5 ± 0.6	18.6 ± 1.4	17.9 ± 1.8	32.5 ± 2.5
	[HCO_3^-]	1150 ± 70	2160 ± 130	1090 ± 120	1940 ± 200
	[H^+]	9.3 ± 0.1	9.2 ± 0.1	17.5 ± 0.4	18.1 ± 0.5

Concentrations of CO_2 (μmol kg^{-1}), HCO_3^- (μmol kg^{-1}) and H^+ (nmol kg^{-1}) were assessed by means of mass spectrometry ($n = 3$; ± SD).
2N LL/HL, diploid life-cycle stage acclimated to low/high light; 1N LL/HL, haploid life-cycle stage acclimated to low/high light; $L_{DIC}H_{pH}$, low dissolved inorganic carbon (DIC)/high pH; $H_{DIC}H_{pH}$, high DIC/high pH; $L_{DIC}L_{pH}$, low DIC/low pH; $H_{DIC}L_{pH}$, high DIC/low pH; nd, not determined.

was determined. $[CO_2]_{BL}$ (μmol kg^{-1}) could be directly taken from measured signals, whereas $[HCO_3^-]_{BL}$ (μmol kg^{-1}) was calculated according to Badger *et al.* (1994):

$$[HCO_3^-]_{BL} = \frac{\frac{dCO_2}{dt}_{BL} + k_+[CO_2]_{BL} - Resp/RQ}{k_-} \quad \text{Eqn 3}$$

(dCO_2/dt_{BL}, steady-state CO_2 evolution in the dark (μmol kg^{-1} min^{-1}); k_+ and k_-, effective rate constants for the conversion of CO_2 to HCO_3^- (min^{-1}) and vice versa; RQ, respiratory quotient of 1 (Burkhardt *et al.*, 2001; Rost *et al.*, 2007)). Following Schulz *et al.* (2007), we applied the calculated effective rate constants derived from the measured pH, temperature and salinity in our assays:

$$k_- = k_{-1}[H^+] + k_{-4} \quad \text{Eqn 4}$$

$$k_+ = k_{+1} + k_{+4}[OH^-] \quad \text{Eqn 5}$$

($[H^+]$ and $[OH^-]$, concentrations of hydrogen and hydroxide ions, respectively (mol kg^{-1}); k_{-1}, k_{+1}, k_{-4} and k_{+4}, rate constants (Zeebe & Wolf-Gladrow, 2001)). To assess $[H^+]$, known [DIC] (μmol kg^{-1}) was added to cell-free medium. From the resulting increase in $[CO_2]$ (μmol kg^{-1}), the ratio of [DIC] : $[CO_2]$ and thus $[H^+]$ could be derived (Zeebe & Wolf-Gladrow, 2001):

$$[H^+] = \frac{-K_1^*[CO_2] - \sqrt{(K_1^*[CO_2])^2 - 4(([CO_2])^2[DIC]K_1^*K_2^*)}}{2([CO_2] - [DIC])} \quad \text{Eqn 6}$$

(K_1^* and K_2^*, stoichiometric equilibrium constants (Roy *et al.*, 1993)). $[DIC]_{BL}$ was derived as the sum of the C_i species, where carbonate ions ($[CO_3^{2-}]_{BL}$) can be assumed to be in equilibrium with $[HCO_3^-]_{BL}$ (Schulz *et al.*, 2006):

$$[DIC]_{BL} = [CO_2]_{BL} + (1 + r)[HCO_3^-]_{BL} \quad \text{Eqn 7}$$

The constant r hereby represents the pH-dependent ratio between $[HCO_3^-]$ and $[CO_3^{2-}]$ (Zeebe & Wolf-Gladrow, 2001; Schulz *et al.*, 2007), which is defined as:

$$r = \frac{[CO_3^{2-}]}{[HCO_3^-]} = \frac{K_2^*}{[H^+]} \quad \text{Eqn 8}$$

Carbonate chemistry at the end of light (EL) $[CO_2]_{EL}$ (μmol kg^{-1}) was directly obtained from measurements, whereas $[HCO_3^-]_{EL}$ (μmol kg^{-1}) was derived following Schulz *et al.* (2007):

$$[HCO_3^-]_{EL} = ([DIC]_{BL} - [DIC]_{consumed} - [CO_2]_{EL})/(1 + r) \quad \text{Eqn 9}$$

$[DIC]_{consumed}$ represents the concentration of DIC that was consumed in the course of the light interval and was defined as the sum of DIC used for photosynthesis ($[O_2]_{evolved}$/PQ, μmol kg^{-1}) and for calcification ($[DIC]_{CaCO3}$, μmol kg^{-1}):

$$[DIC]_{consumed} = \frac{[O_2]_{evolved}}{PQ} + [DIC]_{CaCO_3} \quad \text{Eqn 10}$$

$[O_2]_{evolved}$ hereby represents the concentration of O_2 that evolved over the course of the light phase and PQ is the photosynthetic quotient of 1.1 (Burkhardt *et al.*, 2001; Rost *et al.*, 2007). $[DIC]_{CaCO3}$ was constrained by the measured ratio of particulate inorganic to organic carbon (PIC : POC) of the calcifying diploid life-cycle stage under similar light treatments (1.4 at low-light and 0.8 at high-light acclimations; Rokitta & Rost, 2012) and was assumed to scale linearly with $[O_2]_{evolved}$ (e.g. Paasche, 1999). Additionally, calcite production was normalized to the photoperiod (Schulz *et al.*, 2007):

$$[DIC]_{CaCO_3} = \frac{[O_2]\ evolved}{PQ} \times \frac{16\ Phot - 8\ Resp}{16\ Phot} \times \frac{PIC}{POC} \quad \text{Eqn 11}$$

In the noncalcifying haploid stage, PIC : POC was set to zero. Sensitivity analyses in which the PIC : POC were allowed to vary within typical uncertainties, revealed negligible effects on the calculated carbonate chemistry and photosynthetic fluxes.

Carbon fluxes Knowing the carbonate chemistry, total net CO_2 uptake (CO_2up_{total}, μmol kg^{-1} min^{-1}) was inferred directly from the steady-state CO_2 drawdown in the light following Badger *et al.* (1994):

$$CO_2up_{total} = -\frac{dCO_2}{dt}_{EL} - k_+[CO_2]_{EL} + k_-[HCO_3^-]_{EL} \quad \text{Eqn 12}$$

Total CO_2 uptake can be divided into one part used for photosynthesis (CO_2up_{PS}, μmol kg^{-1} min^{-1}) and another part used for calcification (CO_2up_{CaCO3}, μmol kg^{-1} min^{-1}). As HCO_3^- is the major external C_i source for calcification, we assumed that only 20% of calcification is supplied by external CO_2 (Sikes *et al.*, 1980; Paasche, 2001; Rost *et al.*, 2002). Overall calcification was constrained by photoperiod-normalized PIC : POC ratios and was assumed to scale linearly with the photosynthetic oxygen evolution:

$$CO_2up_{CaCO_3} = 0.2 \times \frac{Phot}{PQ} \times \frac{PIC}{POC} \times \frac{16\ Phot - 8\ Resp}{16\ Phot} \quad \text{Eqn 13}$$

Please note that, similar to PIC : POC ratios, errors in the assumption of the CO_2 usage for calcification can affect the estimated photosynthetic fluxes by relative constant and small offsets, but do not change the overall observed regulation patterns in response to carbonate chemistry. Accounting for the CO_2 uptake for calcification, CO_2up_{PS} could be calculated as:

$$CO_2up_{PS} = CO_2up_{total} - CO_2up_{CaCO_3} \quad \text{Eqn 14}$$

Photosynthetic HCO_3^- uptake (HCO_3^-up, μmol kg^{-1} min^{-1}) was estimated as the difference between photosynthetic net C_i fixation (calculated as Phot PQ^{-1}) and net CO_2 uptake for photosynthesis:

$$HCO_3^-up = \frac{Phot}{PQ} - CO_2up_{PS} \quad \text{Eqn 15}$$

Knowing the photosynthetic net CO_2 uptake, its fraction of the overall net photosynthetic C_i uptake (f_{CO_2}; cf. Kottmeier *et al.*, 2014) was derived as:

$$f_{CO_2} = CO_2up_{PS} / \left(\frac{Phot}{PQ}\right) \quad \text{Eqn 16}$$

Rate normalization All rates were normalized to the amount of chlorophyll *a* (Chl*a*) in the concentrated samples. Known amounts of cell suspension were filtered onto cellulose nitrate filters (0.45 μm; Sartorius, Gottingen, Germany) that were instantly frozen in liquid nitrogen. After extraction in 90% acetone, Chl*a* content was determined fluorimetrically (TD-700 fluorometer; Turner Designs, Sunnyvale, CA, USA) following the protocol of Knap *et al.* (1996).

Statistics

All experiments were carried out in biological triplicates. Fluxes estimated for the different carbonate chemistry conditions and at the same incoming PFD were tested pairwise for significant differences applying two-sided *t*-tests. Effects were called significant when *P*-values were ≤ 0.05. In the figures, such significant differences were indicated by different lower-case characters (e.g. a and b). Values denoted by two letters (e.g. ab) represent data that are not significantly different from a or b.

Results

In the following, we describe treatment-specific differences in short-term responses to altered carbonate chemistry and light. For clarity, only the fluxes of the diplont are shown in Figs 2, 3. Fluxes of the haplont are given in Table 2.

Oxygen fluxes

In both life-cycle stages and light acclimations, net photosynthesis increased under increasing incoming light (Fig. 2a,b; PFD 180 vs 700), whereas dark respiration was generally independent of the light levels applied before the dark phase (Fig. 2c,d). The dependency on carbonate chemistry was stage and acclimation-light specific (Fig. 2a–d; Table 2).

In the diplont acclimated to low light (2N LL), net photosynthesis was significantly stimulated under combined carbonation and acidification ($H_{DIC}L_{pH}$; Fig. 2a). This increase could not be attributed exclusively to carbonation or acidification, but appeared to be a product of both. Respiration in 2N LL decreased under $H_{DIC}L_{pH}$ (significantly only at PFD 180). This effect seemed to be driven by acidification, because the rates decreased significantly under both low-pH conditions, but not with carbonation (Fig. 2c).

In the diplont acclimated to high light (2N HL), net photosynthesis was significantly impaired under $H_{DIC}L_{pH}$ (Fig. 2b).

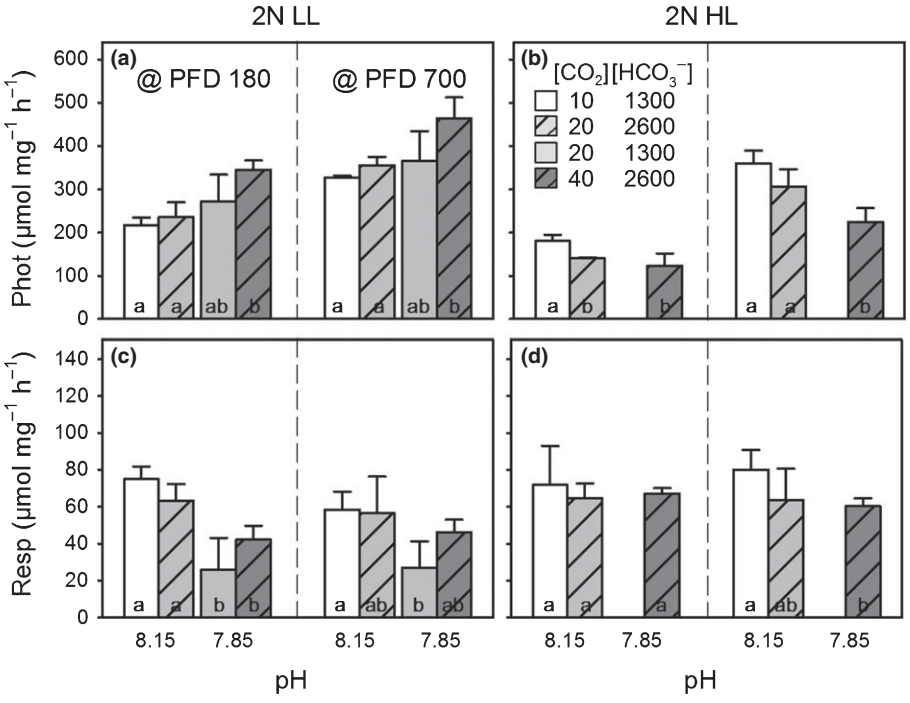

Fig. 2 Short-term modulations in photosynthetic and respiratory O_2 fluxes of *Emiliania huxleyi* in response to low dissolved inorganic carbon (DIC)/high pH ($L_{DIC}H_{pH}$; white bars), as well as carbonation ($H_{DIC}H_{pH}$; dashed, light grey bars), acidification ($L_{DIC}L_{pH}$; light grey bars) and the combination of both ($H_{DIC}L_{pH}$; dashed, dark grey bars): Chl*a*-normalized photosynthetic net O_2 evolution (Phot; a, b) and respiration (Resp; c, d) were measured at low and high photon flux densities (PFD; 180 and 700 μmol photons m^{-2} s^{-1}). Data are shown for the diploid life-cycle stage acclimated to low and high light (2N LL, 2N HL). Note: in 2N HL, no data for the $L_{DIC}L_{pH}$ condition were obtained. Error bar indicate mean ± SD ($n = 3$). Different lower-case characters indicate significant differences between the fluxes obtained at different carbonate chemistry conditions and same PFD.

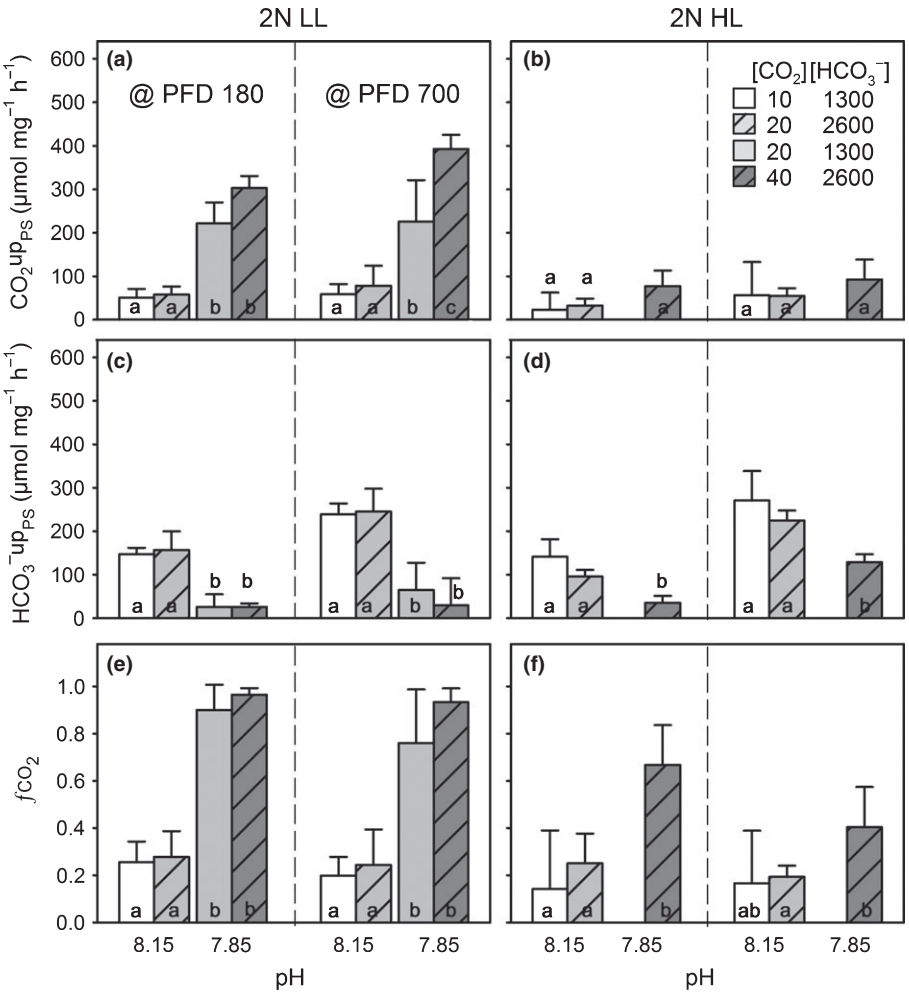

Fig. 3 Short-term modulations in external inorganic carbon (C_i) fluxes of *Emiliania huxleyi* in response to low dissolved inorganic carbon (DIC)/high pH ($L_{DIC}H_{pH}$; white bars), as well as carbonation ($H_{DIC}H_{pH}$; dashed, light grey bars), acidification ($L_{DIC}L_{pH}$; light grey bars) and the combination of both ($H_{DIC}L_{pH}$; dashed, dark grey bars): Chl*a*-normalized photosynthetic net CO_2 uptake (CO_2upt_{PS}; a, b), photosynthetic HCO_3^- uptake ($HCO_3^-upt_{PS}$; c, d) and the fraction of overall photosynthetic net C_i uptake that is covered by net CO_2 uptake (f_{CO_2}; e, f) were measured at low and high photon flux densities (PFD; 180 and 700 µmol photons m^{-2} s^{-1}). Data are shown for the diploid life-cycle stage acclimated to low and high light (2N LL, 2N HL). Note: in 2N HL, no data for the $L_{DIC}L_{pH}$ condition were obtained. Error bar indicate mean ± SD ($n = 3$). Different lower-case characters indicate significant differences between the fluxes obtained at different carbonate chemistry conditions and same PFD.

Also this effect seemed to be caused by carbonation and acidification together, although the drivers could not be identified statistically due to the lack of the $L_{DIC}L_{pH}$ data (Fig. 1; Tables 1, 2). Respiration in 2N HL was largely unaffected by carbonate chemistry (Fig. 2d).

In contrast to the diplont, photosynthesis and respiration in the low- and high-light acclimated haplont (1N LL, 1N HL) were insensitive to the applied carbonate chemistry (Table 2).

Carbon fluxes

In both life-cycle stages and light acclimations, the higher C_i demands imposed by the higher incoming light levels during measurements were in most cases covered by additional HCO_3^- uptake, whereas photosynthetic net CO_2 uptake was largely unaffected by the incoming light (Fig. 3a–d; Table 2; PFD 180 vs PFD 700). The dependency of C_i fluxes on carbonate chemistry was clearly stage and acclimation-light specific (Fig. 3; Table 2).

In 2N LL, the photosynthetic net CO_2 uptake increased significantly under $H_{DIC}L_{pH}$ at both applied light levels, and these higher fluxes seemed to be driven mainly by acidification because CO_2 uptake was strongly increased under both low-pH conditions (Fig. 3a). Carbonation at high pH did not stimulate the CO_2 uptake, whereas carbonation at low pH (LDICLpH vs HDICLpH) additionally increased CO_2 uptake. HCO_3^- uptake in 2N LL decreased significantly under $H_{DIC}L_{pH}$ (Fig. 3c). This decrease was clearly driven by acidification because HCO_3^- uptake was decreased under both low-pH conditions, independent of carbonation. The described opposing short-term regulation of CO_2 and HCO_3^- uptake under $H_{DIC}L_{pH}$ caused significant shifts in f_{CO_2} from ~0.3 to ~0.9 (Fig. 3e).

In 2N HL, photosynthetic net CO_2 uptake was relatively unaffected by carbonate chemistry (Fig. 3b). Similar to the low-light acclimated cells, HCO_3^- uptake for photosynthesis in 2N HL decreased significantly under $H_{DIC}L_{pH}$, presumably also driven by acidification (Fig. 3d). As a consequence of the relatively constant net CO_2 uptake and the decreased HCO_3^- uptake, f_{CO_2} increased significantly from ~0.2 to ~0.7 at a PFD of 180, whereas the increase was insignificant at 700 µmol photons m^{-2} s^{-1} (Fig. 3f).

In 1N LL, photosynthetic net CO_2 uptake was close to zero and the photosynthetic HCO_3^- uptake clearly dominated the C_i fluxes (Table 2). Both CO_2 and HCO_3^- fluxes were unaffected by carbonate chemistry, resulting in constant and low f_{CO_2} values (~0.1 on average; Table 2). In 1N HL, photosynthetic net CO_2 uptake was negative, reflecting a net CO_2 efflux alongside a high HCO_3^- uptake (Table 2). Also here, CO_2 and HCO_3^- fluxes

Table 2 Short-term modulations in photosynthetic O_2 and inorganic carbon (C_i) fluxes of *Emiliania huxleyi* in response to low dissolved inorganic carbon (DIC) and high pH ($L_{DIC}H_{pH}$), as well as carbonation ($H_{DIC}H_{pH}$), acidification ($L_{DIC}L_{pH}$) and the combination ($H_{DIC}L_{pH}$)

Acclimation	PFD	Carbonate chemistry	Phot (μmol mg^{-1} h^{-1})	Resp (μmol mg^{-1} h^{-1})	CO_2upt_{PS} (μmol mg^{-1} h^{-1})	$HCO_3^-upt_{PS}$ (μmol mg^{-1} h^{-1})	f_{CO_2}
2N LL	180	$L_{DIC}H_{pH}$	217 ± 17	75 ± 7	51 ± 20	147 ± 15	0.26 ± 0.09
		$H_{DIC}H_{pH}$	236 ± 34	63 ± 9	58 ± 19	156 ± 43	0.28 ± 0.11
		$L_{DIC}L_{pH}$	271 ± 63	26 ± 17	221 ± 49	25 ± 29	0.90 ± 0.11
		$H_{DIC}L_{pH}$	345 ± 22	42 ± 8	303 ± 28	11 ± 9	0.96 ± 0.03
	700	$L_{DIC}H_{pH}$	327 ± 5	59 ± 10	59 ± 1	239 ± 1	0.20 ± 0.08
		$H_{DIC}H_{pH}$	355 ± 19	57 ± 20	78 ± 1	245 ± 1	0.24 ± 0.15
		$L_{DIC}L_{pH}$	365 ± 69	27 ± 14	226 ± 1	64 ± 1	0.76 ± 0.23
		$H_{DIC}L_{pH}$	464 ± 48	46 ± 7	393 ± 1	29 ± 1	0.93 ± 0.06
2N HL	180	$L_{DIC}H_{pH}$	181 ± 14	72 ± 21	23 ± 39	141 ± 40	0.14 ± 0.25
		$H_{DIC}H_{pH}$	141 ± 2	65 ± 8	32 ± 17	96 ± 15	0.25 ± 0.13
		$L_{DIC}L_{pH}$	nd	nd	nd	nd	nd
		$H_{DIC}L_{pH}$	124 ± 28	67 ± 3	77 ± 36	35 ± 16	0.67 ± 0.17
	700	$L_{DIC}H_{pH}$	360 ± 30	80 ± 11	56 ± 77	271 ± 68	0.17 ± 0.22
		$H_{DIC}H_{pH}$	307 ± 40	64 ± 17	55 ± 18	224 ± 23	0.19 ± 0.05
		$L_{DIC}L_{pH}$	nd	nd	nd	nd	nd
		$H_{DIC}L_{pH}$	225 ± 32	60 ± 4	93 ± 46	129 ± 18	0.40 ± 0.17
1N LL	180	$L_{DIC}H_{pH}$	147 ± 22	38 ± 8	1 ± 8	131 ± 14	0.00 ± 0.06
		$H_{DIC}H_{pH}$	173 ± 69	29 ± 7	28 ± 26	129 ± 39	0.15 ± 0.10
		$L_{DIC}L_{pH}$	202 ± 29	56 ± 12	58 ± 16	126 ± 19	0.31 ± 0.07
		$H_{DIC}L_{pH}$	185 ± 79	29 ± 3	55 ± 83	113 ± 17	0.24 ± 0.33
	700	$L_{DIC}H_{pH}$	223 ± 32	35 ± 4	−6 ± 8	207 ± 23	−0.03 ± 0.04
		$H_{DIC}H_{pH}$	240 ± 56	29 ± 5	7 ± 21	210 ± 41	0.02 ± 0.09
		$L_{DIC}L_{pH}$	286 ± 23	48 ± 11	26 ± 17	225 ± 25	0.11 ± 0.07
		$H_{DIC}L_{pH}$	273 ± 23	32 ± 4	38 ± 52	210 ± 37	0.14 ± 0.19
1N HL	180	$L_{DIC}H_{pH}$	119 ± 13	69 ± 4	−33 ± 7	141 ± 11	−0.31 ± 0.09
		$H_{DIC}H_{pH}$	113 ± 36	54 ± 8	−12 ± 26	114 ± 6	−0.18 ± 0.30
		$L_{DIC}L_{pH}$	136 ± 19	67 ± 19	0 ± 17	124 ± 24	0.00 ± 0.14
		$H_{DIC}L_{pH}$	148 ± 34	79 ± 20	−20 ± 17	154 ± 44	−0.14 ± 0.10
	700	$L_{DIC}H_{pH}$	246 ± 13	68 ± 8	−38 ± 10	261 ± 6	−0.17 ± 0.05
		$H_{DIC}H_{pH}$	196 ± 33	55 ± 9	−29 ± 24	207 ± 24	−0.18 ± 0.15
		$L_{DIC}L_{pH}$	236 ± 25	56 ± 8	−5 ± 8	208 ± 33	−0.02 ± 0.03
		$H_{DIC}L_{pH}$	274 ± 68	75 ± 9	−23 ± 2	272 ± 60	−0.10 ± 0.03

Chl*a*- normalized photosynthetic net O_2 evolution (Phot) and respiration (Resp), photosynthetic net CO_2 uptake (CO_2upt_{PS}), photosynthetic HCO_3^- uptake ($HCO_3^-upt_{PS}$) and the fraction of overall photosynthetic net C_i uptake that is covered by net CO_2 uptake (f_{CO_2}) were measured at low and high photon flux densities (PFD; 180 vs 700 μmol photons m^{-2} s^{-1}; $n = 3$; ± SD).
2N LL/HL, diploid life-cycle stage acclimated to low light/high light; 1N LL/HL, haploid life-cycle stage acclimated to low/high light; $L_{DIC}H_{pH}$, low DIC/high pH; $H_{DIC}H_{pH}$, high DIC/high pH; $L_{DIC}L_{pH}$, low DIC/low pH; $H_{DIC}L_{pH}$, high DIC/low pH; nd, not determined.

were unaffected by carbonate chemistry, resulting in constant and negative f_{CO_2} values (~−0.1).

Discussion

In this study, we investigated *Emiliana huxleyi's* photosynthetic O_2 and C_i fluxes and their short-term modulations in response to changing carbonate chemistry and light. In the diploid life-cycle stage (diplont), cellular fluxes were shown to be highly sensitive and to rapidly respond to the applied conditions. In the haploid stage (haplont), cellular fluxes were rather constant, even across large changes in carbonate chemistry.

H^+-driven increase in CO_2 uptake stimulates photosynthesis in low-light acclimated diplonts

In the low-light acclimated diplont (2N LL), rates of photosynthetic O_2 evolution were in a similar range as measured earlier under comparable conditions (Nielsen, 1995; Rokitta & Rost, 2012). They stayed relatively constant under carbonation or acidification alone, but were strongly stimulated by combined carbonation and acidification (Fig. 2a). Ocean acidification (OA) has earlier been shown to affect cellular fluxes rapidly (Barcelos e Ramos *et al.*, 2010; Kottmeier *et al.*, 2014). An immediate stimulation in photosynthesis, if maintained over longer timescales, could therefore also explain the increase in particulate organic carbon (POC) production that is typically observed in OA-acclimated coccolithophores (Raven & Crawfurd, 2012). Even though the applied carbonate chemistry matrix generally allowed for the distinction between the effects of carbonation and acidification, their differential effects were not evident from the observed O_2 fluxes (Fig. 2a). Only by measuring the underlying C_i acquisition was it possible to identify the drivers behind the photosynthetic responses (Fig. 3a,c): Net CO_2 uptake was strongly promoted under acidification as well as under combined carbonation and acidification (Fig. 3a), whereas HCO_3^- uptake

was strongly downscaled under these conditions (Fig. 3c). As the stimulation in net CO_2 uptake under combined carbonation and acidification exceeded the impairing effect on HCO_3^- uptake, the overall photosynthetic C_i uptake and consequently photosynthetic O_2 evolution were increased under these conditions (Fig. 2a).

The transition from the active HCO_3^- to diffusive CO_2 uptake under short-term acidification is in line with Kottmeier *et al.* (2014), who observed that *E. huxleyi* increases the relative fraction of CO_2 usage when being exposed to high $[CO_2]$/low pH over short timescales. Here we show that this shift is caused by a combination of increased CO_2 uptake and decreased HCO_3^- uptake. The increased CO_2 usage is likely to decrease the energy demand of the cell, because transport of HCO_3^- is considered more costly due to the molecule's negative charge and the large hydration envelope, properties that require an active transport (Burkhardt *et al.*, 2001; Beardall & Raven, 2004; Holtz *et al.*, 2015b). Indeed, we found stimulated photosynthesis and decreased respiration rates under acidification despite the same incoming light (Fig. 2a,c), indicating not only a more efficient CO_2 supply at RubisCO, but also altered energy allocations under these conditions. Such energy reallocations under OA have earlier been attributed to shifts from reductive towards oxidative pathways (Rokitta *et al.*, 2012).

The H^+-driven stimulation in CO_2 uptake contradicts the 'fertilizing effect' of CO_2 that is typically ascribed to OA. Contrary to the common notion that CO_2 uptake for photosynthesis benefits from carbonation, it was here promoted mainly by acidification, at least over the short timescales applied. The higher CO_2 uptake under combined carbonation and acidification compared to acidification alone indicated that high H^+ levels generally increase the cellular CO_2 uptake capacity. Yet, the higher CO_2 availability was able to stimulate its uptake even further – carbonation and acidification acted synergistically. The H^+-driven decrease in cellular HCO_3^- uptake, which occurred independent of the applied dissolved inorganic carbon (DIC) levels, indicated that the HCO_3^- transport capacity is generally downscaled under acidification. Carbonation alone had no effect on HCO_3^- uptake, suggesting that the transporters are substrate-saturated at the applied $[HCO_3^-]$ (~1300 and 2600 μmol kg^{-1}). This is in line with a study by Rost *et al.* (2006) who measured the short-term DIC-dependency of photosynthesis at constant pH and showed that HCO_3^- uptake in *E. huxleyi* was substrate-saturated even below $[HCO_3^-]$ of ~500 μmol kg^{-1}.

The H^+-dependent regulations in C_i fluxes are likely to be similar after acclimation. Bach *et al.* (2011), for instance, acclimated *E. huxleyi* to carbonate chemistry conditions in which either CO_2 or pH varied independently. They could show that POC production increases with DIC if pH is buffered to ~8.0, but it decreases with increasing DIC if pH decreases concomitantly. This suggests that the negative H^+ effects on HCO_3^- uptake are retained after acclimation. However, in contrast to our study, where no short-term carbonation effects were measured, Bach and coworkers found stimulated POC and particulate inorganic carbon (PIC) production after acclimation to carbonation. Consequently, the cells were able to increase their C_i uptake when being exposed to these conditions over longer timescales, possibly by expressing more HCO_3^- transporters. In order to examine how acclimation affects the sensitivity towards changing carbonate chemistry, future studies should investigate which short-term effects manifest over longer timescales.

The strong H^+ effects on CO_2 and HCO_3^- uptake rates, observed in the current study, must originate from processes at the cell membrane or inside the cell, such as electrochemical gradients, enzyme activities and C_i speciation (Mackinder *et al.*, 2010; Suffrian *et al.*, 2011; Taylor *et al.*, 2011). The stimulated net CO_2 uptake under acidification could, for example, be explained by pH-dependent differences in membrane morphology (Leung *et al.*, 2012), which may also affect the CO_2 permeability. It could also be caused by pH-dependent regulations of intracellular fluxes, for instance due to different enzyme activities, which may lead to a stronger inward CO_2 gradient. The decreased HCO_3^- uptake under acidification is apparently caused by a direct H^+-driven inhibition of HCO_3^- transporters at the plasmalemma or chloroplast membrane. The diplont *E. huxleyi* expresses AE1 and AE2-type Cl^-/HCO_3^- transporters of the Solute Carrier 4 (SLC4) family (Herfort *et al.*, 2002; von Dassow *et al.*, 2009; Mackinder *et al.*, 2011; Rokitta *et al.*, 2011; Bach *et al.*, 2013). This enzyme family is well investigated in the context of renal acid/base regulation in mammals, where the activity of the anion exchangers has indeed been shown to be modulated by pH (Alper, 2006).

H^+-driven decrease in HCO_3^- uptake causes carbon-limitation in high-light acclimated diplonts

In high-light acclimated diploid cells (2N HL), photosynthesis was inhibited under combined carbonation and acidification (Fig. 2b). This finding seems puzzling at first because in low-light acclimated cells (2N LL), the same carbonate chemistry had a pronounced beneficial effect on photosynthesis (Fig. 2a). However, light-dependent modulations in the sensitivity towards carbonate chemistry are well in line with other studies (e.g. Kranz *et al.*, 2010; Gao *et al.*, 2012; Rokitta & Rost, 2012; Jin *et al.*, 2013; Hoppe *et al.*, 2015). Rokitta & Rost (2012), for example, found that POC production in *E. huxleyi* is strongly stimulated when acclimated to OA and sub-saturating light, but is relatively unaffected by OA under high light intensities.

Based on our flux measurements, we are able to provide an explanation for such differential OA sensitivities: In contrast to the low-light acclimated cells, where CO_2 uptake was strongly stimulated when being exposed to acidified conditions, CO_2 uptake in the high-light acclimated cells remained unaffected (Fig. 3b). Similar to the low-light acclimated cells, HCO_3^- uptake in the high-light acclimated cells was impaired under acidification (Fig. 3d). As a result, the overall C_i uptake and consequently photosynthetic O_2 evolution were significantly decreased (Fig. 2b). The inability of high-light acclimated cells to increase CO_2 uptake may not only be the reason for the C_i shortage under short-term acidification, but also explains why photosynthesis is often not stimulated after acclimation to OA (Raven & Crawfurd, 2012). However, a detrimental H^+ effect on

photosynthesis in *E. huxleyi* has not yet been observed after acclimation, indicating that either the decrease in HCO_3^- uptake is less pronounced, or the increase CO_2 uptake is more pronounced when cells are exposed to acidified conditions over an extended period of time.

The reduced capability of high-light acclimated cells to increase CO_2 uptake under acidification may derive from adjustments of their CO_2-concentrating mechanism (CCM) to the higher acclimation irradiance. *Emiliana huxleyi* was shown to increase HCO_3^- uptake with increasing irradiance during flux measurements (Fig. 3d; 180 vs 700 PFD). This may indicate that high-light acclimated cells also used a higher fraction of HCO_3^- under the conditions, at which they were cultured (Rost *et al.*, 2006). Cells operating CCMs that are based predominantly on HCO_3^- uptake need to reduce the diffusive losses and therefore downregulate their CO_2 permeability, for example by altering chloroplast morphology (Sukenik *et al.*, 1987).

Recent studies on the combined effects of OA and light indicate that similar mechanisms, as here observed for *E. huxleyi*, also apply to other phytoplankton taxa. In diatoms, for example, growth was shown to increase significantly when cultured under OA and sub-saturating light, whereas these responses were reversed under high light (Gao *et al.*, 2012). Besides light intensity, light fluctuations also have been shown to significantly modulate OA effects (Jin *et al.*, 2013; Hoppe *et al.*, 2015). Hoppe and coworkers, for example, observed that photosynthesis stayed constant under OA and constant light, but decreased under OA and dynamic light. According to our data, OA may generally lower the HCO_3^- uptake capacity of phytoplankton. Although this is apparently not detrimental under low and stable light conditions, the impaired HCO_3^- uptake seems to have severe consequences under high and dynamic light conditions. Under the latter conditions, the phytoplankton cells are dependent primarily on HCO_3^- transport, because the *high* Ci demand under high light and the *varying* Ci demand under dynamic light cannot be covered or adjusted fast enough by diffusive CO_2 uptake. Owing to the impairment of HCO_3^- transporters, these cells are thus more prone to C_i shortage at RubisCO under OA, even though external substrate concentrations are slightly elevated. When RubisCO becomes C_i-limited, the Calvin Cycle is a weaker electron sink, which can cause energetic overloads and higher costs associated with dissipation of energy and repair mechanisms (van de Poll *et al.*, 2007; Gao *et al.*, 2012; Jin *et al.*, 2013; Hoppe *et al.*, 2015). Thus, the high H^+-driven decrease in cellular HCO_3^- uptake can explain why the energy transfer efficiency from photochemistry to biomass production is reduced under OA in combination with high or dynamic light conditions (Gao *et al.*, 2012; Hoppe *et al.*, 2015).

Haplonts are insensitive to carbonate chemistry

The comparison of the two life-cycle stages of *E. huxleyi* revealed that their modes of C_i acquisition strongly diverge. Photosynthetic and respiratory O_2 fluxes in the haploid stage did not respond to the short-term changes in carbonate chemistry (Table 2). Also CO_2 and HCO_3^- uptake were not affected by carbonation or acidification. This agrees with the results of acclimation studies that often found no or few changes in POC production and other cellular processes under OA (Rokitta & Rost, 2012; Kottmeier *et al.*, 2014). The fact that HCO_3^- uptake was unaffected by external H^+ levels implies that the HCO_3^- uptake mechanism of the haplont is different from the one of the diplont (Table 2). Indeed, there are transcriptomic datasets demonstrating that the two life-cycle stages express different isoforms of HCO_3^- transporters of the SLC4 family (von Dassow *et al.*, 2009; Mackinder *et al.*, 2011; Rokitta *et al.*, 2011). Also, the haplont was shown to express stage-specific subunits of a vacuolar H^+ ATPase and other stage-specific ion transporters, e.g. a Ca^{2+}/H^+ antiporters, which may further explain the differential sensitivity towards H^+ levels (von Dassow *et al.*, 2009; Rokitta *et al.*, 2011, 2012).

The consistently high HCO_3^- usage of the haplont was not in line with the results of a ^{14}C disequilibrium method, which estimated generally higher CO_2 contributions and a strong dependency on $[CO_2]$/pH (Kottmeier *et al.*, 2014). This discrepancy may be attributed to the different key assumptions of the MIMS and/or the ^{14}C disequilibrium methods. Regarding the MIMS method, we tested the consequences of potential offsets in key assumptions (e.g. variations in rate constants, PIC : POC, or photosynthetic quotient (PQ)) and found that typical uncertainties cannot explain the strong deviations between the methods. In contrast to the MIMS approach, the ^{14}C disequilibrium technique does not yield actual CO_2 and HCO_3^- uptake rates, but estimates the relative CO_2 uptake for photosynthesis (Lehman, 1971; Espie & Colman, 1986; Elzenga *et al.*, 2000; Kottmeier *et al.*, 2014). In this method, f_{CO_2} is assessed based on the curvature of the cellular photosynthetic ^{14}C incorporation during a transient isotopic $^{14}CO_2$ disequilibrium in the medium. In order to estimate f_{CO_2}, the ^{14}C-incorporation is fitted with a model that is based on a number of parameters (Lehman, 1971; Espie & Colman, 1986). Some of these parameters, including kinetic constants, decay rates and the height of isotopic disequilibria remain error-afflicted and are currently being re-evaluated (S. Thoms *et al.* unpublished). Until these methodological discrepancies are better understood, the conflicting results for the haploid stage remain puzzling.

Impaired HCO_3^- uptake under acidification may affect calcification

Although the strong negative H^+ effects on photosynthetic HCO_3^- uptake have not explicitly been described before, negative H^+ effects on calcification are often discussed (Taylor *et al.*, 2011; Fukuda *et al.*, 2014; Bach *et al.*, 2015; Cyronak *et al.*, 2015). These inhibitory effects have often been attributed to changes in electrochemical gradients and the associated costs of H^+ removal (Mackinder *et al.*, 2010; Raven, 2011; Suffrian *et al.*, 2011; Taylor *et al.*, 2011). In agreement with Fukuda *et al.*, 2014, we here found strong evidence that acidification impairs the HCO_3^- uptake. Assuming that high H^+ levels affect the transport of HCO_3^- across the plasmalemma, the decreased uptake would not only influence photosynthesis, but also

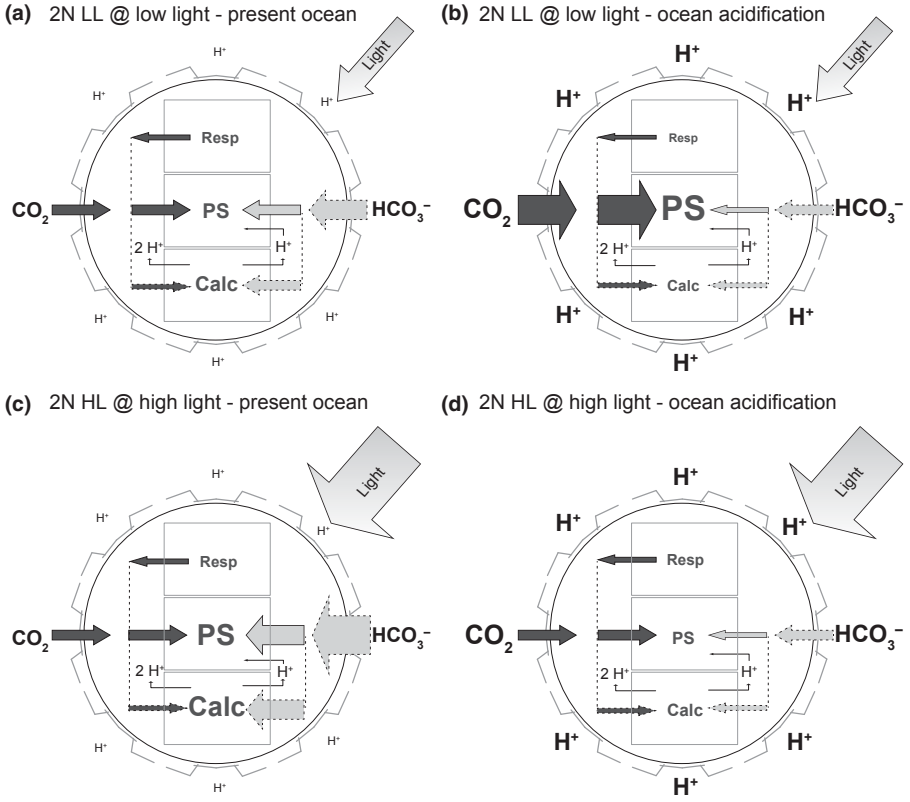

Fig. 4 Schematic illustration of the ocean acidification (OA)-dependent regulations in external inorganic carbon (C_i) fluxes of diploid, low-light acclimated (2N LL; a, b) and high-light acclimated (2N HL; c, d) *Emiliania huxleyi* under acclimation light. Sizes of arrows with solid lines reflect the measured photosynthetic and respiratory fluxes of CO_2 and HCO_3^-. Sizes of arrows with dashed lines reflect estimated fluxes. (a) Low-light acclimated cells mainly use external HCO_3^- as photosynthetic substrate under acclimation pH and achieve similar rates of calcification (Calc) and photosynthesis (PS). (b) When exposing low-light acclimated cells to OA, cells increase CO_2 uptake for photosynthesis, whereas HCO_3^- uptake is downscaled due to the increased H^+ levels. If HCO_3^- fluxes into photosynthesis and calcification were downscaled to the same degree, photosynthesis would disproportionally increase over calcification. (c) High-light acclimated cells perform higher rates of photosynthesis under acclimation light than low-light acclimated cells. The increased C_i demand is covered by additional HCO_3^- uptake. (d) When exposing high-light acclimated cells to OA, they are not able to increase CO_2 uptake rates, but nevertheless experience the H^+-driven decrease in HCO_3^- uptake. As a consequence of the decreased overall C_i supply, photosynthesis and presumably calcification experience C_i shortage and thus decrease.

calcification. Based on flux measurements of this study, we illustrated the presumed cellular C_i fluxes in response to typical OA scenarios under different light acclimations (Fig. 4).

As HCO_3^- fluxes into POC and PIC are similar in magnitude, calcification may serve intrinsic pH regulation (Sikes *et al.*, 1980; Price *et al.*, 2008; Raven, 2011). More specifically, when HCO_3^- is used for photosynthesis, one H^+ is consumed per fixed CO_2, and when HCO_3^- is used for calcification, one H^+ is released per produced $CaCO_3$ (Fig. 4; Holtz *et al.*, 2015a). The additional photosynthetic CO_2 uptake observed under acidification does not interfere with such a pH-homeostatic behaviour. Thus, independent of the external carbonate chemistry and light conditions, the need to exchange H^+ with the environment seems to be generally lower in the calcifying diplont of *E. huxleyi* (Fig. 4). This could provide the calcifying stage with an advantage over noncalcifying HCO_3^- users (such as the haplont), which have to assure constant H^+ uptake to compensate for alkalization during HCO_3^--based photosynthesis (Raven, 1986, 2011). This advantage may add to the diplont's success under bloom conditions, where seawater H^+ levels can become low.

Conclusions

In this study, we reveal a strong H^+-driven regulation of photosynthetic C_i fluxes of *E. huxleyi* that contradicts the commonly assumed 'fertilizing effect' of CO_2. At typical present-day conditions, HCO_3^- was shown to be the major photosynthetic C_i source of both life-cycle stages. High H^+ levels were shown to rapidly inhibit the HCO_3^- uptake and concomitantly to stimulate the CO_2 uptake. This H^+-dependent inhibition in HCO_3^- uptake serves as a mechanistic explanation for the typical OA-dependent decline in calcification of coccolithophores and other marine calcifiers. Such an inhibition may be widespread among various phytoplankton taxa and also elucidates how the light-use efficiency can decrease when phytoplankton communities are grown under OA in combination with high or fluctuating light intensities. Future research should investigate whether similar

H^+-dependent flux regulations are also evident when cells are acclimated to altered conditions.

Acknowledgements

We thank Klaus-Uwe Richter for the technical support and Dieter Wolf-Gladrow, Silke Thoms, Lena Holtz and Clara Hoppe for the constructive comments on this manuscript. We also gratefully acknowledge the feedback of the two anonymous reviewers. S.D.R. and B.R. received funding from the German Federal Ministry for Education and Research (BMBF) under grant no. 031A518C ($ZeBiCa^2$) and 03F0655B (Bioacid II).

Author contributions

D.M.K., S.D.R. and B.R. planned and designed the research. D.M.K. performed experiments and analysed the data. D.M.K., S.D.R. and B.R. interpreted the data and wrote the manuscript.

References

Alper SL. 2006. Molecular physiology of SLC4 anion exchangers. *Experimental Physiology* **91**: 153–161.

Anning T, Nimer NA, Merrett MJ, Brownlee C. 1996. Costs and benefits of calcification in coccolithophorids. *Journal of Marine Systems* **9**: 45–56.

Bach LT, Mackinder LC, Schulz KG, Wheeler G, Schroeder DC, Brownlee C, Riebesell U. 2013. Dissecting the impact of CO_2 and pH on the mechanisms of photosynthesis and calcification in the coccolithophore *Emiliania huxleyi*. *New Phytologist* **199**: 121–134.

Bach LT, Riebesell U, Gutowska MA, Federwisch L, Schulz KG. 2015. A unifying concept of coccolithophore sensitivity to changing carbonate chemistry embedded in an ecological framework. *Progress in Oceanography* **135**: 125–138.

Bach LT, Riebesell U, Schulz KG. 2011. Distinguishing between the effects of ocean acidification and ocean carbonation in the coccolithophore *Emiliania huxleyi*. *Limnology and Oceanography* **56**: 2040–2050.

Badger MR, Palmqvist K, Yu JW. 1994. Measurement of CO_2 and HCO_3^- fluxes in cyanobacteria and microalgae during steady-state photosynthesis. *Physiologia Plantarum* **90**: 529–536.

Barcelos e Ramos J, Müller MN, Riebesell U. 2010. Short-term response of the coccolithophore *Emiliania huxleyi* to abrupt changes in seawater carbon dioxide concentrations. *Biogeosciences* **7**: 177–186.

Beardall J, Raven JA. 2004. The potential effects of global climate change on microalgal photosynthesis, growth and ecology. *Phycologia* **43**: 26–40.

Berry L, Taylor AR, Lucken U, Ryan KP, Brownlee C. 2002. Calcification and inorganic carbon acquisition in coccolithophores. *Functional Plant Biology* **29**: 289–299.

Brown CW, Yoder JA. 1994. Coccolithophorid blooms in the global ocean. *Journal of Geophysical Research-Oceans* **99**: 7467–7482.

Buitenhuis ET, De Baar HJW, Veldhuis MJW. 1999. Photosynthesis and calcification by *Emiliania huxleyi* (Prymnesiophyceae) as a function of inorganic carbon species. *Journal of Phycology* **35**: 949–959.

Burkhardt S, Amoroso G, Riebesell U, Sultemeyer D. 2001. CO_2 and HCO_3^- uptake in marine diatoms acclimated to different CO_2 concentrations. *Limnology and Oceanography* **46**: 1378–1391.

Cyronak T, Schulz KG, Jokiel PL. 2015. The Omega myth: what really drives lower calcification rates in an acidifying ocean. *ICES Journal of Marine Science: Journal du Conseil*, fs075. doi: 10.1093/icesjms/fsv075.

von Dassow P, Ogata H, Probert I, Wincker P, Da Silva C, Audic S, Claverie J-M, De Vargas C. 2009. Transcriptome analysis of functional differentiation between haploid and diploid cells of *Emiliania huxleyi*, a globally significant photosynthetic calcifying cell. *Genome Biology* **10**: R114.

Dickson AG. 1981. An exact definition of total alkalinity and a procedure for the estimation of alkalinity and total inorganic carbon from titration data. *Deep-Sea Research Part II: Topical Studies in Oceanography* **28**: 609–623.

Elzenga JTM, Prins HBA, Stefels J. 2000. The role of extracellular carbonic anhydrase activity in inorganic carbon utilization of *Phaeocystis globosa* (Prymnesiophyceae): a comparison with other marine algae using the isotopic disequilibrium technique. *Limnology and Oceanography* **45**: 372–380.

Espie GS, Colman B. 1986. Inorganic carbon uptake during photosynthesis – a theoretical analysis using the isotopic disequilibrium technique. *Plant Physiology* **80**: 863–869.

Feng Y, Warner ME, Zhang Y, Sun J, Fu FX, Rose JM, Hutchins DA. 2008. Interactive effects of increased pCO_2, temperature and irradiance on the marine coccolithophore *Emiliania huxleyi* (Prymnesiophyceae). *European Journal of Phycology* **43**: 87–98.

Fukuda SY, Suzuki Y, Shiraiwa Y. 2014. Difference in physiological responses of growth, photosynthesis and calcification of the coccolithophore *Emiliania huxleyi* to acidification by acid and CO_2 enrichment. *Photosynthesis Research* **121**: 299–309.

Gao K, Xu J, Gao G, Li Y, Hutchins DA, Huang B, Wang L, Zheng Y, Jin P, Cai X *et al.* 2012. Rising CO_2 and increased light exposure synergistically reduce marine primary productivity. *Nature Climate Change* **2**: 519–523.

Guillard RRL, Ryther JH. 1962. Studies of marine planktonic diatoms. I. *Cyclothella nana* Hustedt and *Detonula confervacea* Cleve. *Canadian Journal of Microbiology* **8**: 229–239.

Herfort L, Thake B, Roberts J. 2002. Acquisition and use of bicarbonate by *Emiliania huxleyi*. *New Phytologist* **156**: 427–436.

Holtz LM, Wolf-Gladrow DA, Thoms S. 2015a. Numerical cell model investigating cellular carbon fluxes in *Emiliania huxleyi*. *Journal of Theoretical Biology* **364**: 305–315.

Holtz LM, Wolf-Gladrow DA, Thoms S. 2015b. Simulating the effects of light intensity and carbonate system composition on particulate organic and inorganic carbon production in *Emiliania huxleyi*. *Journal of Theoretical Biology* **372**: 192–204.

Hoppe CJM, Holtz L-M, Trimborn S, Rost B. 2015. Ocean acidification decreases the light use efficiency in an Antarctic diatom under dynamic but not constant light. *New Phytologist* **207**: 159–171.

Jin P, Gao K, Villafane VE, Campbell DA, Helbling EW. 2013. Ocean acidification alters the photosynthetic responses of a coccolithophorid to fluctuating ultraviolet and visible radiation. *Plant Physiology* **162**: 2084–2094.

Knap A, Michaels A, Close A, Ducklow H, Dickson A. 1996. Protocols for the joint global ocean flux study (JGOFS) core measurements. *JGOFS, Reprint of the IOC Manuals and Guides No. 29, UNESCO 1994* **19**: 1–170.

Kottmeier DM, Rokitta SD, Tortell PD, Rost B. 2014. Strong shift from HCO_3^- to CO_2 uptake in *Emiliania huxleyi* with acidification: new approach unravels acclimation versus short-term pH effects. *Photosynthesis Research* **121**: 265–275.

Kranz SA, Levitan O, Richter KU, Prasil O, Berman-Frank I, Rost B. 2010. Combined effects of CO_2 and light on the N_2-fixing cyanobacterium *Trichodesmium* IMS101: physiological responses. *Plant Physiology* **154**: 334–345.

Langer G, Nehrke G, Probert I, Ly J, Ziveri P. 2009. Strain-specific responses of *Emiliania huxleyi* to changing seawater carbonate chemistry. *Biogeosciences* **6**: 2637–2646.

Lehman JT. 1971. Enhanced transport of inorganic carbon into algal cells and its implications for the biological fixation of carbon. *Journal of Phycology* **14**: 33–44.

Leung C-Y, Palmer LC, Qiao BF, Kewalramani S, Sknepnek R, Newcomb CJ, Greenfield MA, Vernizzi G, Stupp SI, Beyzyk MJ *et al.* 2012. Molecular crystallization controlled by pH regulates mesoscopic membrane morphology. *ACS Nano* **6**: 10901–10909.

Mackinder L, Wheeler G, Schroeder D, von Dassow P, Riebesell U, Brownlee C. 2011. Expression of biomineralization-related ion transport genes in *Emiliania huxleyi*. *Environmental Microbiology* **13**: 3250–3265.

Mackinder L, Wheeler G, Schroeder D, Riebesell U, Brownlee C. 2010. Molecular mechanisms underlying calcification in coccolithophores. *Geomicrobiology Journal* **27**: 585–595.

Nanninga HJ, Tyrrell T. 1996. Importance of light for the formation of algal blooms by *Emiliania huxleyi*. *Marine Ecology Progress Series* **136**: 195–203.

Nielsen MV. 1995. Photosynthetic characteristics of the coccolithophorid *Emiliania huxleyi* (Prymnesiophyceae) exposed to elevated concentrations of dissolved inorganic carbon. *Journal of Phycology* **31**: 715–719.

Nielsen MV. 1997. Growth, dark respiration and photosynthetic parameters of the coccolithophorid *Emiliania huxleyi* (Prymnesiophyceae) acclimated to different day length-irradiance combinations. *Journal of Phycology* **33**: 818–822.

Paasche E. 1964. *A tracer study of the inorganic carbon uptake during coccolith formation and photosynthesis in the coccolithophorid Coccolithus huxleyi*. Lund, Sweden: Scandinavian Society for Plant Physiology.

Paasche E. 1999. Reduced coccolith calcite production under light-limited growth: a comparative study of three clones of *Emiliania huxleyi* (Prymnesiophyceae). *Phycologia* **38**: 508–516.

Paasche E. 2001. A review of the coccolithophorid *Emiliania huxley*i (Prymnesiophyceae), with particular reference to growth, coccolith formation, and calcification–photosynthesis interactions. *Phycologia* **40**: 503–529.

Pierrot D, Lewis E, Wallace D. 2006. *MS Excel program developed for CO_2 system calculations*. ORNL/CDIAC-105. Oak Ridge, TN, USA: Carbon Dioxide Information Analysis Center, Oak Ridge National Laboratory, US Department of Energy.

van de Poll WH, Visser RJ, Buma AG. 2007. Acclimation to a dynamic irradiance regime changes excessive irrandiance sensitivity of *Emiliania huxleyi* and *Thalassiosira weissflogii*. *Limnology and Oceanography* **52**: 1430–1438.

Price GD, Badger MR, Woodger FJ, Long BM. 2008. Advances in understanding the cyanobacterial CO_2-concentrating-mechanism (CCM): functional components, C_i transporters, diversity, genetic regulation and prospects for engineering into plants. *Journal of Experimental Botany* **59**: 1441–1461.

Raitsos D, Lavender S, Pradhan Y, Tyrrell T, Reid P, Edwards M. 2006. Coccolithophore bloom size variation in response to the regional environment of the subarctic North Atlantic. *Limnology and Oceanography* **51**: 2122–2130.

Raven J. 1986. Biochemical disposal of excess H^+ in growing plants? *New Phytologist* **104**: 175–206.

Raven J. 2011. Effects on marine algae of changed seawater chemistry with increasing atmospheric CO_2. *Biology and Environment: Proceedings of the Royal Irish Academy* **111 B**: 1–17.

Raven J, Crawfurd K. 2012. Environmental controls on coccolithophore calcification. *Marine Ecology Progress Series* **470**: 137–166.

Raven J, Johnston A. 1991. Mechanisms of inorganic carbon acquisition in marine phytoplankton and their implications for the use of other resources. *Limnology and Oceanography* **36**: 1701–1714.

Rokitta S, De Nooijer L, Trimborn S, De Vargas C, Rost B, John U. 2011. Transcriptome analyses reveal differential gene expression patterns between life-cycle stages of *Emiliania huxleyi* (Haptophyta) and reflect specialization to different ecological niches. *Journal of Phycology* **47**: 829–838.

Rokitta S, John U, Rost B. 2012. Ocean acidification affects redox-balance and ion-homeostasis in the life-cycle stages of *Emiliania huxleyi*. *PLoS ONE* **7**: e52212.

Rokitta S, Rost B. 2012. Effects of CO_2 and their modulation by light in the life-cycle stages of the coccolithophore *Emiliania huxleyi*. *Limnology and Oceanography* **57**: 607–618.

Rost B, Kranz SA, Richter KU, Tortell PD. 2007. Isotope disequilibrium and mass spectrometric studies of inorganic carbon acquisition by phytoplankton. *Limnology and Oceanography – Methods* **5**: 328–337.

Rost B, Riebesell U. 2004. Coccolithophores and the biological pump: responses to environmental changes. In: Thierstein HR, Young JR, eds. *Coccolithophores – from molecular processes to global impact*. Heidelberg, Germany: Springer, 76–99.

Rost B, Riebesell U, Sültemeyer D. 2006. Carbon acquisition of marine phytoplankton: effect of photoperiod length. *Limnology and Oceanography* **51**: 12–20.

Rost B, Zondervan I, Riebesell U. 2002. Light-dependent carbon isotope fractionation in the coccolithophorid *Emiliania huxleyi*. *Limnology and Oceanography* **47**: 120–128.

Roy RN, Roy LN, Vogel KM, Portermoore C, Pearson T, Good CE, Millero J, Campbell DM. 1993. The dissociation constants of carbonic acid in seawater at salinities 5 to 45 and temperatures 0 to 45°C. *Marine Chemistry* **44**: 249–267.

Sadeghi A, Dinter T, Vountas M, Taylor B, Altenburg-Soppa M, Bracher A. 2012. Remote sensing of coccolithophore blooms in selected oceanic regions using the PhytoDOAS method applied to hyper-spectral satellite data. *Biogeosciences* **9**: 2127–2143.

Schulz KG, Riebesell U, Rost B, Thoms S, Zeebe RE. 2006. Determination of the rate constants for the carbon dioxide to bicarbonate inter-conversion in pH-buffered seawater systems. *Marine Chemistry* **100**: 53–65.

Schulz KG, Rost B, Burkhardt S, Riebesell U, Thoms S, Wolf-Gladrow DA. 2007. The effect of iron availability on the regulation of inorganic carbon acquisition in the coccolithophore *Emiliania huxleyi* and the significance of cellular compartmentation for stable carbon isotope fractionation. *Geochimica et Cosmochimica Acta* **71**: 5301–5312.

Sett S, Bach LT, Schulz KG, Koch-Klavsen S, Lebrato M, Riebesell U. 2014. Temperature modulates coccolithophorid sensitivity of growth, photosynthesis and calcification to increasing seawater pCO_2. *PLoS ONE* **9**: e88308.

Sikes CS, Roer RD, Wilbur KM. 1980. Photosynthesis and coccolith formation: inorganic carbon sources and net inorganic reaction of deposition. *Limnology and Oceanography* **25**: 248–261.

Stojkovic S, Beardall J, Matear R. 2013. CO_2-concentrating mechanisms in three southern hemisphere strains of *Emiliania huxleyi*. *Journal of Phycology* **49**: 670–679.

Stoll MHC, Bakker K, Nobbe GH, Haese RR. 2001. Continuous-flow analysis of dissolved inorganic carbon content in seawater. *Analytical Chemistry* **73**: 4111–4116.

Suffrian K, Schulz KG, Gutowska MA, Riebesell U, Bleich M. 2011. Cellular pH measurements in *Emiliania huxleyi* reveal pronounced membrane proton permeability. *New Phytologist* **190**: 595–608.

Sukenik A, Bennett J, Falkowski P. 1987. Light-saturated photosynthesis – limitation by electron transport or carbon fixation. *Biochimica et Biophysica Acta* **891**: 205–215.

Taylor AR, Chrachri A, Wheeler G, Goddard H, Brownlee C. 2011. A voltage-gated H^+ channel underlying pH homeostasis in calcifying coccolithophores. *PLOS Biology* **9**: e1001085.

Trimborn S, Langer G, Rost B. 2007. Effect of varying calcium concentrations and light intensities on calcification and photosynthesis in *Emiliania huxleyi*. *Limnology and Oceanography* **52**: 2285–2293.

Weiss RF. 1970. The solubility of nitrogen, oxygen and argon in water and seawater. *Deep-Sea Research* **17**: 721–735.

Winter A, Henderiks J, Beaufort L, Rickaby REM, Brown CW. 2013. Poleward expansion of the coccolithophore *Emiliania huxleyi*. *Journal of Plankton Research* **36**: 316–325.

Wolf-Gladrow DA, Riebesell U, Burkhardt S, Bijma J. 1999. Direct effects of CO_2 concentration on growth and isotopic composition of marine plankton. *Tellus Series B – Chemical and Physical Meteorology* **51**: 461–476.

Xu K, Gao K. 2015. Solar UV Irradiances modulate effects of ocean acidification on the coccolithophorid *Emiliania huxleyi*. *Photochemistry and Photobiology* **91**: 92–101.

Zeebe RE, Wolf-Gladrow DA. 2001. *CO_2 in seawater: equilibrium, kinetics, isotopes*. Amsterdam, the Netherlands: Elsevier Science B.V.

Zondervan I, Rost B, Riebesell U. 2002. Effect of CO_2 concentration on the PIC/POC ratio in the coccolithophore *Emiliania huxleyi* grown under light-limiting conditions and different daylengths. *Journal of Experimental Marine Biology and Ecology* **272**: 55–70.

Supporting Information

Additional supporting information may be found in the online version of this article.

Table S1 Acclimation carbonate chemistry

Please note: Wiley Blackwell are not responsible for the content or functionality of any supporting information supplied by the authors. Any queries (other than missing material) should be directed to the *New Phytologist* Central Office.

Chapter 4
Publication III

H^+-driven impairment of HCO_3^- uptake manifests after acclimation and explains declined calcification in coccolithophores

Dorothee M. Kottmeier, Sebastian D. Rokitta, Björn Rost

Submitted to Journal of Experimental Botany

4.1 Abstract

Recent ocean acidification (OA) studies revealed that H^+ levels rather than CO_2 and HCO_3^- levels regulate *short-term* responses in the photosynthetic inorganic carbon (C_i) supply of *Emiliania huxleyi*. Here, we investigated whether *acclimation* to altered carbonate chemistry conditions modulates these regulation patterns and how C_i supply for calcification is affected. To this end, we acclimated *E. huxleyi* to *present-day* conditions (ambient [CO_2], [HCO_3^-] and pH), *carbonation* (high [CO_2] and [HCO_3^-], ambient pH), *acidification* (ambient [CO_2], low [HCO_3^-] and pH) and *OA* (high [CO_2], ambient [HCO_3^-], low pH). Under these conditions, growth, production of particulate inorganic and organic carbon as well as cellular C_i and O_2 fluxes were measured. Responses to *carbonation* differed from short-term responses: Photosynthesis and calcification were strongly stimulated due to additional HCO_3^- uptake, while growth was unaffected. These regulations can, however, not explain responses to typical OA, where [HCO_3^-] stays rather constant. The responses to high [H^+] were similar to short-term responses: Even though the effects of *acidification* and *OA* on photosynthesis and calcification were small, cellular C_i supply was strongly modulated in these low-pH treatments. Photosynthetic CO_2 uptake was significantly stimulated, whereas cellular HCO_3^- uptake was strongly inhibited. Also growth was significantly decreased. The observed flux regulations identify H^+ as the prime driver of coccolithophores' acclimation responses towards OA. The regulatory effort under acidified conditions apparently puts a metabolic burden on the cells, causing the significant decrease in growth.

Keywords:

Calcification, Coccolithophores, CO_2-concentrating mechanism, Irradiance, Photosynthesis, Carbon source, Membrane-inlet mass spectrometry, Ocean acidification, pH, Protons

4.2 Introduction

Emiliania huxleyi is the Earth´s most dominant pelagic calcifier and known to be well adapted to shallow mixed-layer depths with high irradiances (Nanninga & Tyrrell, 1996; Raitsos *et al.*, 2006). Under these conditions, the species is able to form large monospecific blooms with cell concentrations of up to 10 million cells L^{-1} (Holligan *et al.*, 1993; Tyrrell & Merico, 2004). In the process of calcification, CO_3^{2-} precipitates intracellularly with Ca^{2+} to form $CaCO_3$, leading to reduced seawater alkalinity and CO_3^{2-} levels. This production of particulate inorganic carbon (PIC) furthermore increases the partial pressure of carbon dioxide (pCO_2) of seawater and thereby counteracts the effect of photosynthetic production of particulate organic carbon (POC). The relative strength of calcification vs. photosynthesis therefore influences the biogeochemical CO_2 fluxes on regional and global scales (Broecker & Peng, 1987; Rost & Riebesell, 2004).

In the last decades, *E. huxleyi* has become an important model organism, especially because of its high sensitivity towards ocean acidification (OA; Raven & Crawfurd, 2012; Read *et al.*,

2013; Meyer & Riebesell, 2015). This term describes the strong increase in CO_2 and the slight increase in HCO_3 levels (their sum is referred to as carbonation) as well as the decrease in CO_3^{2-} levels and pH (the latter corresponds to an increase in $[H^+]$ and is referred to as acidification), which result from the oceanic uptake of anthropogenic CO_2 (Wolf-Gladrow *et al.*, 1999; Caldeira & Wickett, 2003). A large number of laboratory and field studies on *E. huxleyi* and other coccolithophores found that OA stimulates photosynthesis, but impairs calcification and growth, typically leading to decreased PIC:POC ratios (Raven & Crawfurd, 2012; Kroeker *et al.*, 2013; Meyer & Riebesell, 2015). These responses can yet vary in magnitude, depending on genetic predisposition and other environmental boundary conditions such as light, temperature or nutrient status (Zondervan, 2007; Langer *et al.*, 2009; Lefebvre *et al.*, 2012; Rokitta & Rost, 2012; Sett *et al.*, 2014; Xu & Gao, 2015).

In first attempts to identify the chemical drivers of typical OA responses, *E. huxleyi* was acclimated to decoupled carbonate chemistry, under which carbonation and acidification effects could be distinguished (Bach *et al.*, 2011; Bach *et al.*, 2013). These acclimation studies revealed that POC and PIC production are both stimulated by carbonation, but are reduced when cells are acclimated to acidification. The antagonistic regulation of PIC production by carbonation and acidification was also indicated by a study of Fukuda *et al.* (2014), who showed that calcification is reduced under high $[H^+]$, but that this reduction can be overcome by additional HCO_3^- availability. A recent study investigated the mechanisms underlying short-term carbonation and acidification responses of *E. huxleyi* by means of membrane-inlet mass spectrometry (Kottmeier *et al.*, 2016). Photosynthetic fluxes of *E. huxleyi* were shown to be relatively insensitive towards abrupt increases in CO_2 and HCO_3^- levels, i.e., when being exposed to carbonation for time scales of seconds to minutes. The fluxes were, however, very sensitive towards abrupt increases in H^+ levels, i.e., to acidification. Under the latter conditions, photosynthetic HCO_3^- uptake was strongly inhibited. Low-light acclimated cells were able to overcompensate this inhibition in HCO_3^- uptake with additional CO_2 uptake. High-light acclimated cells were, however, unable to increase CO_2 uptake and therefore suffered from internal shortage of inorganic carbon (C_i) under acidification. These regulations could be different after acclimation, during which cells adjust their metabolism to the altered conditions, e.g., by changing gene expression. Also, we are currently lacking information about C_i fluxes into calcification and their dependence on carbonation and acidification.

In order to understand the differences between *short-term* and *acclimation* responses towards carbonation and acidification, we here acclimated *E. huxleyi* to *present-day* conditions (ambient $[CO_2]$, $[HCO_3^-]$ and pH), *carbonation* (high $[CO_2]$, high $[HCO_3^-]$ and ambient pH), *acidification* (ambient $[CO_2]$, low $[HCO_3^-]$ and low pH) and *OA* (high $[CO_2]$, ambient $[HCO_3^-]$ and low pH; Fig. 4.1). We assessed integrated responses in growth, elemental composition and production rates, as well as *in vivo* fluxes of O_2, CO_2 and HCO_3^- associated with photosynthesis and calcification. By comparing these responses with short-term responses

(Kottmeier *et al.*, 2016), we could identify processes that were manifested or adjusted over the course of the acclimation.

4.3 Methods

Acclimations

Emiliania huxleyi strain RCC1216 was acclimated to four different carbonate chemistry conditions ('*present-day*', '*carbonation*', '*acidification*' and '*OA*'; Fig. 4.1; Table 4.1) under saturating irradiance (400 ±30 μmol photons m^{-2} s^{-1}) for ≥10 generations. Cells were grown as dilute batch cultures in a 16:8 h light:dark cycle at 15 ±1°C in sterile-filtered North Sea seawater (0.2 μm, Sartobran 300, Sartorius, Göttingen, Germany). Phosphate and nitrate were added to yield concentrations of ~7 and ~100 μmol kg^{-1}, respectively. Vitamins and trace metals were adjusted according to F/2 (Guillard & Ryther, 1962). Cells were cultured on roller tables in sterilized, gas-tight 2 L borosilicate bottles (Duran Group, Mainz, Germany). Cultures were irradiated by daylight lamps (FQ 54W/965HO, Osram, Munich, Germany).

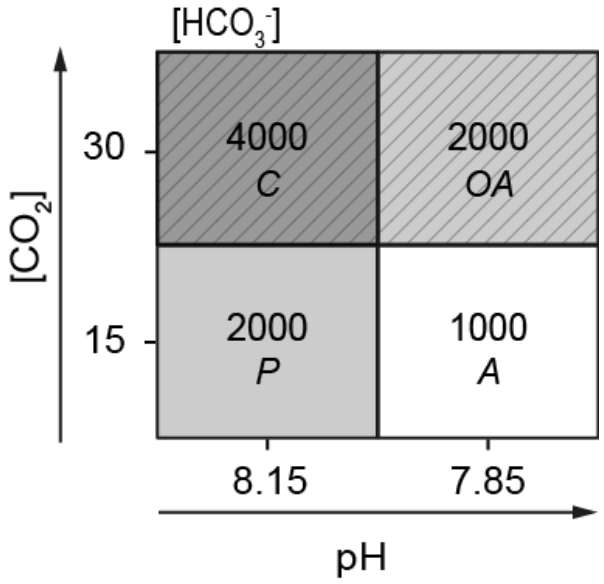

Figure 4.1: Decoupled carbonate chemistry during acclimation of *Emiliania huxleyi* and during cellular flux measurements. Applied conditions were *present-day* (*P*; light grey), *carbonation* (*C*; dark grey, dashed), *acidification* (*A*; white) and *ocean acidification* (*OA*; light grey, dashed). Numbers inside the fields denote concentrations of HCO_3^-. Concentrations are given in μmol kg^{-1}.

Irradiance was adjusted inside seawater-filled culturing bottles and measured with a Universal Light Meter (ULM 500, Walz, Effeltrich, Germany) using a 4π-sensor (US-SQS/L). Carbonate chemistry was adjusted by aerating the media with humidified, 0.2 μm-filtered air (Midisart 2000, Sartorius) containing a pCO_2 of 380 μatm in the *present-day* and *acidification* treatments, and a pCO_2 of 1000 μatm in the *carbonation* and *OA* treatments (Table 4.1). In the *acidification* and *carbonation* treatments, total alkalinity (TA) was adjusted by acid- or base addition (Table 4.1). Gas mixtures were produced with a gas flow controller (CGM 2000, MCZ Umwelttechnik, Bad Nauheim, Germany), mixing defined portions of pure CO_2 (Air Liquide, Duesseldorf, Germany) and CO_2-free air (Air purification system, Parker Zander, Kaarst, Germany). Carbonate chemistry of the media was controlled at the beginning as well as at the end of the acclimation period, and was calculated based on pH_{NBS} and TA measurements using CO2sys (Table 4.1; Pierrot *et al.*, 2006).

Measurements of pH were performed with a Metrohm pH meter (826 pH mobile, Metrohm, Filderstadt, Germany) using an Aquatrode Plus electrode with integrated temperature sensor (measurement reproducibility ±0.01 pH units). TA was determined with potentiometric titration (TitroLine alpha plus, measurement reproducibility ±7 μmol kg^{-1}, Schott Instruments, Mainz, Germany) of sterile-filtered samples (0.2 μm, cellulose acetate syringe filters, Thermo Fisher Scientific, Waltham, MA, USA) and was corrected with certified reference materials (CRM; provided by A. Dickson; Scripps Institution of Oceanography, USA). Dissolved inorganic carbon (DIC) was controlled with colorimetric measurements of sterile-filtered samples with a QuAAtro autoanalyser (measurement reproducibility ±5 μmol kg^{-1}, Seal Analytical, Norderstedt, Germany) following the method of (Stoll *et al.*, 2001).

Growth and production rates

Cellular quotas of POC, PIC and particulate organic nitrogen (PON; pg $cell^{-1}$) were measured with an Automated Nitrogen Carbon Analyser mass spectrometer (ANCA-SL 20-20, Sercon Ltd., Crewe, UK). Known volumes of cell suspension were vacuum-filtered (-200 mbar relative to atmosphere) onto precombusted (12h, 500°C) GF/F filters (1.2 μm; Whatman, Maidstone, UK) six to eight hours after the beginning of the light phase. POC filters were soaked with HCl (0.2 M) to remove calcite prior to measurements. Cellular quotas of PIC were assessed as the difference in carbon quotas between acidified and non-acidified filters. Quotas of chlorophyll *a* (Chl *a*; pg $cell^{-1}$) were assessed by filtering defined volumes of cell suspension onto cellulose nitrate filters (0.45 μm, Sartorius, Göttingen, Germany), which were subsequently frozen in liquid nitrogen and stored at -80°C until analysis. Chl *a* was extracted in 90% acetone (v/v, Sigma, Munich, Germany) and determined fluorometrically (TD-700 fluorometer, Turner Designs, Sunnyvale, CA, USA) according to Knap *et al.* (1996). The fluorometer was calibrated with an *Anacystis nidulans* Chl *a* standard (Sigma). Cell growth was determined by daily cell counting with a Coulter Counter (Beckman-Coulter, Fullerton, CA, USA), and the growth constant μ (d^{-1}) was determined as:

$$\mu = \frac{\ln c_2 - \ln c_1}{t_2 - t_1} \quad (4.1)$$

with c_2 and c_1 being the cell concentrations (cells mL^{-1}) at the two sampling time points t_1 and t_2 (d). Production rates of POC and PIC (pg $cell^{-1}$ d^{-1}) were approximated as

$$POC\ production = \text{POC quota} \cdot \mu \quad (4.2)$$

$$PIC\ production = \text{PIC quota} \cdot \mu \quad (4.3)$$

Cellular oxygen and carbon fluxes

Photosynthetic *real time* fluxes of oxygen (O_2) and C_i were measured by means of membrane-inlet mass spectrometry (MIMS; Isoprime, GV Instruments, Manchester, UK) at conditions resembling the *in situ* carbonate chemistry and irradiance (Table 4.1). Fluxes were estimated following the disequilibrium method by Badger *et al.* (1994). In this technique, calculations of photosynthetic CO_2 and HCO_3^- fluxes across the plasmalemma are based on the chemical disequilibrium between the two C_i species during their light-dependent uptake. To account for calcification, we followed the modifications introduced by Schulz *et al.* (2007) and Kottmeier *et al.* (2016) and applied measured PIC:POC ratios of the cells that were acclimated to the respective carbonate chemistry conditions. Prior to measurements, acclimated *E. huxleyi* cells were concentrated by gentle vacuum filtration (-200 mbar relative to atmosphere) over a polycarbonate filter (Isopore TSTP, 3 μm, Merck, Darmstadt, Germany). Culture medium was exchanged with 50 mM N,N-bis(2-hydroxyethyl)glycine (BICINE)-buffered DIC-free seawater medium of the appropriate pH, and 8 mL of the concentrated and buffered cell suspension (5 - 10 x 10^6 cells mL^{-1}) were transferred into the MIMS cuvette. Carbonate chemistry was adjusted by adding the corresponding concentrations of $NaHCO_3$ (Table 4.1). During a first dark phase prior to the actual measurement intervals, membrane-impermeable dextran-bound sulphonamide (25 μM, DBS; Synthelec, Lund, Sweden) was added to inhibit any potential activity of external carbonic anhydrase. Chl *a* samples of the concentrated cell suspensions were taken to quantify the assayed biomass.

Fluxes of O_2 and C_i were measured in consecutive, 6-minute light and dark phases in a temperature-controlled cuvette. Steady-state photosynthetic net O_2 evolution (*Phot*) was measured in the light, whereas respiratory O_2 uptake (*Resp*) was measured in the subsequent dark phase. Photosynthetic and respiratory O_2 fluxes were converted to C_i fluxes by applying a photosynthetic quotient (*PQ*) of 1.1 and a respiratory quotient of 1.0, respectively (Burkhardt *et al.*, 2001; Kottmeier *et al.*, 2016). C_i fluxes into calcification (Cal_{MIMS}) were derived by multiplying photosynthetic net C_i fixation with light-phase normalized PIC:POC ratios ($PIC{:}POC_{light}$) in order to account for continuous respiration of POC during the 8-hour dark phase (Schulz *et al.*, 2007):

$$PIC{:}POC_{light} = \frac{PIC\ quota}{POC\ quota} \times \frac{16\ Phot - 8\ Resp}{16\ Phot} \quad (4.4)$$

$$Cal_{MIMS} = \frac{Phot}{PQ} \times PIC{:}POC_{light} \quad (4.5)$$

Cellular CO_2 uptake was deduced from steady-state CO_2 drawdown in the light, and corrected for the simultaneous inter-conversion between CO_2 and HCO_3^- according to Badger *et al.* (1994). Because calcification is predominantly supplied by external HCO_3^- (Sikes *et al.*, 1980; Rost *et al.*, 2002), we assumed that the CO_2 uptake for calcification (CO_2up_{CaCO3}) was 20% of overall Cal_{MIMS} (Kottmeier *et al.*, 2016). Accordingly, HCO_3^- uptake for calcification ($HCO_3^-up_{CaCO3}$) was assumed to be 0.8 × Cal_{MIMS}. Photosynthetic CO_2 uptake (CO_2up_{PS}) was calculated by subtracting CO_2up_{CaCO3} from overall cellular CO_2 uptake. The fraction of overall photosynthetic C_i uptake that is covered by CO_2 (fCO_2) was obtained according to Kottmeier *et al.* (2016). Photosynthetic HCO_3^- uptake ($HCO_3^-up_{PS}$) was calculated as the difference between overall photosynthetic C_i uptake and photosynthetic CO_2 uptake. Total HCO_3^- uptake ($HCO_3^-up_{tot}$) was calculated as the sum of HCO_3^- uptake for calcification ($HCO_3^-up_{CaCO3}$) and HCO_3^- uptake for photosynthesis ($HCO_3^-up_{PS}$). For further details on the calculations of the photosynthetic fluxes, we refer to Kottmeier *et al.* (2016).

Table 4.1: Carbonate chemistry in the *present-day* (*P*), *carbonation* (*C*), *acidification* (*A*) and the *ocean acidification* (*OA*) treatments in cell-free media (Control), at the time of harvesting (Acc), and during cellular flux measurements with membrane-inlet mass spectrometry (MIMS). For acclimation conditions, attained pCO_2 (μatm), $[H^+]$ (nmol kg^{-1}), DIC (μmol kg^{-1}), $[CO_2]$ (μmol kg^{-1}), $[HCO_3^-]$ (μmol kg^{-1}), $[CO_3^{2-}]$ (μmol kg^{-1}), and $\Omega_{calcite}$ were calculated based on measured pH_{NBS} and TA using CO2sys (Pierrot *et al.*, 2006). Results are reported for 15°C (n≥3; ±SD). Input parameters for CO2sys calculations were salinity (31), pressure (0.1 dbar), as well as phosphate (7 μmol kg^{-1}) and silicate (7 μmol kg^{-1}). Equilibrium constants by Mehrbach *et al.* (1973), refit by Dickson and Millero (1987) and dissociation constants for sulfuric acid by Dickson (1990) were applied. For MIMS conditions, carbonate chemistry was measured mass-spectrometrically (Badger *et al.*, 1994; Schulz *et al.*, 2007). The pCO_2 was calculated after (Zeebe & Wolf-Gladrow, 2001).

Treatment		pCO_2	pH_{NBS}	$[H^+]$	TA	DIC	$[CO_2]$	$[HCO_3^-]$	$[CO_3^{2-}]$	$\Omega_{calcite}$
	Control	403 ± 4	8.13 ± 0.00	9.9 ± 0.1	2341 ± 4	2129 ± 4	15 ± 0	1961 ±5	153 ± 1	3.7 ± 0.0
P	Acc	384 ± 17	8.14 ± 0.01	9.9 ± 0.1	2280 ± 19	2068 ± 23	15 ± 1	1903 ± 25	151 ± 3	3.7 ± 0.1
	MIMS	486 ± 17	8.15 ± 0.01	9.3 ± 0.2	-	2323 ± 180	21 ± 3	2252 ± 264	160 ± 5	-
	Control	868 ± 109	8.16 ± 0.02	9.5 ± 0.1	5317 ± 560	4899 ± 529	33 ± 4	4493 ± 489	373 ± 38	9.1 ± 0.9
C	Acc	805 ± 84	8.18 ± 0.00	8.9 ± 0.3	5223 ± 527	4791 ± 491	31 ± 3	4379 ± 450	382 ± 39	9.3 ± 0.9
	MIMS	883 ± 13	8.18 ± 0.02	8.5 ± 0.4	-	4648 ± 69	36 ± 0	4263 ± 64	333 ± 5	-
	Control	418 ± 12	7.83 ± 0.00	20.1 ± 0.2	1122 ± 19	1056 ± 19	16 ± 0	1002 ±19	38 ± 0	0.9 ± 15
A	Acc	410 ± 51	7.83 ± 0.04	19.0 ± 1.1	1119 ± 31	1052 ± 37	16 ± 2	997 ± 37	39 ± 2	1.0 ± 0.1
	MIMS	405 ± 12	7.88 ± 0.02	17.3 ± 0.8	-	1037 ± 31	17 ± 1	980 ± 30	38 ± 1	-
	Control	998 ± 15	7.78 ± 0.01	22.5 ± 0.2	2312 ± 2	2238 ± 2	38 ± 1	2127 ± 2	73 ± 1	1.8 ± 0.0
OA	Acc	964 ± 8	7.79 ± 0.00	22.1 ± 0.2	2287 ± 4	2211 ± 4	37 ± 0	2100 ± 4	73 ± 1	1.8 ± 0.0
	MIMS	942 ± 28	7.87 ± 0.02	17.8 ± 0.7	-	2357 ± 70	38 ± 1	2230 ± 67	85 ± 3	-

Statistics

All experiments were carried out in biological triplicates. Differences between the *present-day*, *carbonation*, *acidification* and *OA* treatments were tested pairwise for significance by applying two-sided t-tests. Effects were considered statistically significant when p-values were ≤0.05. In the figures and tables 4, significant differences were indicated by different lower-case characters (e.g., a and b). Values denoted by two letters (e.g., ab) represent data that are not significantly different from a and b.

4.4 Results

Integrated responses

Cellular growth was unaltered after acclimation to *carbonation*, but decreased from ~1.1 at *present-day* to ~1.0 d^{-1} after acclimation to *acidification* or *OA* (Fig. 4.2 A, Table 4.2). Cellular POC production was increased under *carbonation* (~15%), but constant under *acidification* and slightly decreased (~10%) under *OA* (Fig. 4.4.2 B, Table 4.2). Also PIC production was strongly stimulated under *carbonation* (~45%), but decreased under *acidification* and *OA* (~15%; Fig. 4. 2 C, Table 4.2). The ratio of PIC:POC increased by ~20% under *carbonation*, but decreased slightly under *acidification* and *OA* (~10%). Cellular Chl *a* quotas and Chl *a*:POC ratios, as well as the ratio of POC:PON were not affected by carbonate chemistry (Table 4.2). Scanning electron microscopy did not reveal malformations of coccoliths under any of the acclimation conditions (data not shown).

Cellular fluxes

We measured cellular O_2 and C_i fluxes of the acclimated cells under *in situ* carbonate chemistry conditions in order to identify the alterations in fluxes that caused the alterations in the integrated responses. Similar to the POC production, also Chl *a*-normalized O_2 evolution (*Phot*) indicated that photosynthesis was increased under *carbonation* (~30%), but unaffected by *acidification* or *OA* (Fig. 4.3 A, Table 4.2). Photosynthetic CO_2 uptake (CO_2up_{PS}) was low under *present-day*, became negative under *carbonation* (i.e., cells exhibited a CO_2 net efflux), but increased under *acidification* and *OA* (~600%; Fig. 4.3 B, Table 4.2). Photosynthetic HCO_3^- uptake ($HCO_3^-up_{PS}$) was generally high and was further stimulated by *carbonation* (~45%), but decreased under *acidification* and *OA* (~50%; Fig. 4.3 C, Table 4.2). As a consequence of these antagonistic regulations in CO_2 and HCO_3^- uptake, the ratio of photosynthetic CO_2 uptake to the overall photosynthetic C_i uptake (f_{CO_2}) decreased from ~0.1 to ~-0.1 under *carbonation*, but increased to ~0.4 under *acidification* and *OA* (Fig. 4.3 D, Table 4.2). Respiration (*Resp*) and the ratio of net photosynthesis to respiration (*Phot:Resp*) were relatively constant in all applied carbonate chemistry treatments (Table 4.2).

Calcification as estimated from light-normalized PIC:POC ratios and MIMS measurements (Cal_{MIMS}) strongly increased under *carbonation* (~60%), but stayed constant under

acidification and *OA* (Fig. 4.3 E, Table 4.2). Yet, an apparent negative trend in calcification under the low-pH treatments was observed (Fig. 4.3 E, Table 4.2). Also CO_2 and HCO_3^- uptake for calcification (CO_2up_{CaCO3}, $HCO3^-up_{CaCO3}$) increased under *carbonation* (~60%), but remained relatively constant under *acidification* and *OA* (Fig. 4.3 F, Table 4.2). The total cellular HCO_3^- uptake ($HCO_3^-up_{tot}$), i.e., the fluxes into both, photosynthesis and calcification, was generally increased under *carbonation* (~50%), whereas it decreased under *acidification* and *OA* (~25%; Fig. 4.3 G, Table 4.2). The ratio of HCO_3^- uptake for calcification to HCO_3^- uptake for photosynthesis ($HCO_3^-{}_{CaCO3}$:$HCO_3^-{}_{PS}$) was not affected by *carbonation*, but strongly increased under *acidification* and *OA* (~50%, Fig. 4.3 F, Table 4.2).

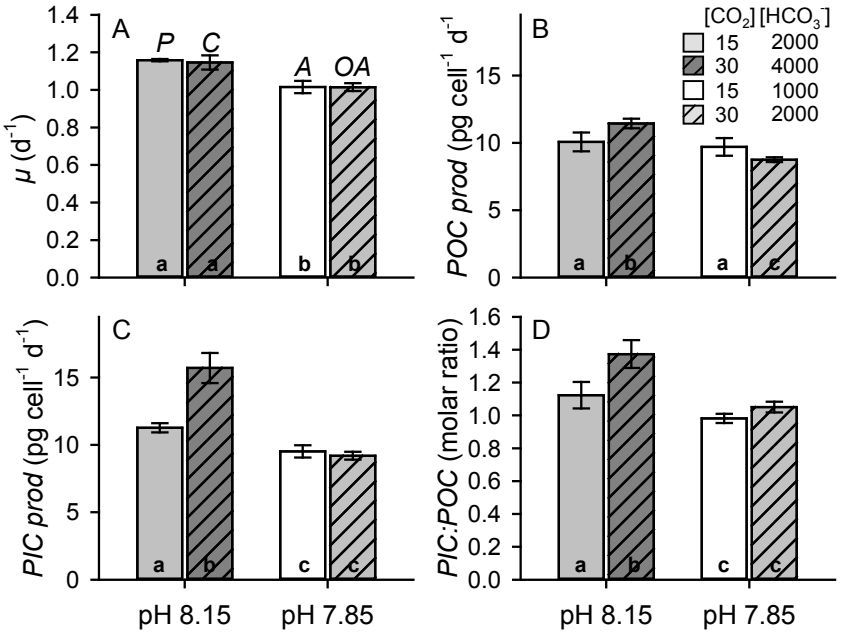

Figure 4.2: Integrated responses to *present-day* (*P*; light grey), *carbonation* (*C*; dark grey, dashed), *acidification* (*A*; white) and *ocean acidification* (*OA*; light grey, dashed): A) Cellular growth constants (μ), B) production rates of particulate organic carbon (POC) C) production rates of particulate inorganic carbon (PIC) and D) PIC:POC ratios. Error bars indicate SD (n = 3). The different lower-case characters indicate significant differences between the data obtained at different carbonate chemistry conditions, e.g., data labeled 'a' are statistically different from bars labeled 'b' or 'c'.

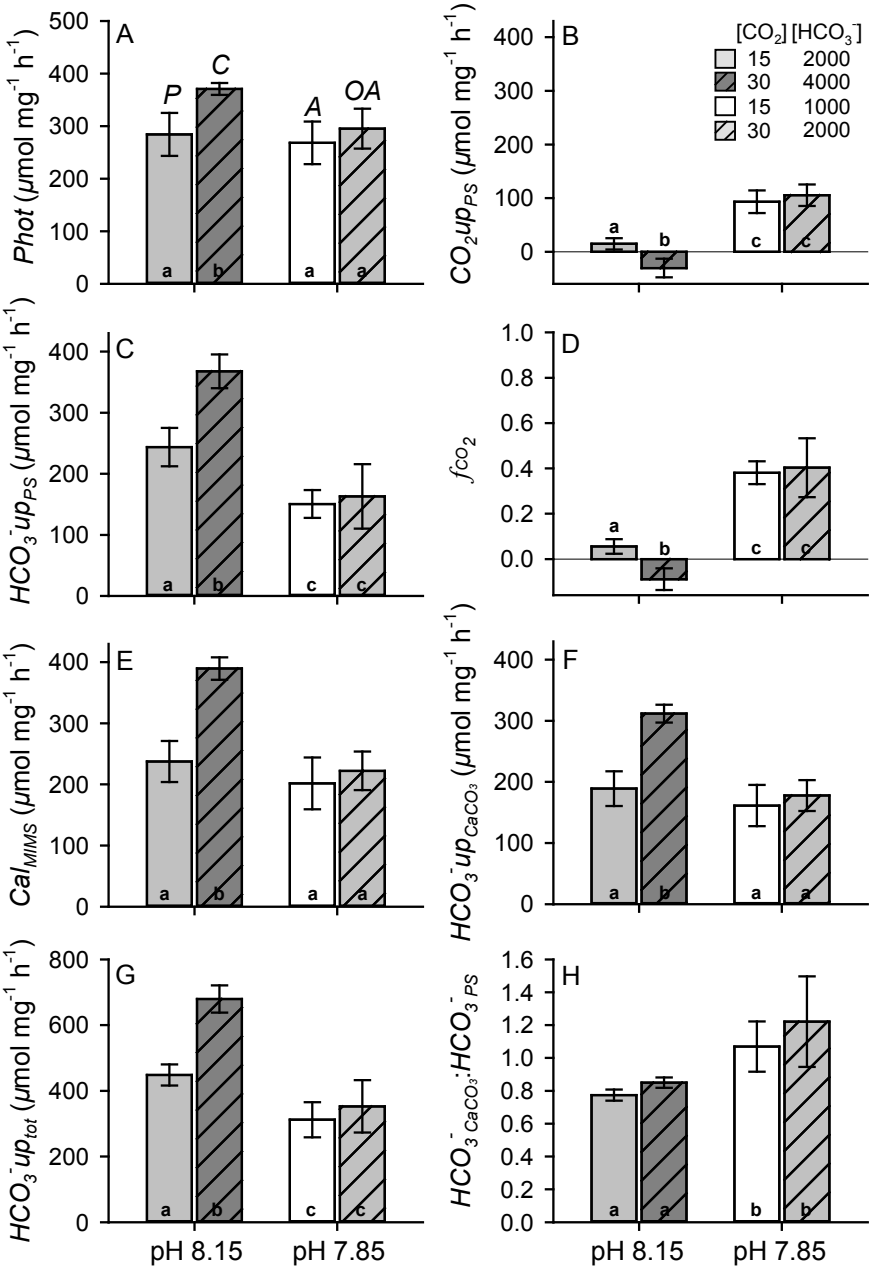

Figure 4.3: Cellular O_2 and C_i fluxes of *Emiliania huxleyi* in the *present-day* (*P*; light grey), *carbonation* (*C*; dark grey), *acidification* (*A*; white) and *ocean acidification* (*OA*; dashed, light grey) treatments: A) photosynthetic net O_2 evolution (*Phot*), **B)** photosynthetic CO_2 uptake (CO_2up_{PS}), **C)** photosynthetic HCO_3^- uptake ($HCO_3^-up_{PS}$), **D)** ratio of photosynthetic CO_2 uptake to overall photosynthetic C_i uptake (fCO_2), **E)** calcification rates (Cal_{MIMS}), **F)** HCO_3^- uptake for calcification ($HCO_3^-up_{CaCO3}$), **G)** Total HCO_3^- uptake ($HCO_3^-up_{tot}$), **H)** Ratio of HCO_3^- uptake for calcification to HCO_3^- uptake for photosynthesis ($HCO_3^-{}_{CaCO3}:HCO_3^-{}_{PS}$). All rates were normalized to Chl *a*. Error bars indicate SD (n = 3). Different lower-case characters indicate significant differences between the fluxes obtained at different carbonate chemistry conditions.

Table 4.2 - Integrated responses and underlying cellular fluxes of *Emiliania huxleyi* in the *present-day* (*P*), *carbonation* (*C*), *acidification* (*A*) and *ocean acidification* (*OA*) treatments: Different lower-case characters in superscript indicate statistically significant differences between the fluxes obtained at different carbonate chemistry conditions.

Parameter (unit)	*P*	*C*	*A*	*OA*
μ (d^{-1})	1.16 ± 0.01^{a}	1.15 ± 0.04^{a}	1.02 ± 0.03^{b}	1.01 ± 0.02^{b}
POC quota (pg $cell^{-1}$)	8.9 ± 0.6^{a}	10.2 ± 0.3^{b}	9.7 ± 0.7^{ab}	8.9 ± 0.2^{a}
POC production (pg $cell^{-1}$ d^{-1})	10.1 ± 0.7^{a}	11.4 ± 0.4^{b}	9.7 ± 0.7^{a}	8.8 ± 0.2^{c}
PIC quota (pg $cell^{-1}$)	10.0 ± 0.3^{a}	14.0 ± 1.0^{b}	9.5 ± 0.5^{a}	9.5 ± 0.3^{c}
PIC production (pg $cell^{-1}$ d^{-1})	11.3 ± 0.3^{a}	15.7 ± 1.1^{b}	9.5 ± 0.5^{c}	9.2 ± 0.3^{c}
PIC:POC (molar ratio)	1.12 ± 0.08^{a}	1.37 ± 0.08^{b}	0.98 ± 0.03^{c}	1.05 ± 0.03^{a}
$PIC:POC_{light}$ (molar ratio)	0.87 ± 0.02^{a}	1.15 ± 0.03^{b}	0.82 ± 0.06^{a}	0.88 ± 0.02^{a}
Chl a quota (pg $cell^{-1}$)	0.13 ± 0.01^{a}	0.13 ± 0.01^{a}	0.12 ± 0.01^{a}	0.12 ± 0.01^{a}
Chl a: POC (pg pg^{-1})	0.014 ± 0.001^{a}	0.013 ± 0.001^{a}	0.013 ± 0.004^{a}	0.014 ± 0.002^{a}
POC:PON (molar ratio)	6.9 ± 0.2^{a}	6.8 ± 0.4^{a}	6.9 ± 0.3^{a}	6.6 ± 0.2^{a}
Phot (μmol (mg Chl *a*)$^{-1}$ h^{-1})	284 ± 41^{a}	371 ± 11^{b}	268 ± 41^{a}	295 ± 38^{a}
μ_{MIMS} (d^{-1})	1.06 ± 0.15^{a}	1.22 ± 0.04^{a}	0.88 ± 0.13^{a}	1.07 ± 0.12^{a}
CO_2up_{PS} (μmol (mg Chl *a*)$^{-1}$ h^{-1})	15 ± 11^{a}	-30 ± 17^{b}	93 ± 21^{c}	105 ± 20^{c}
$HCO_3^-up_{PS}$ (μmol (mg Chl *a*)$^{-1}$ h^{-1})	244 ± 34^{a}	368 ± 27^{b}	151 ± 23^{c}	163 ± 53^{c}
fCO_2	0.06 ± 0.03^{a}	-0.09 ± 0.05^{b}	0.38 ± 0.05^{c}	0.40 ± 0.13^{c}
Cal_{MIMS}	237 ± 34^{a}	390 ± 18^{b}	202 ± 42^{a}	222 ± 32^{a}
CO_2up_{CaCO3} (μmol (mg Chl *a*)$^{-1}$ h^{-1})	47 ± 7^{a}	78 ± 4^{b}	40 ± 8^{a}	50 ± 2^{a}
$HCO_3^-up_{CaCO3}$ (μmol (mg Chl *a*)$^{-1}$ h^{-1})	189 ± 28^{a}	312 ± 15^{b}	161 ± 34^{a}	178 ± 25^{a}
$HCO_3^-up_{tot}$ (μmol (mg Chl *a*)$^{-1}$ h^{-1})	448 ± 32^{a}	679 ± 41^{b}	312 ± 54^{c}	352 ± 80^{c}
$HCO_3^-up_{CaCO3}:HCO_3^-upt_{PS}$	0.77 ± 0.03^{a}	0.85 ± 0.03^{a}	1.07 ± 0.15^{b}	1.22 ± 0.28^{b}
Resp (μmol (mg Chl *a*)$^{-1}$ h^{-1})	100 ± 27^{a}	107 ± 12^{a}	77 ± 16^{a}	85 ± 4^{a}
Phot:Resp	3.0 ± 0.8^{a}	3.5 ± 0.4^{a}	3.6 ± 1.1^{a}	3.5 ± 0.4^{a}

4.5 Discussion

In this study, we measured the differential effects of acclimation to carbonation and acidification on growth, elemental composition and production rates in high-light grown *E. huxleyi*. In order to explain the observed integrated cellular responses, we measured the *in vivo* O_2, CO_2 and HCO_3^- fluxes of the acclimated cells under *in situ* conditions by means of MIMS.

Acclimation to *carbonation* boosts POC and PIC production by stimulating the uptake of HCO_3^-

Rates of POC production were strongly increased in the *carbonation* treatment, but were relatively unaffected under acidified conditions, i.e., in the *acidification* and *OA* treatments (Fig. 4.2 A). The increase in biomass buildup under *carbonation* was also reflected in elevated rates of photosynthetic net O_2 evolution (Fig. 4.3 A). Besides POC production, also PIC production and the MIMS-based estimates of calcification were significantly elevated under *carbonation* (Fig. 4. 2 C, Fig. 4.3 E, Fig. 4.4 B). The carbonation-driven increase in PIC production was larger than the increase in POC production, i.e., PIC:POC ratios increased (Fig. 4.2 C, Table 4.2). This suggests that photosynthesis and calcification share a common intracellular C_i pool, of which the residual C_i is directed towards calcification when photosynthesis is substrate-saturated. A redirection of C_i from photosynthesis to calcification was also observed under nutrient limitation, when cells cannot not sustain photosynthetic biomass production and excess C_i is therefore available (Paasche & Brubak, 1994; van Bleijswijk *et al.*, 1994; Paasche, 1998). On the other hand, PIC:POC ratios were shown to decrease when DIC levels become too low to sustain both processes (Buitenhuis *et al.*, 1999; Zondervan *et al.*, 2002; Bach *et al.*, 2013). Under these conditions, maintaining photosynthesis seems to be more important than sustaining calcification. Apparently, increased calcification acts as a 'sink' for excess C_i, while decreased calcification acts as a C_i 'source' for photosynthesis when intracellular C_i becomes sparse.

By measuring cellular CO_2 and HCO_3^- fluxes, the effects of carbonation on photosynthesis and calcification (Fig. 4.2 B, C, Fig. 4.3 A, E) could be attributed to a stimulated HCO_3^- uptake supplying these processes (Fig. 4. 3 C, F, Fig. 4.4 B). Stimulating carbonation effects are in line with the studies of Bach *et al.* (2011, 2013) and Buitenhuis *et al.* (1999), who found that POC and PIC production are, at constant pH, correlated with external $[HCO_3^-]$. The flux regulations after *acclimation* to carbonation, however, differed from those under *short-term* carbonation, where neither CO_2 uptake nor HCO_3^- uptake were stimulated (Kottmeier *et al.*, 2016). These differences indicate that cells, when being exposed to carbonation over several generations, adjust their metabolism to allow for higher HCO_3^- uptake, especially when light-energization is sufficient (Price *et al.*, 2008). Higher HCO_3^- uptake rates could be achieved by increasing the number of HCO_3^- transporters and/or by shifting from high-affine forms with low transport capacities to low-affine forms with high transport capacities

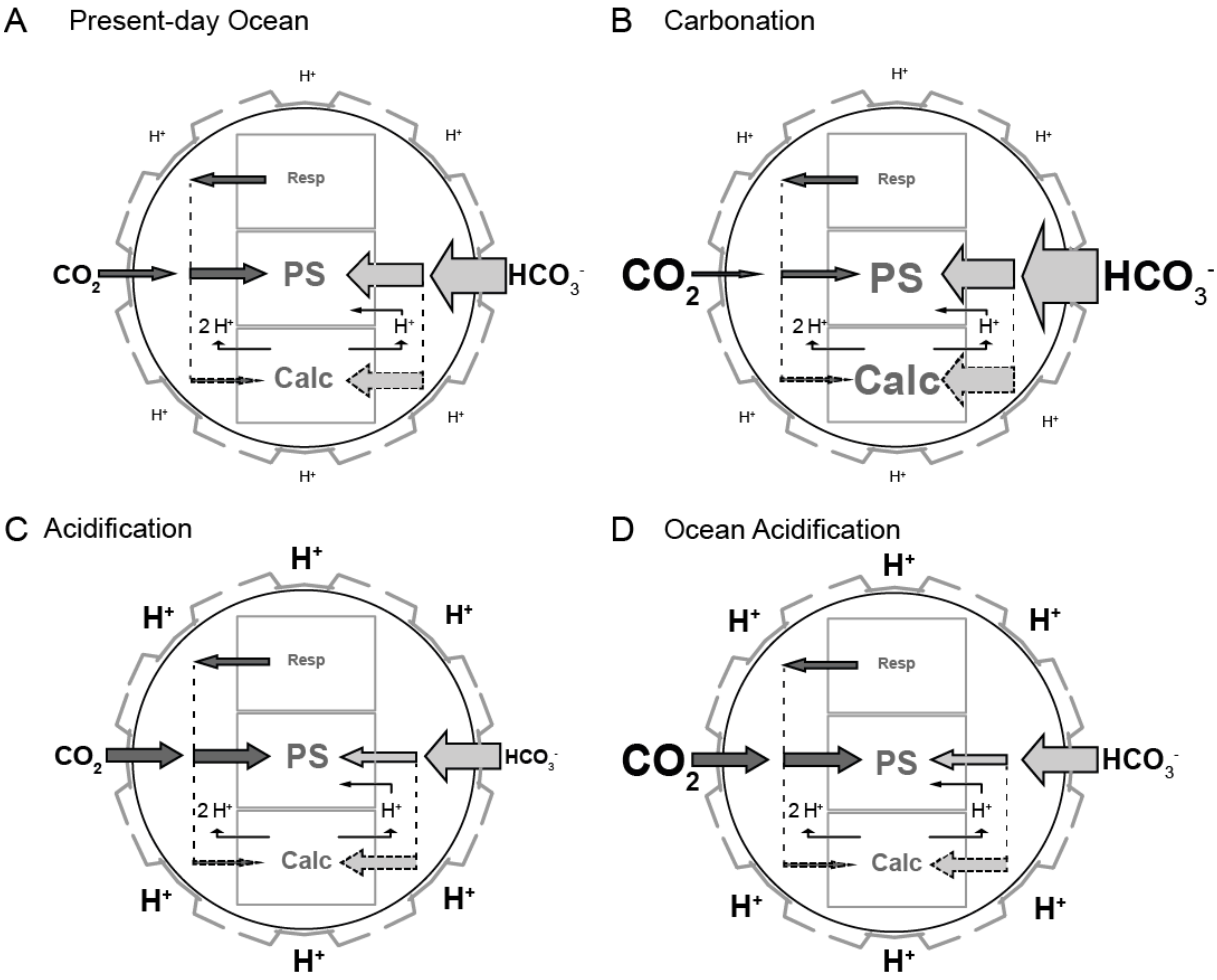

Figure 4.4: Schematic illustration of C_i fluxes in *Emiliania huxleyi* acclimated to different carbonate chemistry settings under high irradiances: A) Under *present-day* conditions, HCO_3^- is the main external substrate for photosynthesis and calcification. Fluxes of HCO_3^- into photosynthesis are slightly higher than HCO_3^- fluxes into calcification, leading to a small consumption of H^+ by photosynthesis. **B)** Under *carbonation*, photosynthesis and calcification are both stimulated by increased HCO_3^- uptake. The increase in calcification is stronger than in photosynthesis, indicating that excess C_i is directed into calcification. The uptake of CO_2 is slightly downscaled, indicating that photosynthesis is largely independent of external [CO_2]. **C)** Under *acidification*, cells maintain constant rates of photosynthesis, whereas calcification is slightly reduced. The photosynthetic C_i requirements are covered by increased proportions of CO_2 uptake, compensating for the reduced uptake of HCO_3^-. The decrease in calcification is likely caused by an inhibited cellular HCO_3^- transport. The ratio of HCO_3^- uptake for calcification vs. HCO_3^- uptake for photosynthesis increases, implying excess production of H^+. **D)** Under *OA*, fluxes are very similar to the fluxes in the *acidification* treatment, indicating that under typical OA scenarios where overall DIC levels are relatively unaffected, acidification effects are more pronounced than carbonation effects. Please note: Sizes of arrows are proportional with the measured fluxes under *in situ* conditions. Dashed arrows represent fluxes that were estimated based on measured PIC:POC ratios at the given conditions.

(Eberlein *et al.*, 2014). Genes involved in C_i uptake were indeed shown to be differentially expressed under changing DIC levels (Bach *et al.*, 2013). Such carbonation effects may have been of importance in the Cretaceous when coccolithophores thrived, because at these times TA, DIC and pH were considerably higher than today (Stanley *et al.*, 2005; Hönisch *et al.*, 2012). However, under the OA scenarios expected for the future, carbonation mainly involves increases in [CO_2] with relatively small increases in [HCO_3^-]. Consequently, typical OA responses cannot be explained by the HCO_3^--driven stimulation of POC and PIC production observed here, but must rather derive from acidification (Fig. 4.4 D).

Acclimation to *acidified conditions* causes opposing regulations in photosynthetic HCO_3^- uptake and CO_2 uptake

Photosynthesis in *E. huxleyi* was relatively unaffected by increased [H^+]: Rates of POC production stayed unaltered after acclimation to *acidification* and only slightly decreased after acclimation to *OA* (Fig. 4.2 B). Also, rates of net O_2 evolution were unaltered in these low-pH treatments (Fig. 4. 3 A). The rather small acidification-sensitivity of high-light grown cells is in line with a previous acclimation study, which found OA responses to become less pronounced with increasing light intensities (Rokitta & Rost, 2012). The acclimation responses observed here, however, were different from short-term responses: When high-light grown *E. huxleyi* cells were exposed to high [H^+] over time scales of minutes, net O_2 evolution significantly decreased (Kottmeier *et al.*, 2016). This inhibition was caused by an impairment of HCO_3^- uptake at concomitantly unaltered CO_2 uptake, leading to an overall decrease in cellular C_i uptake and thus insufficient CO_2 supply at RubisCO. In the current *acclimation* study, such detrimental H^+ effects on overall C_i uptake were not apparent. Instead, *E. huxleyi* was able to reestablish sufficiently high C_i uptake by mitigating the inhibitory H^+ effect on HCO_3^- uptake and slightly increasing CO_2 uptake for photosynthesis (Fig 3 B, C; cf. Fig 3 B, D in Kottmeier *et al.*, 2016.). However, the modified CCM, or other cellular adjustments under low pH, seemed to impose a metabolic burden that resulted in lowered growth (Fig. 4.2 A).

Despite the apparent insensitivity of photosynthesis to acidified conditions, the associated CO_2 and HCO_3^- supply was strongly affected when cells were acclimated to high [H^+]: Photosynthetic CO_2 uptake was significantly stimulated under *acidification* and *OA*, whereas photosynthetic and also total cellular HCO_3^- uptake were significantly decreased (Fig. 4. 3 B, C, G; Fig. 4.4 C, D). The shift in the photosynthetic C_i source is in line with the responses observed under short-term exposure to high [H^+] (Kottmeier *et al.*, 2014; Kottmeier *et al.*, 2016) and shows that typical OA responses are driven by acidification rather than by carbonation, also after acclimation. OA effects on CCMs have often been attributed to the increased seawater CO_2 levels that were thought to enhance diffusive supply for RubisCO. Our results show that this stimulation in CO_2 uptake is actually driven by increased seawater H^+ levels (Kottmeier *et al.*, 2016). The H^+-dependent transition from HCO_3^- uptake to CO_2 uptake may decrease the cells' energetic costs, because HCO_3^- uptake is energy-driven in

E. huxleyi (Kottmeier *et al.*, 2016), while CO_2 is thought to enter phytoplankton cells primarily by diffusion (Giordano *et al.*, 2005; Holtz *et al.*, 2015b; Raven & Beardall, 2016). Respiration, being an indicator for cellular energy demand, was indeed slightly, but insignificantly downscaled under acidified conditions (Table 4.2). However, overall growth was concomitantly also reduced and no obvious reinvestments into other processes, e.g., into POC or PIC production, were observed (Fig. 4.2 A). Thus, there were no indications for a more efficient energy budgeting, at least at the high light levels applied here (Rokitta & Rost, 2012).

H^+-driven shift in C_i source explains the often observed decrease in PIC:POC ratios under OA

Because calcification depends on the same HCO_3^- uptake mechanism as photosynthesis, and both processes share the intracellular C_i pool (Paasche, 1964; Nimer & Merrett, 1996; Holtz *et al.*, 2015a), it is plausible that calcification is also affected by the H^+-driven inhibition of cellular HCO_3^- uptake (Fig. 4.4 C, D). Our data revealed that PIC production was indeed slightly decreased under *acidification* and *OA* (Fig. 4.2 C). The relatively small decrease is likely a result of the applied high light intensities (Rokitta & Rost, 2012). The reason for the decreased PIC production is probably an impairment of cellular HCO_3^- uptake, even though this decrease could not be fully resolved by the MIMS measurements (Fig 4.3 F), possibly because the uncertainties were larger than the effects. An interaction of a H^+-driven decrease (as seen under *acidification* and *OA*) and a HCO_3^--driven increase in calcification (as seen under *carbonation*; Fig 4.2 C) explains the often observed pseudo-correlation with the carbonate saturation state (Ω), which has been discussed recently (Bach, 2015; Cyronak *et al.*, 2015; Rickaby *et al.*, 2016).

A decreased HCO_3^- supply for calcification, next to the increased CO_2 supply for photosynthesis and the prioritization of photosynthesis over calcification under C_i-shortage, may explain the decreases in PIC:POC ratios under OA that were often observed in *E. huxleyi* and other coccolithophores (Raven & Crawfurd, 2012; Meyer & Riebesell, 2015). Depending on species- and strain-specific features (e.g., size and morphotype) and environmental conditions (e.g., irradiance, nutrient status and temperature), either the positive H^+ effect on CO_2 uptake for photosynthesis or the negative H^+ effect on cellular HCO_3^- uptake may overweigh. As a consequence, POC production can be stimulated (e.g., Riebesell *et al.*, 2000; Zondervan *et al.*, 2002), remain constant (e.g., Langer *et al.*, 2009; Müller *et al.*, 2015) or be decreased (e.g., Fiorini *et al.*, 2011; Müller *et al.*, 2015). Because PIC production is mainly affected by the impairment of the HCO_3^- uptake, it typically decreases (e.g., Riebesell *et al.*, 2000; Zondervan *et al.*, 2002; Langer *et al.*, 2009; Müller *et al.*, 2015) or stays constant under OA (e.g., Zondervan *et al.*, 2002; Langer *et al.*, 2009; Fiorini *et al.*, 2011). At times, when photosynthesis benefits from a H^+-driven increase in CO_2 uptake, more HCO_3^- could be directed from POC to PIC production, which could even explain beneficial OA effects on calcification (e.g., Iglesias-Rodriguez *et al.*, 2008).

The above described processes also explain the optimum curvature of PIC and POC production that are often observed in coccolithophores (e.g., Langer *et al.*, 2006; Sett *et al.*, 2014; Bach *et al.*, 2015; Zhang *et al.*, 2015). At very high pCO_2, the negative H^+ effect on HCO_3^- uptake increasingly overweighs the stimulatory H^+ effect on CO_2 uptake, and consequently, production rates decrease. The recently observed shift of production optima towards lower pCO_2 with increasing acclimation light (Zhang *et al.*, 2015) could be a consequence of the fact that the H^+-driven stimulation in photosynthetic CO_2 uptake becomes less pronounced with increasing light (Kottmeier *et al.*, 2016). This also explains why high-light grown phytoplankton can already experience an energetic overload at pCO_2 levels, at which low-light acclimated cells still function properly (Gao *et al.*, 2012; Hoppe *et al.*, 2015; Zhang *et al.*, 2015; Kottmeier *et al.*, 2016).

Decreased growth under elevated [H^+] and irradiance poses a risk for *E. huxleyi* in the future ocean

In the applied low-pH treatments, *E. huxleyi* was, despite the strong flux regulations, able to maintain rather constant photosynthesis, calcification, respiration, POC:PON ratios and Chl *a* quotas (Table 4.2). This was likely possible due to the high energization (400 µmol m^{-2} s^{-1}). However, the ability to maintain these traits seemed to be accomplished at the expense of cellular growth (Fig. 4.2 A). Under acidified conditions, cells may, for example, face increased costs for acid-base regulation, because the decreased seawater pH directly leads to a decreased cytosolic pH (Mackinder *et al.*, 2010; Suffrian *et al.*, 2011; Taylor *et al.*, 2011; Rokitta *et al.*, 2012). Our flux measurements revealed higher biological 'H^+ generation' in the low-pH treatments, i.e., the ratio of HCO_3^- flux into calcification (a pathway that generates H^+) over the HCO_3^- flux into photosynthesis (a pathway that consumes H^+) was significantly increased (Fig. 4.3 H; 4.4 C, D; cf., Holtz *et al.*, 2015a; Kottmeier *et al.*, 2016). Such a H^+ imbalance may become even larger with increasing irradiances, because the overall HCO_3^- fluxes are higher under these conditions, and consequently more H^+ are released intracellularly. This explains why *E. huxleyi* may face lowered growth in a future ocean, especially under high light (this study; Langer *et al.*, 2009; Rokitta & Rost, 2012; Kottmeier *et al.*, 2014).

The future of coccolithophores is often predicted based on their sensitivity in POC and PIC production rates. Changes in growth, even when being seemingly small, can yet have large consequences that are not necessarily reflected in production rates: The observed drop in growth under high [H^+] from ~1.15 to 1.00 d^{-1} would, for example, lead to a 50% discrepancy in the POC buildup of a population over the course of only four days. Even though *E. huxleyi* is known to exhibit an exceptional tolerance for high irradiances (Nanninga & Tyrrell, 1996; Nielsen, 1997; Trimborn *et al.*, 2007; Ragni *et al.*, 2008), the decreased growth under high light and low pH, and the higher susceptibility to photoinhibition (Kottmeier *et al.*, 2016), suggest that under future OA, *E. huxleyi* will be close to the upper limit of its physiological scope. Under the dynamic light in natural environments, the balancing of variable C_i demands

with the limited C_i uptake capacities under OA may become even more challenging (Rost *et al.*, 2006; Jin *et al.*, 2013; Hoppe *et al.*, 2015; Xing *et al.*, 2015; Xu & Gao, 2015). Because *E. huxleyi* forms blooms in summer, i.e., in high-light conditions, the species may face difficulties in sustaining its growth and partially lose its exceptional blooming capacities in a future ocean.

Conclusions

In this study, we confirmed the strong acidification-dependent regulations of C_i fluxes in *E. huxleyi* that were earlier observed after short-term exposure to high $[H^+]$. We found that, at typical OA scenarios, acidification effects dominate over carbonation effects. The verification of the strong H^+ dependency in flux regulations, also after acclimation, now allows us to explain the integrated OA responses of coccolithophores measured in the last decades: The common pattern of decreased PIC:POC ratios under OA can be attributed to the H^+-driven decrease in cellular HCO_3^- uptake and the concomitant increase in photosynthetic CO_2 uptake. Because calcification cannot access CO_2 as a compensatory C_i source, it is generally more affected by increasing $[H^+]$ and therefore decreases relative to photosynthesis. Overall, the strength of the antagonistic H^+ effects on HCO_3^- and CO_2 uptake can, however, vary and thereby determine the magnitude and direction of OA responses.

Acknowledgements

We thank Christian Großmann for supporting us with the culture work, carbonate chemistry measurements and cell harvesting, and Klaus-Uwe Richter and David Stronzek for the technical support with the mass spectrometer. Our thanks also go to Beate Müller, Ulrike Richter and Anja Terbrüggen for measuring the DIC, ANCA and nutrient samples. The interpretation of our data strongly profited from the fruitful discussions with Lena Holtz. The project was financially supported by funding from the German Federal Ministry for Education and Research (BMBF) in the framework of the project Bioacid II (03F0655B) and ZeBiCa^2 (grant no. 031A518C).

4.6 References

Bach LT. 2015. Reconsidering the role of carbonate ion concentration in calcification by marine organisms. *Biogeosciences Discussions* **12**(9): 6689-6722.

Bach LT, Mackinder LC, Schulz KG, Wheeler G, Schroeder DC, Brownlee C, Riebesell U. 2013. Dissecting the impact of CO_2 and pH on the mechanisms of photosynthesis and calcification in the coccolithophore *Emiliania huxleyi*. *New Phytologist* **199**(1): 121-134.

Bach LT, Riebesell U, Gutowska MA, Federwisch L, Schulz KG. 2015. A unifying concept of coccolithophore sensitivity to changing carbonate chemistry embedded in an ecological framework. *Progress in Oceanography* **135**: 125-138.

Bach LT, Riebesell U, Schulz KG. 2011. Distinguishing between the effects of ocean acidification and ocean carbonation in the coccolithophore *Emiliania huxleyi*. *Limnology and Oceanography* **56**(6): 2040-2050.

Badger MR, Palmqvist K, Yu JW. 1994. Measurement of CO_2 and HCO_3^- fluxes in cyanobacteria and microalgae during steady-state photosynthesis. *Physiologia Plantarum* **90**(3): 529-536.

Broecker WS, Peng TH. 1987. The role of $CaCO_3$ compensation in the glacial to interglacial atmospheric CO_2 change. *Global Biogeochemical Cycles* **1**(1): 15-29.

Buitenhuis ET, De Baar HJW, Veldhuis MJW. 1999. Photosynthesis and calcification by *Emiliania huxleyi* (Prymnesiophyceae) as a function of inorganic carbon species. *Journal of Phycology* **35**(5): 949-959.

Burkhardt S, Amoroso G, Riebesell U, Sultemeyer D. 2001. CO_2 and HCO_3^- uptake in marine diatoms acclimated to different CO_2 concentrations. *Limnology and Oceanography* **46**(6): 1378-1391.

Caldeira K, Wickett ME. 2003. Anthropogenic carbon and ocean pH - The coming centuries may see more oceanic acidification than the past 300 million years. *Nature* **425**(365): 365.

Cyronak T, Schulz KG, Jokiel PL. 2015. The Omega myth: what really drives lower calcification rates in an acidifying ocean. *ICES Journal of Marine Science: Journal du Conseil*: fsv075.

Eberlein T, Van de Waal DB, Rost B. 2014. Differential effects of ocean acidification on carbon acquisition in two bloom-forming dinoflagellate species. *Physiol Plant* **151**(4): 468-479.

Fiorini S, Middelburg JJ, Gattuso JP. 2011. Effects of elevated CO2 partial pressure and temperature on the coccolithophore Syracosphaera pulchra. *Aquatic Microbial Ecology* **64**(3): 221-232.

Fukuda SY, Suzuki Y, Shiraiwa Y. 2014. Difference in physiological responses of growth, photosynthesis and calcification of the coccolithophore *Emiliania huxleyi* to acidification by acid and CO_2 enrichment. *Photosynthesis Research* **121**(2-3): 299-309.

Gao K, Xu J, Gao G, Li Y, Hutchins DA, Huang B, Wang L, Zheng Y, Jin P, Cai X, et al. 2012. Rising CO_2 and increased light exposure synergistically reduce marine primary productivity. *Nature Climate Change* **2**(7): 519-523.

Giordano M, Beardall J, Raven JA. 2005. CO_2 concentrating mechanisms in Algae: mechanisms, environmental modulation, and evolution. *Annual Review of Plant Biology* **56**(1): 99-131.

Guillard RRL, Ryther JH. 1962. Studies of marine planktonic diatoms. *Canadian Journal of Microbiology* **8**: 229-239.

Holligan PM, Fernandez E, Aiken J, Balch WM, Boyd P, Burkill PH, Finch M, Groom SB, Malin G, Muller K, et al. 1993. A biogeochemical study of the coccolithophore, *Emiliania huxleyi,* in the North-Atlantic. *Global Biogeochemical Cycles* **7**(4): 879-900.

Holtz LM, Wolf-Gladrow DA, Thoms S. 2015a. Numerical cell model investigating cellular carbon fluxes in *Emiliania huxleyi*. *Journal of Theoretical Biology* **364**: 305-315.

Holtz LM, Wolf-Gladrow DA, Thoms S. 2015b. Simulating the effects of light intensity and carbonate system composition on particulate organic and inorganic carbon production in *Emiliania huxleyi*. *Journal of Theoretical Biology* **372**: 192-204.

Hönisch B, Ridgwell A, Schmidt DN, Thomas E, Gibbs SJ, Sluijs A, Zeebe R, Kump L, Martindale RC, Greene SE, et al. 2012. The geological record of ocean acidification. *Science* **335**(6072): 1058-1063.

Hoppe CJM, Holtz L-M, Trimborn S, Rost B. 2015. Ocean Acidification decreases the light use efficiency in an Antarctic diatom under dynamic but not constant light. *New Phytologist* **207**(1): 159-171.

Iglesias-Rodriguez MD, Halloran PR, Rickaby RE, Hall IR, Colmenero-Hidalgo E, Gittins JR, Green DR, Tyrrell T, Gibbs SJ, von Dassow P, et al. 2008. Phytoplankton calcification in a high-CO_2 world. *Science* **320**(5874): 336-340.

Jin P, Gao K, Villafane VE, Campbell DA, Helbling EW. 2013. Ocean acidification alters the photosynthetic responses of a coccolithophorid to

fluctuating ultraviolet and visible radiation. *Plant Physiology* **162**(4): 2084-2094.

Knap A, Michaels A, Close A, Ducklow H, Dickson A. 1996. Protocols for the joint global ocean flux study (JGOFS) core measurements. Reprint of the IOC Manuals and Guides No. 29. Oak Ridge: UNESCO 1994.

Kottmeier DM, Rokitta SD, Rost B. 2016. Acidification, not carbonation, is the major regulator of carbon fluxes in the coccolithophore *Emiliania huxleyi*. *New Phytologist*.

Kottmeier DM, Rokitta SD, Tortell PD, Rost B. 2014. Strong shift from HCO_3^- to CO_2 uptake in *Emiliania huxleyi* with acidification: new approach unravels acclimation versus short-term pH effects. *Photosynthesis Research* **121**(2-3): 265-275.

Kroeker KJ, Kordas RL, Crim R, Hendriks IE, Ramajo L, Singh GS, Duarte CM, Gattuso JP. 2013. Impacts of ocean acidification on marine organisms: quantifying sensitivities and interaction with warming. *Global Change Biology* **19**(6): 1884-1896.

Langer G, Geisen M, Baumann KH, Kläs J, Riebesell U, Thoms S, Young JR. 2006. Species-specific responses of calcifying algae to changing seawater carbonate chemistry. *Geochemistry Geophysics Geosystems* **7**(9).

Langer G, Nehrke G, Probert I, Ly J, Ziveri P. 2009. Strain-specific responses of *Emiliania huxleyi* to changing seawater carbonate chemistry. *Biogeosciences* **6**(11): 2637-2646.

Lefebvre SC, Benner I, Stillman JH, Parker AE, Drake MK, Rossignol PE, Okimura KM, Komada T, Carpenter EJ. 2012. Nitrogen source and pCO_2 synergistically affect carbon allocation, growth and morphology of the coccolithophore *Emiliania huxleyi*: potential implications of ocean acidification for the carbon cycle. *Global Change Biology* **18**(2): 493-503.

Mackinder L, Wheeler G, Schroeder D, Riebesell U, Brownlee C. 2010. Molecular mechanisms underlying calcification in coccolithophores. *Geomicrobiology Journal* **27**: 585-595.

Meyer J, Riebesell U. 2015. Reviews and Syntheses: Responses of coccolithophores to ocean acidification: a meta-analysis. *Biogeosciences* **12**(6): 1671-1682.

Müller MN, Trull TW, Hallegraeff GM. 2015. Differing responses of three Southern Ocean *Emiliania huxleyi* ecotypes to changing seawater carbonate chemistry. *Marine Ecology Progress Series* **531**: 81-90.

Nanninga HJ, Tyrrell T. 1996. Importance of light for the formation of algal blooms by *Emiliania huxleyi*. *Marine Ecology Progress Series* **136**(1-3): 195-203.

Nielsen MV. 1997. Growth, dark respiration and photosynthetic parameters of the coccolithophorid *Emiliania huxleyi* (Prymnesiophyceae) acclimated to different day length-irradiance combinations. *Journal of Phycology* **33**(5): 818-822.

Nimer NA, Merrett MJ. 1996. The development of a CO_2-concentrating mechanism in *Emiliania huxleyi*. *New Phytologist* **133**(3): 383-389.

Paasche E 1964. A tracer study of the inorganic carbon uptake during coccolith formation and photosynthesis in the coccolithophorid *Coccolithus huxleyi*. Lund: Scandinavian Society for Plant Physiology.

Paasche E. 1998. Roles of nitrogen and phosphorus in coccolith formation in *Emiliania huxleyi* (Prymnesiophyceae). *European Journal of Phycology* **33**(1): 33-42.

Paasche E, Brubak S. 1994. Enhanced calcification in the coccolithophorid *Emiliania huxleyi* (Haptophyceae) under phosphorus limitation. *Phycologia* **33**(5): 324-330.

Pierrot D, Lewis E, Wallace D 2006. MS Excel program developed for CO_2 system calculations. *ORNL/CDIAC-105. Carbon Dioxide Information Analysis Center, Oak Ridge National Laboratory, US Department of Energy, Oak Ridge, Tennessee*.

Price GD, Badger MR, Woodger FJ, Long BM. 2008. Advances in understanding the cyanobacterial CO_2-concentrating-mechanism (CCM): functional components, C_i transporters, diversity, genetic regulation and prospects for engineering into plants. *Journal of Experimental Botany* **59**(7): 1441-1461.

Ragni M, Airs RL, Leonardos N, Geider RJ. 2008. Photoinhibition of PSII in *Emiliania huxleyi* (Haptophyta) under high light stress: The roles of photoacclimation, photoprotection, and photorepair. *Journal of Phycology* **44**(3): 670-683.

Raitsos D, Lavender S, Pradhan Y, Tyrrell T, Reid P, Edwards M. 2006. Coccolithophore bloom size variation in response to the regional environment of the subarctic North Atlantic. *Limnology and Oceanography* **51**(5): 2122-2130.

Raven J, Crawfurd K. 2012. Environmental controls on coccolithophore calcification. *Marine Ecology Progress Series* **470**: 137-166.

Raven JA, Beardall J. 2016. The ins and outs of CO_2. *Journal of Experimental Botany* **67**(1): 1-13.

Read BA, Kegel J, Klute MJ, Kuo A, Lefebvre SC, Maumus F, Mayer C, Miller J, Monier A, Salamov A, et al. 2013. Pan genome of the phytoplankton *Emiliania* underpins its global distribution. *Nature* **499**(7457): 209-213.

Rickaby RE, Hermoso M, Lee RB, Rae BD, Heureux AM, Balestreri C, Chakravarti L, Schroeder DC, Brownlee C. 2016. Environmental carbonate chemistry selects for phenotype of recently

isolated strains of Emiliania huxleyi. *Deep Sea Research Part II: Topical Studies in Oceanography*.

Riebesell U, Zondervan I, Rost B, Tortell PD, Zeebe E, Morel FMM. 2000. Reduced calcification in marine plankton in response to increased atmospheric CO_2. *Nature* **407**: 634-637.

Rokitta S, John U, Rost B. 2012. Ocean acidification affects redox-balance and ion-homeostasis in the life-cycle stages of *Emiliania huxleyi*. *PLOS ONE* **7**(12): e52212.

Rokitta S, Rost B. 2012. Effects of CO_2 and their modulation by light in the life-cycle stages of the coccolithophore *Emiliania huxleyi*. *Limnology and Oceanography* **57**(2): 607-618.

Rost B, Riebesell U 2004. Coccolithophores and the biological pump: responses to environmental changes. In: Thierstein HR, Young JR eds. *Coccolithophores - From Molecular Processes to Global Impact*. Heidelberg: Springer, 76–99.

Rost B, Riebesell U, Sültemeyer D. 2006. Carbon acquisition of marine phytoplankton: effect of photoperiod length. *Limnology and Oceanography* **51**(1): 12-20.

Rost B, Zondervan I, Riebesell U. 2002. Light-dependent carbon isotope fractionation in the coccolithophorid *Emiliania huxleyi*. *Limnology and Oceanography* **47**(1): 120-128.

Schulz KG, Rost B, Burkhardt S, Riebesell U, Thoms S, Wolf-Gladrow DA. 2007. The effect of iron availability on the regulation of inorganic carbon acquisition in the coccolithophore *Emiliania huxleyi* and the significance of cellular compartmentation for stable carbon isotope fractionation. *Geochimica et Cosmochimica Acta* **71**: 5301-5312.

Sett S, Bach LT, Schulz KG, Koch-Klavsen S, Lebrato M, Riebesell U. 2014. Temperature modulates coccolithophorid sensitivity of growth, photosynthesis and calcification to increasing seawater pCO_2. *PLOS ONE* **9**(2): e88308.

Sikes CS, Roer RD, Wilbur KM. 1980. Photosynthesis and coccolith formation: inorganic carbon sources and net inorganic reaction of deposition. *Limnology and Oceanography* **25**(2): 248-261.

Stanley SM, Ries JB, Hardie LA. 2005. Seawater chemistry, coccolithophore population growth, and the origin of Cretaceous chalk. *Geology* **33**(7): 593.

Stoll MHC, Bakker K, Nobbe GH, Haese RR. 2001. Continuous-flow analysis of dissolved inorganic carbon content in seawater. *Analytical Chemistry* **73**(17): 4111-4116.

Suffrian K, Schulz KG, Gutowska MA, Riebesell U, Bleich M. 2011. Cellular pH measurements in *Emiliania huxleyi* reveal pronounced membrane proton permeability. *New Phytologist* **190**(3): 595-608.

Taylor AR, Chrachri A, Wheeler G, Goddard H, Brownlee C. 2011. A voltage-gated H^+ channel underlying pH homeostasis in calcifying coccolithophores. *PLOS Biology* **9**(6): e1001085.

Trimborn S, Langer G, Rost B. 2007. Effect of varying calcium concentrations and light intensities on calcification and photosynthesis in *Emiliania huxleyi*. *Limnology and Oceanography* **52**(5): 2285-2293.

Tyrrell T, Merico A 2004. *Emiliania huxleyi*: bloom observations and the conditions that induce them. *Coccolithophores: From Molecular Processes to Global Impact*, 75-97.

van Bleijswijk JD, Kempers RS, Veldhuis MJ, Westbroek P. 1994. Cell and growth characteristics of types A and B of *Emiliania huxleyi* (Prymnesiophyceae) as determined by flow cytometry and chemical analyses. *Journal of Phycology* **30**(2): 230-241.

Wolf-Gladrow DA, Riebesell U, Burkhardt S, Bijma J. 1999. Direct effects of CO_2 concentration on growth and isotopic composition of marine plankton. *Tellus Series B - Chemical and Physical Meteorology* **51**(2): 461-476.

Xing T, Gao K, Beardall J. 2015. Response of Growth and Photosynthesis of *Emiliania huxleyi* to Visible and UV Irradiances under Different Light Regimes. *Photochemistry and Photobiology*.

Xu K, Gao K. 2015. Solar UV Irradiances modulate effects of ocean acidification on the coccolithophorid *Emiliania huxleyi*. *Photochemistry and Photobiology* **91**(1): 92-101.

Zeebe RE, Wolf-Gladrow DA. 2001. *CO_2 in seawater: equilibrium, kinetics, isotopes*. Amsterdam: Elsevier Science B.V.

Zhang Y, Bach LT, Schulz KG, Riebesell U. 2015. The modulating effect of light intensity on the response of the coccolithophore *Gephyrocapsa oceanica* to ocean acidification. *Limnology and Oceanography* **60**(6): 2145-2157.

Zondervan I. 2007. The effects of light, macronutrients, trace metals and CO_2 on the production of calcium carbonate and organic carbon in coccolithophores - A review. *Deep-Sea Research Part II: Topical Studies in Oceanography* **54**(5-7): 521-537.

Zondervan I, Rost B, Riebesell U. 2002. Effect of CO_2 concentration on the PIC/POC ratio in the coccolithophore *Emiliania huxleyi* grown under light-limiting conditions and different daylengths. *Journal of Experimental Marine Biology and Ecology* **272**(1): 55-70.

Chapter 5
Synthesis

5.1 Major findings of this thesis

By conducting three studies on the physiological adjustments of *Emiliania huxleyi* to changing carbonate chemistry and light, fundamentals in the species' mechanisms of photosynthetic inorganic carbon (C_i) acquisition, calcification, growth, pH homeostasis and energy budgets could be characterized in this thesis (Fig. 5.1). With this knowledge, the mechanisms underlying typical ocean acidification (OA) responses in *E. huxleyi* and other coccolithophores could be resolved.

Publication I: Strong shift from HCO_3^- to CO_2 uptake in *Emiliania huxleyi* with acidification: new approach unravels acclimation versus short-term pH effects

In the first publication, effects of decreasing pH and the associated increases in seawater [CO_2] on the photosynthetic C_i source of *E. huxleyi* were investigated. To this end, both life-cycle stages were acclimated to present-day and OA conditions. After acclimation, the integrated responses towards the changing conditions were assessed and a ^{14}C disequilibrium technique was conducted at ecologically relevant pH values (pH 7.9 - 8.7) and constant DIC, measuring the C_i source of the differently acclimated cells.

Acclimation to OA caused increased rates of particulate organic carbon (POC) production and decreased rates particulate inorganic carbon (PIC) production in the diploid life-cycle stage, and had no significant effect on the integrated responses of the haploid stage. Apparently, both life-cycle stages of *E. huxleyi* increased their relative CO_2 usage with decreasing pH. When measurements of differently acclimated cells were done at the same pH, no significant differences in the C_i source could be detected. Hence, the shifts in the C_i source occurred on time scales of seconds to minutes and overruled potential acclimation effects.

The increased CO_2 usage at low pH/high [CO_2] in the diploid stage can explain the often observed beneficial OA-effects on photosynthetic biomass production (Raven & Crawfurd, 2012). The absence of acclimation effects indicated that the change in the C_i source is not a result of changing gene expression, but is directly driven by the external carbonate chemistry. This implies that, in order to explain integrated OA-responses, C_i sources should be measured at the same pH values/carbonate chemistry as applied under *in situ* conditions, rather than at pH-standardised conditions as it is often the case. The similar regulations in the diploid and haploid stages were rather unexpected, because the haploid stage has been shown to be relatively insensitive towards changing carbonate chemistry.

Publication II: Acidification, not carbonation, is the major regulator of carbon fluxes in the coccolithophore *Emiliania huxleyi*

The aim of the second study was to resolve the drivers behind the observed flux regulations by means of membrane-inlet mass spectrometry (MIMS; Badger *et al.*, 1994; Schulz *et al.*, 2007), i.e., to test whether increased CO_2, HCO_3^- or H^+ levels were responsible for the

observed shift in the C_i source. This approach moreover served as a method comparison between the ^{14}C and the MIMS approach, that were earlier shown to yield comparable results despite the strong difference in the applied pH values (Rost *et al.*, 2007).

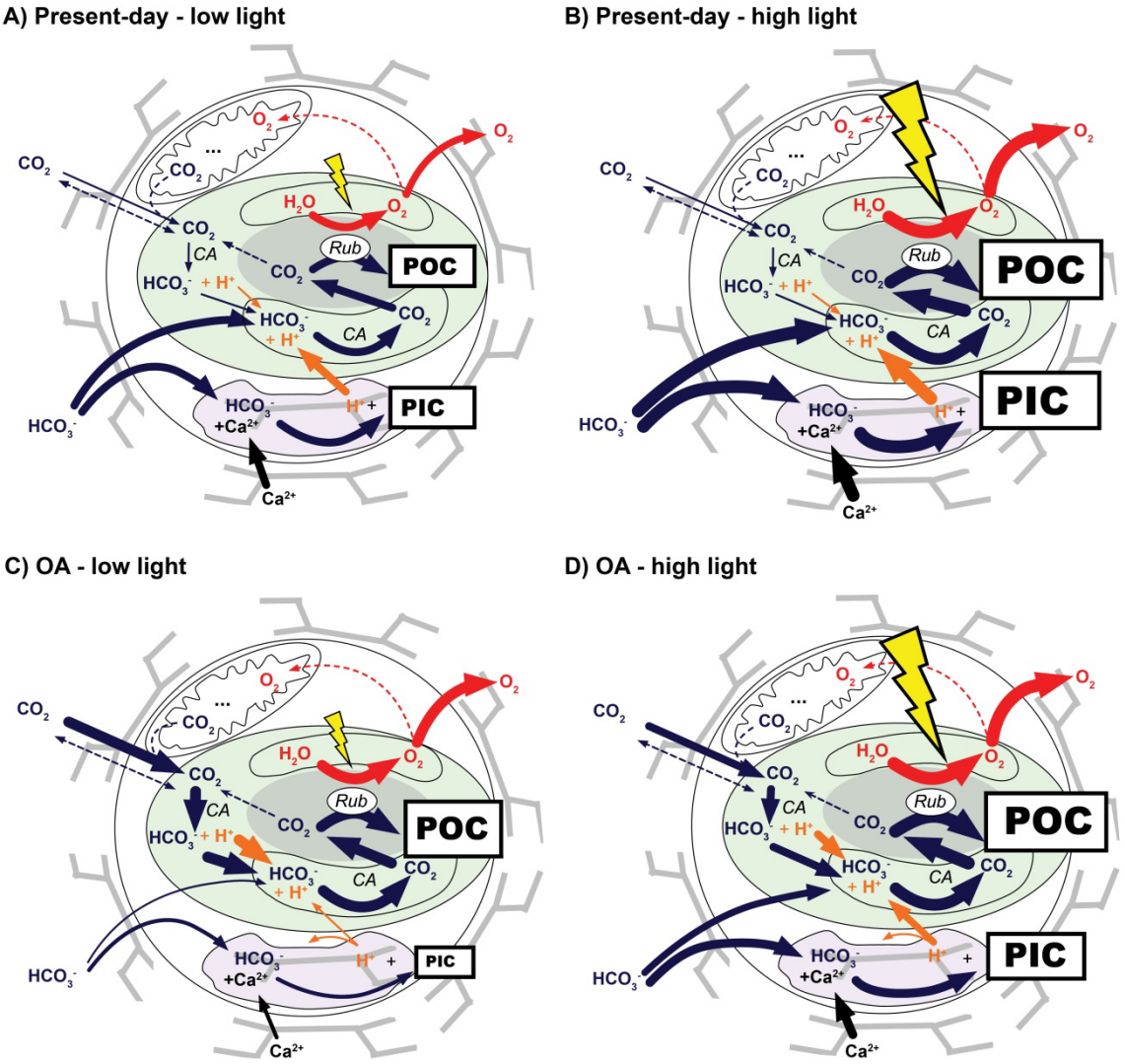

Figure 5.1: Summary of the flux regulations in *E. huxleyi* observed in this thesis. A) Under present-day and low-light conditions, the major part of the cellular C_i demand is covered by HCO_3^-, being equally distributed between photosynthesis and calcification. A similar amount of H^+ is consumed in HCO_3^--based photosynthesis, as being produced by HCO_3^--based calcification. This reduces the necessity of H^+ pumping over the plasmalemma. **B)** The increased C_i demand under high irradiances is covered by additional HCO_3^-, also being equally distributed between photosynthesis and calcification. **C)** After acclimation to OA and low-light conditions, cellular HCO_3^- is strongly inhibited by the increased $[H^+]$, leading to decreased calcification. The decreased HCO_3^- uptake for photosynthesis is overcompensated by additional CO_2 uptake, leading to stimulated photosynthesis. **D)** After acclimation to OA and high-light conditions, the H^+ effects on CO_2 and HCO_3^- uptake are less pronounced than under low light, resulting in relatively little changes in calcification and photosynthesis. However, high-light acclimated cells are less flexible in increasing the C_i uptake when the demand quickly becomes higher and are therefore more prone to C_i limitation.

Present-day acclimated diploid and haploid life-cycle stages of *E. huxleyi* were exposed to a matrix of two pH levels (8.15, 7.85) and two levels of dissolved inorganic carbon (1400, 2800 µmol kg^{-1}) and their *real-time* fluxes under these conditions were measured utilizing MIMS. Since light has previously been shown to modulate OA-responses in *E. huxleyi* and other phytoplankton taxa (Kranz *et al.*, 2010; Rokitta & Rost, 2012), flux regulations were measured in low- as well as high-light acclimated cells and, additionally, low and high irradiances were applied during the flux measurements.

Regarding the increased CO_2 uptake under low pH/high [CO_2], flux regulations in the diploid stage were similar to the regulations observed with the ^{14}C disequilibrium approach. CO_2 uptake was stimulated under acidified conditions. Contrary to the commonly assumed hypothesis that the photosynthetic C_i source is driven by [CO_2], these regulations were instead driven by the external [H^+]. Acidification significantly inhibited HCO_3^- uptake and increased the photosynthetic net CO_2 uptake (Fig. 5.1). The effects were, however, different in magnitude between low- and high-light acclimated cells: Low-light acclimated cells experienced a very pronounced beneficial H^+ effect on CO_2 uptake that even overcompensated for the lowered HCO_3^- uptake and led to increased photosynthesis (Fig. 5.1). High-light acclimated cells maintained almost constant CO_2 uptake rates despite the inhibited HCO_3^- uptake and therefore experienced an insufficient C_i supply for photosynthesis. In contrast to the ^{14}C measurements, which showed that CO_2 was the primary external C_i source at typical oceanic pH values (~8.1), the MIMS-measurements revealed that HCO_3^- was the primary C_i species taken up for photosynthesis at these conditions (Fig. 5.1). In the haplont, cellular C_i acquisition was relatively insensitive to carbonate chemistry. Also here, ^{14}C and MIMS measurements yielded offsets in the assessed C_i source.

The ability of low-light acclimated cells to increase their CO_2 uptake under high [H^+], explained their pronounced increase in biomass production under typical OA conditions (Fig. 5.1; Rokitta & Rost, 2012). The absence of an additional CO_2 uptake in high-light acclimated cells, despite the same decrease in HCO_3^- uptake, explained why photosynthesis does not benefit from OA in these cells (e.g., Rokitta & Rost, 2012), and indicated that they are more prone to C_i limitation in the future ocean. The contradicting results in terms of C_i source between the ^{14}C and the MIMS measurements led to the conclusion that the mathematical models and assumptions underlying the two methods should be reassessed (see section 5.3).

Publication III: H^+-driven impairment of HCO_3^- uptake manifests after acclimation and explains declined calcification in coccolithophores

In order to answer the question how cellular fluxes are regulated after acclimation to altered conditions and how fluxes into calcification are regulated, *real-time* fluxes underlying the integrated responses to carbonation, acidification and their combination were measured. The diploid life-cycle stage of *E. huxleyi* was acclimated to a matrix of two CO_2 (15 and 30 µmol kg^{-1}) and two pH levels (8.15 and 7.85) under irradiances of 400 μmol photons m^{-2} s^{-1} and the

integrated responses in terms of elemental composition and growth as well as the cellular fluxes associated with photosynthesis and respiration were measured under *in situ* conditions. Using the measured ratios of PIC:POC, also the C_i fluxes into calcification could be estimated.

The strong H^+ effects on photosynthetic C_i fluxes being evident under short-term acidification in the first and second study, was also observed on longer time scales: Acidification slightly stimulated the photosynthetic CO_2 uptake and reduced the HCO_3^- uptake for both, photosynthesis and calcification (Fig. 5.1). Overall, diploid *E. huxleyi* cells were able to adjust their C_i acquisition in order to sustain constant photosynthesis under the applied light levels. Thus, the decrease in HCO_3^- uptake was slightly less pronounced and the increase in CO_2 uptake was slightly higher after acclimation. The metabolic adjustment to acidification were apparently performed at the cost of overall growths. Surprisingly, carbonation had no stimulating effects on CO_2 uptake, but strongly increased HCO_3^- uptake.

The fact that calcification could not switch to an alternative external C_i source under acidification explained why OA had generally a detrimental effect on calcification, while biomass production remained unaffected or even increased. As HCO_3^- levels are relatively stable under natural OA, the observed carbonation effects on HCO_3^- supply likely do not contribute strongly to the typical OA responses (Fig. 5.1).

5.2 Flux regulations in *Emiliania huxleyi*

The CO_2-concentrating mechanism of *Emiliania huxleyi* is highly sensitive to protons

In this thesis, a strong H^+ influence on cellular C_i and O_2 fluxes in *E. huxleyi* was observed and shown to be responsible for the bulk of observed OA responses in the species. Next to earlier findings that changes in external [H^+] rapidly propagate into intracellular compartments (Suffrian *et al.*, 2011), *Publication II and III* revealed that this intracellular acidification may partly be due to a positive biological feedback to external acidification: The ratio between HCO_3^--based photosynthesis that consumes H^+, and HCO_3^--based calcification that releases H^+ was decreased and therefore caused an overall increase in the intracellular H^+ production (Fig. 5.1; *Publication II and III*). Acidification has moreover been suggested to impair the H^+ efflux through voltage-gated H_v1 H^+ channels that rely on a trans-membrane H^+ electrochemical gradient (Taylor *et al.*, 2011). All in all, there are external and internal processes that cause intracellular acidification in coccolithophores, which, in turn, can theoretically affect all proteins or enzymes involved in photosynthesis and calcification.

Proton-dependent regulations of enzymatic processes at different molecular levels are a basic principle in biochemistry. The functional pH-optima of enzymes are often defined by the (de)protonation behavior of accessible sidechains, affecting the affinities of enzymes towards substrates or their allosteric modulators (Berg *et al.*, 2002). Protons can also function as

substrate or allosteric modulator itself, e.g., as an allosteric regulator of the O_2-binding hemoglobin (Wurm & Albers, 1989). They are furthermore a substrate for numerous H^+ channels and transporters, e.g., of voltage-gated H^+ channels, Ca^{2+}/H^+ antiporters, or different ATPases. Affecting the overall morphology of the headgroups of the membrane lipid bilayers (Leung, 2012; Leung *et al.*, 2013), H^+ could also effect the permeability for CO_2 or other molecules.

From the data obtained in this thesis, it appears that acidification directly or indirectly inhibits HCO_3^- transport. While the observed regulations in CO_2 and O_2 fluxes were very diverse, the inhibition under high $[H^+]$ was a conserved pattern because it appeared independently of the applied light conditions and exposure times. The inhibitory effects of H^+ on HCO_3^- transporters, which were previously suggested by Fukuda *et al.* (2014), explain why calcification becomes typically affected by OA (Raven and Crawfurd, 2011). This H^+ dependency in HCO_3^- uptake together with the strong stimulatory effect of H^+ on the photosynthetic CO_2 uptake solves the longstanding puzzle why C_i acquisition in an apparent HCO_3^- users is strongly impacted by OA, even though the external $[HCO_3^-]$ is not considerably increased under elevated pCO_2 (cf., Fig. 1.6; Rost & Riebesell, 2004).

The influence of light-energization on ocean acidification responses

In this work, the immediate effects of light on the C_i uptake behavior were compared with acclimation responses to changing light. When exposing *E. huxleyi* to increased irradiances over short time-scales, CO_2 uptake was relatively unaffected while HCO_3^- uptake was strongly stimulated (*Publication III*). This hinted at CO_2 uptake taking place passively, but HCO_3^- taking place by active transport mechanisms. The stimulatory effect of light on HCO_3^- uptake was also evident under acidified conditions. Hence, cellular energization as the driver of HCO_3^- transport could, to a certain degree, compensate for the inhibition by high $[H^+]$. Acclimation to different light intensities affected the cell's capacity for CO_2 uptake under acidified conditions: While low-light acclimated cells were able to strongly increase photosynthetic CO_2 uptake under high $[H^+]$, high-light acclimated cells were not able do this. Such differences may be consequence of morphological adjustments, allowing the cells to perform under their different demands and availabilities. While low-light grown cells are light-limited and can therefore cover a higher proportion of its lower C_i demand by the "cheaper" CO_2 uptake, high-light grown cells are more prone to be C_i-limited and thus need to investigate more energy into active pumping of HCO_3^- (Rost *et al.*, 2006; Raven, 2011).

The sum of these immediate and acclimation effects explains the difference in OA-responses between low- and high-light acclimated cells (*Publication I, II*). POC production in low-light grown cells benefits strongly from the H^+ driven stimulation in CO_2 uptake, but these cells lack the energy to act against the inhibitory H^+ effect in calcification. The PIC:POC ratio therefore strongly decreased under OA (Fig. 5.1). High-light grown cells can partly compensate for the decreased HCO_3^- uptake under high $[H^+]$, sustaining higher rates of both, POC and PIC production. These adjustments to acidification, however, seemed to be

performed at the expense of overall growth (Fig. 5.2; *Publication III*). This underlines that high-light acclimated cells of *E. huxleyi* are at the limit of their C_i uptake capacities, which supports recent findings that high-light grown cells are more prone to photoinhibition under OA (*Publication II*; Gao *et al.*, 2012; Hoppe *et al.*, 2015). Inhibited growth in *E. huxleyi* acclimated to OA is a commonly observed response that may have strong ecological and biogeochemical consequences. Even though the effect size is seemingly small, the decrease is carried forward exponentially, i.e., a culture with decreased calcification and constant growth produces more PIC than a culture with constant calcification and decreased growth (Fig. 5.3; *Publication III*).

5.3 How do measurement techniques affect our view?

Synchronized growth in *E. huxleyi*

Photosynthetic fluxes and their regulations are traditionally investigated on different time scales and by different methods. Effects of environmental conditions to cellular responses can be measured as integrated responses, i.e., as the averaged values of the cell culture, in which processes that occurred over time have summed up. Such integrated responses are, for example, growth or cellular elemental quotas (e.g., POC and PIC quotas; pg $cell^{-1}$) and can, in a first approximation, be used to draw conclusions about processes that caused these effects. As the integrated responses do not take into account diurnal variations and interference of processes, *in vivo* flux measurements, e.g., of O_2 evolution or C_i fixation, can be more suitable

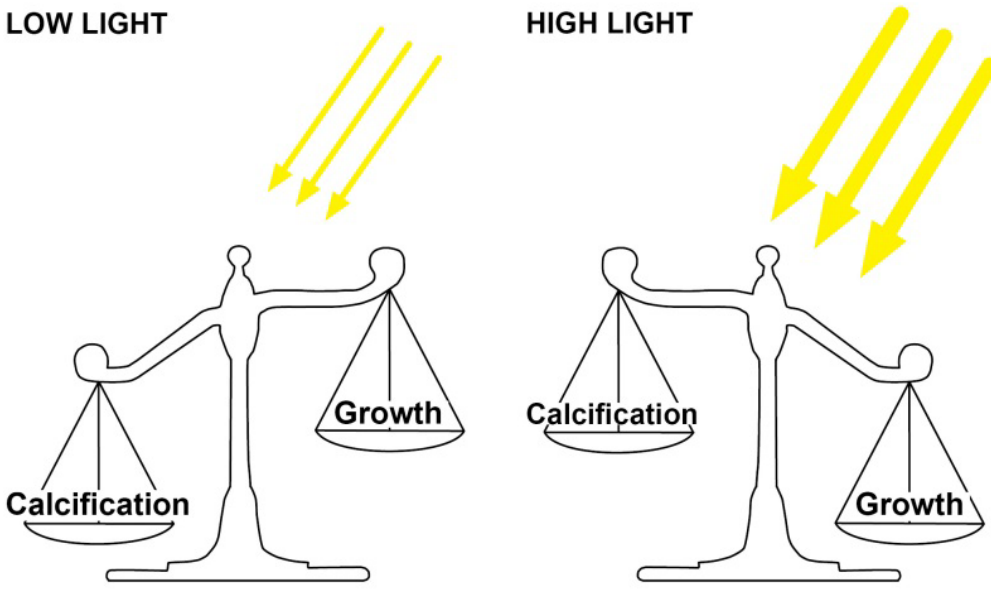

Figure 5.2: "**Trade-off" between calcification and growth.** In the *E. huxleyi* strain RCC 1612, low-light acclimated cells can sustain growth, but calcification is decreased under a pCO_2 of ~1000 μatm. High-light acclimated cells exhibit decreased growth but only slightly decreased calcification under these conditions (*Publication III*; Langer *et al.*, 2009; Rokitta & Rost, 2012).

to get a detailed process understanding (Behrenfeld & Falkowski, 1997; Halsey & Jones, 2015).

Emiliania huxleyi is known to divide in a relatively synchronized manner when acclimated to a light:dark cycle (Zondervan *et al.*, 2002; Müller *et al.*, 2008). As the cells divide during and shortly after the dark period and build biomass during the light period, POC and PIC quotas increase over the course of the light period (Fig. 5.3 A). As a consequence, POC and PIC production (pg cell^{-1} d^{-1}) become larger when measured in the late light phase (Fig. 5.3 B). When production rates are compared within one experiment at similar experimental conditions, the time-dependencies in the production rates may not be as relevant. However, when comparing rates between experiments and different sampling times, e.g. morning versus afternoon, the time-dependency will lead to comparably high offsets. Also, when production rates are different (e.g. between low and high irradiances or when comparing photosynthesis with calcification), the offset between both estimates can becomes larger during the course of the light phase.

One possibility to take into account the diurnal behavior in POC production rates is the normalization to a parameter, which itself is time-dependent, e.g., Chl *a*. Such a normalization expresses the photosynthetic efficiency under the given conditions rather than the cellular performance. For example, an increase in Chl *a*-normalized POC production rates can indicate a more efficient CO_2 supply at RubisCO. As cellular photosynthetic features such as pigments contents react very sensitive to diverse environmental conditions, especially to light, it is yet necessary to measure and analyze data in accordance with the specific research question.

Another factor that comes into play, when determining POC and PIC production as the product of a cellular quota (pg cell^{-1}) times the growth rate μ (d^{-1}), is the fact that growth is usually determined after a full light:dark cycle, while production takes place only during the light phase. Therefore, to express the "real" instaneous production rate the cells perform during light, a light-normalized μ should be applied that is accordingly higher (e.g., in a 16:8 light:dark cycle, μ_{light} would be higher by a factor of (16+8)/16). Thus, "convential" POC and PIC production rates, which integrate also the dark phase, usually underestimate the *real-time* production in the light.

In terms of cell-normalized POC production, rates averaging over a complete light:dark cycle or full light phase can give a more comparable measure between experiments. The (time-) averaged production during light (in pg cell^{-1} d^{-1}) can be estimated analytically from measured μ and the sampling time, assuming exponential increase in the POC quota over the course of the light phase:

$$\text{POC production}_{\text{average, } light} = \text{POC quota} \times e^{\mu \frac{1}{LP}(LP-t)} \qquad (5.1)$$

with the POC quota (pg cell^{-1}) at the sampling time point t (in hours of light phase) and *LP* being the length of the light phase (in hours). This light-phase averaged POC production and

the "convential" POC production (based on a μ which is not normalized to the light phase) are, after all, very similar in magnitude when assessing POC quotas at the end of a light phase

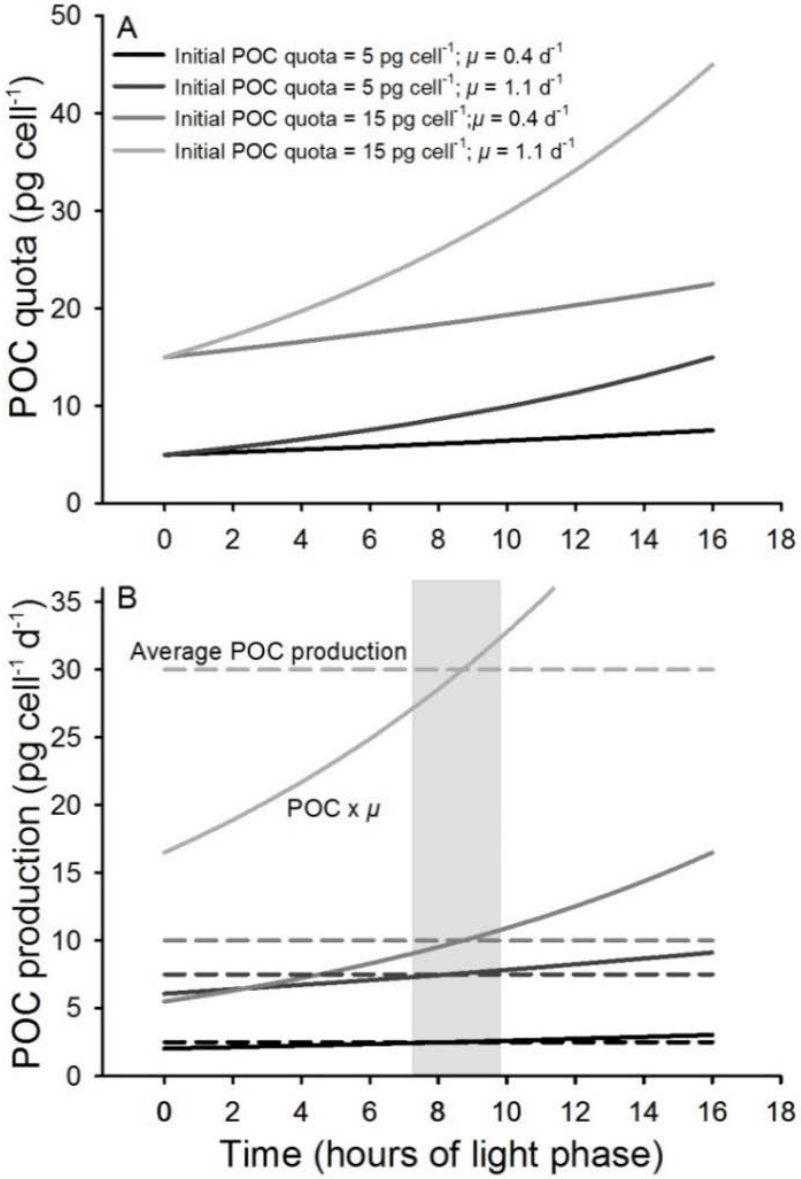

Figure 5.3: **POC production in cultures with synchronized cell growth. A)** Modelled changes in average POC quotas over the course of the light phase assuming exponential growths that is restricted to the light phase. Each grey scale exemplifies different initial conditions in terms of POC quota and μ. **B)** Time-dependent POC production rates (solid lines) and average POC production (over the course of a complete light:dark cycle) calculated after Eq. 5.2 (dashed lines) for the POC quotas illustrated in **A.** Shaded areas represent the time of the light phase where both production quantities are similar in magnitude.

(independent of μ, initial POC quota or length of light phase). In order to compare production rates of synchronised cultures with production rates of continuous cultures, POC production should be averaged to the full light:dark cycle (which is typically 24 hours in laboratory studies):

$$\text{POC production}_{\text{average, } 24h} = \text{POC quota} \times e^{\mu \frac{1}{24\ h}(LP-t)} \qquad (5.2)$$

This measure is also more relevant in terms of biogeochemical impacts. The 24 h-averaged production rates (pg cell^{-1} d^{-1}) and the "conventional" POC production are similar when measuring POC quotas shortly after the middle of the light phase (grey shaded area in Fig 5.3 B). This is why the majority of POC production rates stated in the literature, which are often measured in the middle of the day, are coincidently expressing such 24 h averaged production rates and are therefore to some degree comparable. However, the time-dependency of flux measurements should be taken into account and discussed in the context of CCM and OA research, and can probably explain part of the variability between different experiments.

In vivo measurements and the effects of standardization

In vivo measurements comprise ^{14}C or ^{18}O tracer techniques (e.g., Paasche, 1964; Sültemeyer & Rinast, 1996; Buitenhuis *et al.*, 1999; Rost *et al.*, 2007), CO_2 or O_2 exchange measurements (e.g., Badger *et al.*, 1994; Schulz *et al.*, 2007; Ploug *et al.*, 2011) or fluorometric methods investigating the ETC (e.g., Suggett *et al.*, 2007; Hoppe *et al.*, 2015). Such flux measurements are traditionally applied under standardized conditions (e.g., in terms of pH values and light) to investigate how certain treatments affect cellular capacities, e.g., the maximum photosynthetic rates or half-saturation constants (Burns & Beardall, 1987; MacIntyre, 2002; Rost *et al.*, 2003). Depending on the applied method to investigate photosynthetic C_i acquisition, the measurement conditions can largely vary.

For *E. huxleyi*, the conditions applied during measurements also varied between studies. MIMS measurements have often been performed at a standardized pH of 8.0 (Rost *et al.*, 2003; Tchernov *et al.*, 2003; Schulz *et al.*, 2007; Trimborn *et al.*, 2007). The ^{14}C disequilibrium method has typically been applied at pH 8.5 (Espie & Colman, 1986; Elzenga *et al.*, 2000; Rost *et al.*, 2007; Rokitta & Rost, 2012), while semi-quantitative ^{14}C studies have been applied at a pH of 8.0 (Sikes *et al.*, 1980; Sikes & Wheeler, 1982; Stojkovic *et al.*, 2013). The applied conditions do, however, strongly influence the outcome of the method (*Publication I-III*) and thus the results of the different methods are not only incomparable, but also often do not represent *in situ* conditions. This explains part of the high variability between studies, e.g., with respect to differences in C_i use, and also why no strong C_i flux regulations under typical OA conditions were yet resolved (e.g., Rokitta & Rost, 2012). Such "biases" due to standardization may also apply to measurements of other cellular parameters, such as DIC-, CO_2 and HCO_3^- affinities, the expression of carbonic anhydrases or leakage.

The ^{14}C disequilibrium method as well as the MIMS-based approach both revealed strong pH-dependent short-term regulations in photosynthetic C_i fluxes, with cells transitioning from CO_2 to HCO_3^- usage when going from low to high pH (*Publication I-III*). Despite these overall consistent findings for the diploid stage, the MIMS method estimated a considerably lower CO_2 contribution for photosynthesis in both life-cycle stages and hardly any regulation in C_i source in the haploid stage. Such discrepancies may partly be attributable to the different scales of fluxes that both methods detect, and on the different key assumptions that they are based on.

The MIMS method is based on simultaneous measurements of O_2 and CO_2 over consecutive light and dark phases. While changes in O_2 and CO_2 concentration can be directly measured, CO_2 uptake is deduced from the depletion in CO_2 concentration during steady-state photosynthesis, accounting for the interconversion of CO_2 and HCO_3^-. The HCO_3^- uptake is then derived from the mass balance between CO_2 uptake and total C_i fixation. These calculations include variables such as rates constants as well as photosynthetic and respiratory quotients, which are often associated with some uncertainties. In sensitivity studies, the consequences of potential offsets in these variables were tested (data not shown), confirming that these could not explain the strong difference between the ^{14}C and the MIMS method. The MIMS-based approach furthermore involves several "internal" controls. For instance, carbonate chemistry of the seawater media, which is adjusted prior to measurements, and the assumed rate constants can be verified by means of MIMS. Mass balances between O_2, CO_2 and HCO_3^- fluxes allow to assess whether the order of magnitudes of the measured fluxes are in agreement.

The ^{14}C disequilibrium method, on the other hand, assesses the C_i source based on short-term C_i fixation, i.e., a parameter that may undergo lag phases due to slow labelling, especially in cells with larger intracellular C_i pools and slower turnover than in *E. huxleyi* (Paasche 2002). In contrast to the MIMS approach, the technique is not able to detect actual O_2 and C_i uptake rates, but yields relative estimates of C_i usage as the proportion of CO_2 relative to overall DIC uptake (f_{CO_2}). The f_{CO_2} is assessed based on the curvature of the cellular photosynthetic ^{14}C incorporation during a transient isotopic $^{14}CO_2$ disequilibrium in the medium. In order to calculate the C_i source, a curve fit is applied, which models the expected ^{14}C-incorporation curve at the given conditions with the unknown f_{CO_2}. The fit function is based on a number of variables and constraints that strongly affect the outcome (Lehman, 1971; Espie & Colman, 1986). Experimental conditions can, however, hardly be verified by independent measurements and some of the assumptions within the fit function, namely of the kinetic constants, decay rates and degree of isotopic disequilibria require reevaluation (Thoms et al. in prep.). Being an "all-in-one" approach, which does not allow for any intrinsic controls, the $^{14}CO_2$ disequilibrium method thus appears more error-prone than the MIMS. Hence, methodological problems should be taken into consideration in future research.

5.4 The future of coccolithophores

In line with most literature, the studies performed within this thesis found that *E. huxleyi* is severely affected by OA. The observed flux regulations as a function of pH explained the mechanisms leading to the high OA-sensitivity of the species (*Publication I-III*). Due to the similarities in OA responses within coccolithophores (Raven & Crawfurd, 2012; Meyer & Riebesell, 2015) it is likely that analogous concepts also apply to other representatives of this important group of calcifiers. Especially the pronounced antagonistic H^+ dependence of cellular CO_2 and HCO_3^- uptake may be a comon pattern, because H^+ effects are similar in many biological systems and because phytoplankton share typical components of CCMs (Giordano *et al.*, 2005; Reinfelder, 2011; Mackey *et al.*, 2015). Thus, in order to allow for an improved forecasting of the OA-effects and their modulations by other environmental factors, such overarching concepts should also be investigated in other phytoplankton taxa.

In this thesis, calcification was shown to give *E. huxleyi* physiological apparent advantages over non-calcifiers (*Publication II, III*). The species was, for example, shown to have the ability to redirect HCO_3^- from calcification to photosynthesis in times of low DIC or low energy, as well as the ability to dissipate energy and to redirect C_i to the process of calcification in times of high DIC or high energy. Also the capacity to balance intracellular H^+ levels by HCO_3^--based photosynthesis and HCO_3^--based calcification could give calcifiers an benefit over non-calcifiers, as they do not require excessive H^+ pumping over the plasmalemma. This could not only save overall cellular costs (Raven, 2011), but be especially advantageous at bloom conditions, where external H^+ levels can become low. Under these conditions, photosynthesis of non-calcifying "HCO_3^- users" requires the concomitant uptake of H^+ in order to keep pH homeostasis, which can become challenging. These apparent advantages, however, became restricted under acidification. Under acidified conditions, *E huxleyi* apparently became more inflexible in terms of C_i redistribution between photosynthesis and calcification, because the overall intracellular HCO_3^- pool became smaller (*Publication III*). Furthermore, the species' ability to maintain intracellular pH constant was impacted, as the external acidification not only directly led to decreased intracellular pH values, but also created to a positive feedback on biogenic H^+ production (*Publication II and III*). In future OA scenarios, *E. huxleyi* may therefore lose its current physiological and ecological advantages that is has under late bloom and high light conditions.

In accordance with literature, *E. huxleyi* was shown to experience strong decreases in calcification in this thesis, especially when light energization was low. Moreover, the measurements revealed that the species faces the risk to become C_i-limited when being grown under high light combined with acidification (*Publication II, Publication III*). Under the more dynamic conditions in natural habitats, C_i acquisition may become even more demanding, because cells have to constantly deal with the low energetic availability under low irradiances and the high C_i demands under high irradiances (van de Poll *et al.*, 2007; Jin *et al.*, 2013; Hoppe *et al.*, 2015). Balancing these opposing demands, *E. huxleyi* and other coccolithophores may run into severe difficulties in a future ocean with lowered pH. This will

certainly strongly affect marine ecosystems, not only the species' distribution and competetive abilities, but also other trophic levels. Regarding biogeochemistry and climate change, a reduction of biogenic calcification (in terms of reduced $CaCO_3$ per cell or in reduced overall growth of coccolithophores) could indeed lead to an enhanced CO_2 uptake capacity of the ocean. However, whether the CO_2 uptake capacity really changes, strongly depends on whether the consequences of the reduced "carbonate counter pump" really dominate over the consequences of the reduced "organic carbon pump". Thus, to predict the biogeochemical and ecological consequences of the observed OA effects, process understanding should be coupled with field studies and model-based estimations in future research.

5.5 Conclusions

In this thesis, carbonate-chemistry- and light-dependent cellular flux regulations associated with photosynthesis, calcification and respiration in the coccolithophore *E. huxleyi* were investigated in order to understand how these processes will be affected in the future ocean. The performed studies, in which different physiological measurements were applied, revealed a strong H^+ sensitivity in the C_i acquisition for photosynthesis and calcification that can explain the typical decrease in PIC:POC ratios observed under OA. In contrast to the common notion that CO_2 has a "fertilizing" effect on primary production, the results of this thesis showed that beneficial OA effects are indeed rather independent of carbonation but mainly caused by acidification. The results furthermore revealed that acidification causes cellular HCO_3^- uptake to decrease, which can explain why calcification is strongly impacted by OA. Beyond the biological insights into the flux regulations, it was investigated how measuring conditions (specifically the carbonate chemistry), different methodologies (^{14}C disequilibrium vs. MIMS measurements) and time scales (short-term responses vs. acclimation responses, and integrated signals vs. *real-time* measurements) affects measuring results. With this, the insights gained in this thesis do not only contribute to a better understanding of OA effects on important primary producers and calcifiers, but also to an improvement of the techniques deployed to measure these effects.

Chapter 6
References

Allemand D, Tambutté É, Zoccola D, Tambutté S 2011. Coral Calcification, cells to reefs. In: Dubinsky Z, Stambler N eds. *Coral Reefs: An Ecosystem in Transition*: Springer Netherlands, 119-50.

Anning T, Nimer NA, Merrett MJ, Brownlee C. 1996. Costs and benefits of calcification in coccolithophorids. *J Marine Syst* 9(1): 45-56.

Araki Y, Gonzalez EL. 1998. V- and P-type Ca^{2+}-stimulated ATPases in a calcifying strain of *Pleurochrysis sp.* (Haptophyceae). *J Phycol* 34(1): 79-88.

Archer D, Maier-Reimer E. 1994. Effect of deep-sea sedimentary calcite preservation on atmospheric CO_2 concentration. *Nature* 367(6460): 260-63.

Armstrong RA, Lee C, Hedges JI, Honjo S, Wakeham SG. 2002. A new, mechanistic model for organic carbon fluxes in the ocean based on the quantitative association of POC with ballast minerals. *Deep-Sea Res Pt II* 49(1-3): 219-36.

Arrhenius S. 1896. On the influence of carbonic acid in the air upon the temperature of the ground. *Philosophical Magazine and Journal of Science* 41(5): 237-76.

Asada K. 1999. The water-water cycle in chloroplasts: scavenging of active oxygens and dissipation of excess photons. *Annu Rev Plant Physiol Plant Mol Biol* 50: 601–39.

Bach LT, Mackinder LC, Schulz KG, Wheeler G, Schroeder DC, et al. 2013. Dissecting the impact of CO_2 and pH on the mechanisms of photosynthesis and calcification in the coccolithophore *Emiliania huxleyi*. *New Phytol* 199(1): 121-34.

Badger MR, Andrews TJ, Whitney SM, Ludwig M, Yellowlees DC. 1998. The diversity and co-evolution of Rubisco, plastids, pyrenoids and chloroplast-based CO_2-concentrating mechanisms in algae. *Can J Bot* 76: 1052-71.

Badger MR, Palmqvist K, Yu JW. 1994. Measurement of CO_2 and HCO_3^- fluxes in cyanobacteria and microalgae during steady-state photosynthesis. *Physiol Plant* 90(3): 529-36.

Barnola JM, Raynaud D, Lorius D, Barkov NI. 2003. Historical CO_2 record from the Vostok ice core. Trends: A Compendium of Data on Global Change. Carbon Dioxide Information Analysis Center, Oak Ridge National Laboratory, US Department of Energy, Oak Ridge, Tennessee, USA.

Bauerfeind E, Nötig E-M, Beszczynska A, Fahl K, Kaleschke L, et al. 2009. Particle sedimentation patterns in the eastern Fram Strait during 2000–2005: Results from the Arctic long-term observatory HAUSGARTEN. *Deep-Sea Res Pt. I* 56: 1471-87.

Beardall J, Raven JA. 2013. Calcification and ocean acidification: new insights from the coccolithophore *Emiliania huxleyi*. *New Phytol* 199(1): 1-3.

Beaufort L, Probert I, de Garidel-Thoron T, Bendif EM, Ruiz-Pino D, et al. 2011. Sensitivity of coccolithophores to carbonate chemistry and ocean acidification. *Nature* 476(7358): 80-83.

Becks L, Agrawal AF. 2010. Higher rates of sex evolve in spatially heterogeneous environments. *Nature* 468(7320): 89-92.

Behrenfeld MJ, Falkowski PG. 1997. Photosynthetic rates derived from satellite-based chlorophyll concentration. *Limnol Oceanogr* 42(1): 1-20

Behrenfeld MJ, Halsey KH, Milligan AJ. 2008. Evolved physiological responses of phytoplankton to their integrated growth environment. *Phil trans R Soc B* 363(1504): 2687-703.

Berg JM, Tymoczko JL, Stryer L. 2002. Biochemistry: Freeman and co. New York

Billard C, Inoye I 2004. What is new in coccolithophore biology? In: Thierstein HR, Young JR eds. *Coccolithophores - From Molecular Processes to Global Impact*: Springer Heidelberg, 1-29.

Boller AJ, Thomas PJ, Cavanaugh CM, Scott KM. 2011. Low stable carbon isotope fractionation by coccolithophore RubisCO. *Geochim Cosmochim Acta* 75(22): 7200-07.

Borkhsenious ON, Mason CB, Moroney JV. 1998. The intracellular localization of ribulose-1,5-bisphosphate Carboxylase/Oxygenase in *Chlamydomonas reinhardtii*. *Plant Physiol* 116(4): 1585-91.

Bown PR, Lees JA, Young JR 2004. Calcareous nannoplankton evolution and diversity through time. In: Thierstein HR, Young JR eds. *Coccolithophores - From Molecular Processes to Global Impact*: Springer Heidelberg, 481-508.

Brewer PG, Goldman JC. 1980. Alkalinity changes generated by phytoplankton growth. *Limnol Oceanogr* 21(1): 108-17.

Broecker WS, Peng TH. 1987. The role of $CaCO_3$ compensation in the glacial to interglacial atmospheric CO_2 change. *Global Biogeochem Cy* 1(1): 15-29.

Brown CW, Yoder JA. 1994. Coccolithophorid blooms in the global ocean. *J Geophys Res-Oceans* 99(C4): 7467-82.

Brownlee C, Taylor A 2004. Calcification in coccolithophores: A cellular perspective. In: Thierstein HR, Young JR eds. *Coccolithophores - From Molecular Processes to Global Impact*: Springer Heidelberg, 31-49.

Brussaard C, Kempers R, Kop A, Riegman R, Heldal M. 1996. Virus-like particles in a summer bloom of *Emiliania huxleyi* in the North Sea. *Aquat Microb Ecol* 10(2): 105-13.

Buitenhuis ET, De Baar HJW, Veldhuis MJW. 1999. Photosynthesis and calcification by *Emiliania huxleyi* (Prymnesiophyceae) as a function of inorganic carbon species. *J Phycol* 35(5): 949-59.

Burns DB, Beardall J. 1987. Utilization of inorganic carbon by marine microalgae. *J Exp Mar Biol Ecol* 107: 75.

Caldeira K, Wickett ME. 2003. Anthropogenic carbon and ocean pH - The coming centuries may see more oceanic acidification than the past 300 million years. *Nature* 425(365): 365.

Ciais P, Sabine C, Bala G, Bopp L, Brovkin V, et al. 2013. Carbon and other biogeochemical cycles. In: Stocker TF, Qin D, Plattner G-K et al eds. *Climate change 2013: the physical science basis. Contribution of Working Group I to the fifth Assessment report of the Intergovernmental Panel on Climate Change*. Cambridge, United Kingdom and New York, NY, USA: Cambridge University Press, 465-570.

Coelho SM, Peters AF, Charrier B, Roze D, Destombe C, et al. 2007. Complex life cycles of multicellular eukaryotes: new approaches based on the use of model organisms. *Gene* 406(1-2): 152-70.

Coolen MJ. 2011. 7000 years of *Emiliania huxleyi* viruses in the Black Sea. *Science* 333(6041): 451-2.

Corstjens PL, Van Der Kooij A, Linschooten C, Brouwers GJ, Westbroek P, et al. 1998. GPA, a calcium-binding protein in the coccolithophorid *Emiliania huxleyi* (Prymnesiophyceae). *J Phycol* 34(4): 622-30.

Cyronak T, Schulz KG, Jokiel PL. 2015. The Omega myth: what really drives lower calcification rates in an acidifying ocean. *ICES J Mar Sci*.

von Dassow P, Ogata H, Probert I, Wincker P, Da Silva C, et al. 2009. Transcriptome analysis of functional differentiation between haploid and diploid cells of *Emiliania huxleyi*, a globally significant photosynthetic calcifying cell. *Genome Biol.* (10): R114.

von Dassow P, John U, Ogata H, Probert I, Bendif el M, et al. 2015. Life-cycle modification in open oceans accounts for genome variability in a cosmopolitan phytoplankton. *ISME J* 9(6): 1365-77.

De Bodt C, Van Oostende N, Harlay J, Sabbe K, Chou L. 2010. Individual and interacting effects of pCO_2 and temperature on *Emiliania huxleyi* calcification: study of the calcite production, the coccolith morphology and the coccosphere size. *Biogeosciences* 7(5): 1401-12.

van de Poll WH, Visser RJ, Buma AG. 2007. Acclimation to a dynamic irradiance regime changes excessive irrandiance sensitivity of *Emiliania huxleyi* and *Thalassiosira weissflogii*. *Limnol Oceanogr* 52(4): 1430-38.

de Vargas C, Sáez AG, Medlin LK, Thierstein HR 2004. Super-species in the calcareous plankton. In: Thierstein HR, Young J eds. *Coccolithophores - From Molecular Processes to Global Impact*, 271-98.

van der Wal P, van Bleijswijk JD, Egge JK. 1994. Primary productivity and calcification rate in blooms of the coccolithophorid *Emiliania huxleyi* (Lohmann) Hay et Mohler developing in mesocosms. *Sarsia* 79(4): 401-08.

Dickson AG. 1981. An exact definition of total alkalinity and a procedure for the estimation of alkalinity and total inorganic carbon from titration data. *Deep-Sea Res Pt II* 28(6): 609-23.

Doney SC, Fabry VJ, Feely RA, Kleypas JA. 2009. Ocean acidification: the other CO_2 problem. *Annu Rev Mar Sci* 1: 169-92.

Egge JK, Heimdal BR. 1994. Blooms of phytoplankton including *Emiliania huxleyi* (Haptophyta). Effects of nutrient supply in different N : P ratios. *Sarsia* 79(4): 333-48.

Elzenga JTM, Prins HBA, Stefels J. 2000. The role of extracellular carbonic anhydrase activity in inorganic carbon utilization of *Phaeocystis globosa* (Prymnesiophyceae): A comparison with other marine algae using the isotopic disequilibrium technique. *Limnol Oceanogr* 45(2): 372-80.

Espie GS, Colman B. 1986. Inorganic carbon uptake during photosynthesis - a theoretical analysis using the isotopic disequilibrium technique. *Plant Physiol* 80: 863-69.

Falkowski P, Scholes RJ, Boyle E, Canadell J, Canfield D, et al. 2000. The global carbon cycle: A test of our knowledge of earth as a system. *Science* 290(5490): 291-96.

Falkowski PG, Katz ME, Knoll AH, Quigg A, Raven JA, et al. 2004. The evolution of modern eukaryotic phytoplankton. *Science* 305(5682): 354-60.

Falkowski PG, Raven JA. 2013. *Aquatic Photosynthesis*: Princeton University Press.

Field CB, Behrenfeld MJ, Randerson JT, Falkowski P. 1998. Primary Production of the Biosphere: Integrating Terrestrial and Oceanic Components. *Science* 281(5374): 237-40.

Fourier JBJ. 1822. *Théorie analytique de la chaleur*: Chez Firmin Didot, père et fils.

Frada M, Probert I, Allen MJ, Wilson WH, De Vargas C. 2008. The "Cheshire Cat" escape strategy of the coccolithophore *Emiliania huxleyi* in response to viral infection. *PNAS* 105(41): 15944-49.

Fukuda SY, Suzuki Y, Shiraiwa Y. 2014. Difference in physiological responses of growth, photosynthesis and calcification of the coccolithophore *Emiliania huxleyi* to acidification by acid and CO_2 enrichment. *Photosynth Res* 121(2-3): 299-309.

Gao K, Xu J, Gao G, Li Y, Hutchins DA, et al. 2012. Rising CO_2 and increased light exposure synergistically reduce marine primary productivity. *Nat Clim Chang* 2(7): 519-23.

Gaylord B, Kroeker KJ, Sunday JM, Anderson KM, Barry JP, et al. 2015. Ocean acidification through the lens of ecological theory. *Ecology* 96(1): 3-15.

Gehlen M, Gruber N, Gangstø R, Bopp L, Oschlies A. 2012. Biogeochemical consequences of ocean acidification and feedbacks to the earth system. In: Gattuso JH, Hansson L. eds. Ocean Acidification: Oxford University Press, 230-48.

Giordano M, Beardall J, Raven JA. 2005. CO_2 concentrating mechanisms in Algae: mechanisms, environmental modulation, and evolution. *Ann Rev Plant Biol* 56(1): 99-131.

Green JC, Course PA, Tarran GA. 1996. The life-cycle of *Emiliania huxleyi*: A brief review and a study of relative ploidy levels analysed by flow cytometry. *J Marine Syst* 9(1-2): 33-44.

Halsey KH, Jones BM. 2015. Phytoplankton strategies for photosynthetic energy allocation. *Ann Rev Mar Sci* 7: 265-97.

Herfort L, Thake B, Roberts J. 2002. Acquisition and use of bicarbonate by *Emiliania huxleyi*. *New Phytol* 156(3): 427-36.

Herfort L, Loste E, Meldrum F, Thake B. 2004. Structural and physiological effects of calcium and magnesium in *Emiliania huxleyi* (Lohmann) Hay and Mohler. *J Struct Biol* 148(3): 307-14.

Holligan PM, Viollier M, Harbour DS, Camus P, Champagnephilippe M. 1983. Satellite and ship studies of coccolithophore production along a continental-shelf edge. *Nature* 304(5924): 339-42.

Holtz L-M, Langer G, Rokitta SD, Thoms S, Rai M, et al. 2013a. Synthesis of nanostructured calcite particles in coccolithophores, unicellular algae. *Green biosynthesis of nanoparticles: mechanisms and applications*: 132-47.

Holtz L-M, Thoms S, Langer G, Wolf-Gladrow DA. 2013b. Substrate supply for calcite precipitation in *Emiliania huxleyi*: assessment of different model approaches. *J Phycol* 49(2): 417-26.

Holtz LM, Wolf-Gladrow DA, Thoms S. 2015a. Numerical cell model investigating cellular carbon fluxes in *Emiliania huxleyi*. *J Theor Biol* 364: 305-15.

Holtz LM, Wolf-Gladrow DA, Thoms S. 2015b. Simulating the effects of light intensity and carbonate system composition on particulate organic and inorganic carbon production in *Emiliania huxleyi*. *J Theor Biol* 372: 192-204.

Hoppe CJM, Langer G, Rost B. 2011. *Emiliania huxleyi* shows identical responses to elevated pCO_2 in TA and DIC manipulations. *J Exp Mar Biol Ecol* 406(1): 54-62.

Hoppe CJM, Holtz L-M, Trimborn S, Rost B. 2015. Ocean Acidification decreases the light use efficiency in an Antarctic diatom under dynamic but not constant light. *New Phytol* 207(1): 159-71.

Houdan A, Probert I, Van Lenning K, Lefebvre SC. 2005. Comparison of photosynthetic responses in diploid and haploid life-cycle phases of *Emiliania huxleyi* (Prymnesiophyceae). *Mar Ecol-Prog Ser* 292: 139-46.

Howes EL, Joos F, Eakin CM, Gattuso J-P. 2015. An updated synthesis of the observed and projected impacts of climate change on the chemical, physical and biological processes in the oceans. *Frontiers in Marine Science* 2.

Hughes JS, Otto SP. 1999. Ecology and the evolution of biphasic life cycles. *The American naturalist* 154(3): 306-20.

Iglesias-Rodriguez MD, Halloran PR, Rickaby RE, Hall IR, Colmenero-Hidalgo E, et al. 2008. Phytoplankton calcification in a high-CO_2 world. *Science* 320(5874): 336-40.

IPCC 2013. Summary for Policymakers. In: Stocker TF, Qin D, Plattner G-K et al. eds. Climate Change 2013: The Physical Science Basis. Contribution of Working Group I to the Fifth Assessment Report of the Intergovernmental Panel on Climate Change. Cambridge, United Kingdom and New York, NY, USA: Cambridge University Press, 1–30.

Jin P, Gao K, Villafane VE, Campbell DA, Helbling EW. 2013. Ocean acidification alters the photosynthetic responses of a coccolithophorid to fluctuating ultraviolet and visible radiation. *Plant Physiol* 162(4): 2084-94.

Johnson KS. 1982. Carbon dioxide hydration and dehydration kinetics in seawater. *Limnol Oceanogr* 27(5): 849-55.

Kaltz O, Bell G. 2002. The ecology and genetics of fitness in *Chlamydomonas* XII. Repeated sexual episodes increase rates of adaptation to novel environments. *Evolution* 56(9): 1743-53.

Keeling RF, Piper SC, Bollenbacher AF, Walker JS 2009. Atmospheric CO_2 records from sites in the SIO air sampling network: Carbon Dioxide Information Analysis Center, Oak Ridge National Laboratory, U.S. Department of Energy, Oak Ridge, Tenn.

Klaas C, Archer DE. 2002. Association of sinking organic matter with various types of mineral ballast in the deep sea: Implications for the rain ratio. *Global Biogeochem Cy* 16(4): 63-71.

Klaveness D. 1972. *Coccolithus huxleyi* (Lohm.) Kamptn II. The flagellate cell, aberrant cell types, vegetative propagation and life cycles. *British Phycological Journal* 7(3): 309-18.

Kroeker KJ, Kordas RL, Crim R, Hendriks IE, Ramajo L, et al. 2013. Impacts of ocean acidification on marine organisms: quantifying sensitivities and interaction with warming. *Glob Change Biol* 19(6): 1884-96.

Kump LR, Brantley SL, Arthur MA. 2000. Chemical weathering, atmospheric CO_2, and climate. *Annu Rev Earth Pl Sc* 28: 611-67.

Lam PJ, Doney SC, Bishop JKB. 2011. The dynamic ocean biological pump: Insights from a global compilation of particulate organic carbon, $CaCO_3$, and opal concentration profiles from the mesopelagic. *Global Biogeochem Cy* 25(3).

Langer G, Nehrke G, Probert I, Ly J, Ziveri P. 2009. Strain-specific responses of *Emiliania huxleyi* to changing seawater carbonate chemistry. *Biogeosciences* 6(11): 2637-46.

Laws. 1991. Photosynthetic quotients, new production and net community production in the open ocean. *Deep-Sea Res* 38(1): 143-67.

Le Quéré C, Moriarty R, Andrew RM, Peters GP, Ciais P, et al. 2014. Global carbon budget 2014. *Earth System Science Data Discussions* 7(2): 521-610.

Lefebvre SC, Benner I, Stillman JH, Parker AE, Drake MK, et al. 2012. Nitrogen source and pCO_2 synergistically affect carbon allocation, growth and morphology of the coccolithophore *Emiliania huxleyi*: potential implications of ocean acidification for the carbon cycle. *Glob Change Biol* 18(2): 493-503.

Lehman. 1971. Enhanced transport of inorganic carbon into algal cells and its implications for the biological fixation of carbon. *J. Phycol*. (14): 33-44

Leonardos N, Read B, Thake B, Young JR. 2009. No mechanistic dependence of photosynthesis on calcification in the coccolithophorid *Emiliania Huxleyi* (Haptophyta). *J Phycol* 45(5): 1046-51.

Leung C-Y, Palmer LC, Qiao BF, Kewalramani S, Sknepnek R, et al. 2012. Molecular crystallization controlled by pH regulates mesoscopic membrane morphology. *ACS NANO* 6(12): 10901–09.

Leung C-Y, Palmer LC, Kewalramani S, Qiao B, Stupp SI, et al. 2013. Crystalline polymorphism induced by charge regulation in ionic membranes. *PNAS* 110(41): 16309-14.

Loebl M, Cockshutt AM, Campbell DA, Finkel ZV. 2010. Physiological basis for high resistance to photoinhibition under nitrogen depletion in *Emiliania huxleyi*. *Limnol Oceanogr* 55(5): 2150-60.

Losh JL, Young JN, Morel FM. 2013. Rubisco is a small fraction of total protein in marine phytoplankton. *New Phytol* 198(1): 52-8.

Lovelock JE. 1979. *Gaia: A new look at life on earth*: Oxford University Press, Oxford.

Luthi D, Le Floch M, Bereiter B, Blunier T, Barnola JM, et al. 2008. High-resolution carbon dioxide concentration record 650,000-800,000 years before present. *Nature* 453(7193): 379-82.

MacIntyre HL, Anning T, Geider RJ 2002. Photoacclimation of photosynthesis irradiance response curves and photosynthetic pigrments in microalgae and cyanobacteria. *J. Phycol* (38):17-38

Mackey K, Morris JJ, Morel F, Kranz S. 2015. Response of photosynthesis to ocean Acidification. *Oceanography* 25(2): 74-91.

Mackinder L, Wheeler G, Schroeder D, Riebesell U, Brownlee C. 2010. Molecular mechanisms underlying calcification in coccolithophores. *Geomicrobiology J* 27: 585-95.

Mackinder L, Wheeler G, Schroeder D, von Dassow P, Riebesell U, et al. 2011. Expression of biomineralization-related ion transport genes in *Emiliania huxleyi*. *Environ Microbiol* 13(12): 3250-65.

Maier-Reimer E, Hasselmann K. 1987. Transport and storage of CO_2 in the ocean - an inorganic ocean-circulation carbon cycle model. *Climate dynamics* 2(2): 63-90.

Marsh ME. 2003. Regulation of $CaCO_3$ formation in coccolithophores. *Comparative Biochemistry and Physiology B-Biochemistry & Molecular Biology* 136(4): 743-54.

Meyer J, Riebesell U. 2015. Reviews and Syntheses: Responses of coccolithophores to ocean acidification: a meta-analysis. *Biogeosciences* 12(6): 1671-82.

Milliman JD. 1993. Production and accumulation of calcium carbonate in the ocean: budget of a non-steady state. *Global Biogeochem Cy* 7: 927-57.

Moroney JV, Jungnick N, DiMario RJ, Longstreth DJ. 2013. Photorespiration and carbon concentrating mechanisms: two adaptations to high O_2, low CO_2 conditions. *Photosynth Res* 117(1-3): 121-31.

Müller MN, Antia AN, La Roche J. 2008. Influence of cell cycle phase on calcification in the coccolithophore *Emiliania huxleyi*. *Limnol Oceanogr* 53(2): 506-12.

Nanninga HJ, Tyrrell T. 1996. Importance of light for the formation of algal blooms by *Emiliania huxleyi*. *Mar Ecol-Prog Ser* 136(1-3): 195-203.

Nielsen MV. 1995. Photosynthetic characteristics of the coccolithophorid *Emiliania huxleyi* (Prymnesiophyceae) exposed to elevated concentrations of dissolved inorganic carbon. *J Phycol* 31(5): 715-19.

Nimer NA, Guan Q, Merrett MJ. 1994. Extra- and intra-cellular carbonic anhydrase in relation to culture age in a high-calcifying strain of *Emiliania huxleyi* Lohmann. *New Phytol* 126: 601-07.

Nimer NA, Merrett MJ. 1996. The development of a CO_2-concentrating mechanism in *Emiliania huxleyi*. *New Phytol* 133(3): 383-89.

Orr JC, Fabry VJ, Aumont O, Bopp L, Doney SC, et al. 2005. Anthropogenic ocean acidification over the twenty-first century and its impact on calcifying organisms. *Nature* 437(7059): 681-6.

Paasche E 1964. A tracer study of the inorganic carbon uptake during coccolith formation and photosynthesis in the coccolithophorid *Coccolithus huxleyi*. Lund: Scandinavian Society for Plant Physiology.

Paasche E. 2001. A review of the coccolithophorid *Emiliania huxley*i (Prymnesiophyceae), with particular reference to growth, coccolith formation, and calcification-photosynthesis interactions. *Phycologia* 40(6): 503-29.

Petit JR, Jouzel J, Raynaud D, Barkov NI, Barnola JM, et al. 1999. Climate and atmospheric history of the past 420,000 years from the Vostok ice core, Antarctica. *Nature* 399(6735): 429-36.

Ploug H, Adam B, Musat N, Kalvelage T, Lavik G, et al. 2011. Carbon, nitrogen and O_2 fluxes associated with the cyanobacterium *Nodularia spumigena* in the Baltic Sea. *ISME J* 5(9): 1549-58.

Pörtner HO, Karl D, Boyd PW, Cheung W, Lluch-Cota SE, et al. 2014. Ocean systems. In: Field CB, Barros VR, Dokken DJ et al. eds. Climate Change 2014: Impacts, Adaptation, and Vulnerability. Part A: Global and Sectoral Aspects. Contribution of Working Group II to the Fifth Assessment Report of the Intergovernmental Panel of Climate Change. Cambridge, United Kingdom and New York, NY, USA: Cambridge University Press, 411-84.

Post WM, Peng TH, Emanuel WR, King AW, Dale VH, et al. 1990. The global carbon cycle. *Am Sci* 78(4): 310-26.

Raitsos D, Lavender S, Pradhan Y, Tyrrell T, Reid P, et al. 2006. Coccolithophore bloom size variation in response to the regional environment of the subarctic North Atlantic. *Limnol Oceanogr* 51(5): 2122-30.

Raven J. 2011. Effects on marine algae of changed seawater chemistry with increasing atmospheric CO_2. *PNAS* 111 B(1): 1-17.

Raven J, Johnston A. 1991. Mechanisms of inorganic carbon acquisition in marine phytoplankton and their implications for the use of other resources. *Limnol Oceanogr* 36(8): 1701-14.

Raven JA, Giordano M, Beardall J. 2008. Insights into the evolution of CCMs from comparisons with other resource acquisition and assimilation processes. *Physiol Plantarum* 133(1): 4-14.

Raven J, Crawfurd K. 2012. Environmental controls on coccolithophore calcification. *Mar Ecol-Prog Ser* 470: 137-66.

Raven JA. 2013. Rubisco: still the most abundant protein of Earth? *New Phytol* 198(1): 1-3.

Redfield. 1958. The biological control of the chemical factors in the environment. *Am Sci* 46: 205-21

Reinfelder JR. 2011. Carbon concentrating mechanisms in eukaryotic marine phytoplankton. *Annu Rev Mar Sci* 3: 291-315.

Reusch TB, Boyd PW. 2013. Experimental evolution meets marine phytoplankton. *Evolution* 67(7): 1849-59.

Rhein M, Rintoul SR, Aoki S, Campos E, Chambers D, et al. 2013. Observations: Ocean. In: Stocker TF, Qin D, Plattner G-Ket al eds. *Climate Change 2013: The Physical Science Basis. Contribution of Working Group I to the Fifth Assessment Report of the Intergovernmental Panel on Climate Change*. Cambridge, United Kingdom and New York, NY, USA: Cambridge University Press, 255–316.

Richier S, Fiorini S, Kerros ME, Von Dassow P, Gattuso JP. 2011. Response of the calcifying coccolithophore *Emiliania huxleyi* to low pH/high pCO_2: from physiology to molecular level. *Mar Biol* 158: 551-60.

Riebesell U, Wolf-Gladrow DA, Smetacek V. 1993. Carbon dioxide limitation of phytoplankton growth rates. *Nature* 361(6409): 249-51.

Riebesell U, Zondervan I, Rost B, Tortell PD, Zeebe E, et al. 2000. Reduced calcification in marine plankton in response to increased atmospheric CO_2. *Nature* 407: 634-37.

Riebesell U, Fabry VJ, Hansson L, Gattuso J-P. 2010. *Guide to best practices for ocean acidification research and data reporting*: Publications Office of the European Union Luxembourg.

Ridgwell A, Zeebe RE. 2005. The role of the global carbonate cycle in the regulation and evolution of the Earth system. *Earth Planet Sc Lett* 234(3-4): 299-315.

Riegman R, Stolte W, Noordeloos AA, Slezak D. 2000. Nutrient uptake and alkaline phosphatase (EC 3: 1: 3: 1) activity of *Emiliania huxleyi* (Prymnesiophyceae) during growth under N and P limitation in continuous cultures. *J Phycol* 36(1): 87-96.

Rokitta S, De Nooijer L, Trimborn S, De Vargas C, Rost B, et al. 2011. Transcriptome analyses reveal differential gene expression patterns between life-cycle stages of *Emiliania huxleyi* (Haptophyta) and reflect specialization to different ecological niches. *J Phycol* 47: 829-38.

Rokitta S, Rost B. 2012. Effects of CO_2 and their modulation by light in the life-cycle stages of the coccolithophore *Emiliania huxleyi*. *Limnol Oceanogr* 57(2): 607-18.

Rokitta S, John U, Rost B. 2012. Ocean acidification affects redox-balance and ion-homeostasis in the life-cycle stages of *Emiliania huxleyi*. *PLOS ONE* 7(12): e52212.

Rokitta SD, Von Dassow P, Rost B, John U. 2014. *Emiliania huxleyi* endures N-limitation with an efficient metabolic budgeting and effective ATP synthesis. *BMC Genomics* 15:1051

Rost B, Zondervan I, Riebesell U. 2002. Light-dependent carbon isotope fractionation in the coccolithophorid *Emiliania huxleyi*. *Limnol Oceanogr* 47(1): 120-28.

Rost B, Riebesell U, Burkhardt S, Sültemeyer D. 2003. Carbon acquisition of bloom-forming marine phytoplankton. *Limnol Oceanogr* 48(1): 55-67.

Rost B, Riebesell U 2004. Coccolithophores and the biological pump: responses to environmental changes. In: Thierstein HR, Young JR eds. *Coccolithophores - From Molecular Processes to Global Impact*: Springer Heidelberg, 76–99.

Rost B, Riebesell U, Sültemeyer D. 2006. Carbon acquisition of marine phytoplankton: effect of photoperiod length. *Limnol Oceanogr* 51(1): 12-20.

Rost B, Kranz SA, Richter KU, Tortell PD. 2007. Isotope disequilibrium and mass spectrometric studies of inorganic carbon acquisition by phytoplankton. *Limnol Oceanogr-Meth* 5: 328-37.

Rost B, Zondervan I, Wolf-Gladrow DA. 2008. Sensitivity of phytoplankton to future changes in ocean carbonate chemistry: Current knowledge, contradictions and research directions. *Mar Ecol-Prog Ser* 373: 227-37.

Rouco M, Branson O, Lebrato M, Iglesias-Rodriguez MD. 2013. The effect of nitrate and phosphate availability on *Emiliania huxleyi* (NZEH) physiology under different CO_2 scenarios. *Front Microbiol* 4: 155.

Royer DL, Berner RA, Park J. 2007. Climate sensitivity constrained by CO_2 concentrations over the past 420 million years. *Nature* 446(7135): 530-32.

Sabine CL, Feely RA, Gruber N, Key RM, Lee K, et al. 2004. The oceanic sink for anthropogenic CO_2. *Science* 305(5682): 367-71.

Sadeghi A, Dinter T, Vountas M, Taylor B, Altenburg-Soppa M, et al. 2012. Remote sensing of coccolithophore blooms in selected oceanic regions using the PhytoDOAS method applied to hyper-spectral satellite data. *Biogeosciences* 9(6): 2127-43.

Sarmiento JL. 2013. *Ocean biogeochemical dynamics*: Princeton University Press.

Schulz KG, Rost B, Burkhardt S, Riebesell U, Thoms S, et al. 2007. The effect of iron availability on the regulation of inorganic carbon acquisition in the coccolithophore *Emiliania huxleyi* and the significance of cellular compartmentation for stable carbon isotope fractionation. *Geochim Cosmochim Acta* 71: 5301-12.

Sett S, Bach LT, Schulz KG, Koch-Klavsen S, Lebrato M, et al. 2014. Temperature modulates coccolithophorid sensitivity of growth, photosynthesis and calcification to increasing seawater pCO_2. *PLOS ONE* 9(2): e88308.

Shiraiwa Y. 2003. Physiological regulation of carbon fixation in the photosynthesis and calcification of coccolithophorids. *Comp Biochem Phys B* 136(4): 775-83.

Sikes CS, Roer RD, Wilbur KM. 1980. Photosynthesis and coccolith formation: inorganic carbon sources and net inorganic reaction of deposition. *Limnol Oceanogr* 25(2): 248-61.

Sikes CS, Wheeler A. 1982. Carbonic anhydrase and carbon fixation in coccolithophorids. *J Phycol* 18(3): 423-26.

Soto AR, Zheng H, Shoemaker D, Rodriguez J, Read BA, et al. 2006. Identification and preliminary characterization of two cDNAs encoding unique carbonic anhydrases from the marine alga *Emiliania huxleyi*. *Appl Environ Microbiol* 72(8): 5500-11.

Spreitzer RJ, Salvucci ME. 2002. Rubisco: Structure, regulatory interactions, and possibilities for a better enzyme. *Ann Rev Plant Biol* 53: 449-75.

Stanley SM, Hardie LA. 1998. Secular oscillations in the carbonate mineralogy of reef-building and sediment-producing organisms driven by tectonically forced shifts in seawater chemistry. *Palaeogeography, Palaeoclimatology, Palaeoecology* 144(1): 3-19.

Stojkovic S, Beardall J, Matear R. 2013. CO_2-concentrating mechanisms in three southern hemisphere strains of *Emiliania huxleyi*. *J Phycol* 49(4): 670-79.

Suffrian K, Schulz KG, Gutowska MA, Riebesell U, Bleich M. 2011. Cellular pH measurements in *Emiliania huxleyi* reveal pronounced membrane proton permeability. *New Phytol* 190(3): 595-608.

Suggett DJ, Le Floc'H E, Harris GN, Leonardos N, Geider RJ. 2007. Different strategies of photoacclimation by two strains of *Emiliania huxleyi* (Haptophyta). *J Phycol* 43(6): 1209-22.

Sundquist ET. 1990. Influence of deep-sea benthic processes on atmospheric CO_2. *Phil Trans R Soc A* 331(1616): 155-65.

Sültemeyer D, Rinast K-A. 1996. The CO_2 permeability of the plasma membrane of *Chlamydomonas reinhardtii*: mass-spectrometric ^{18}O exchange measurements from $^{13}C^{18}O_2$ in suspension of carbonic anhydrase-loaded plasma-membrane vesicles. *Planta* 200: 358–36.

Taylor AR, Brownlee C. 2005. Unravelling the mechanisms of calcium transport in coccolithophores. *Phycologia* 44(4): 14-15.

Taylor AR, Chrachri A, Wheeler G, Goddard H, Brownlee C. 2011. A voltage-gated H^+ channel underlying pH homeostasis in calcifying coccolithophores. *PLOS Biol* 9(6): e1001085.

Tchernov D, Silverman J, Luz B, Reinhold L, Kaplan A. 2003. Massive light-dependent cycling of inorganic carbon between oxygenic photosynthetic microorganisms and their surroundings. *Photosynth Res* 77(2-3): 95-103.

Thierstein H, Geitzenauer K, Molfino B, Shackleton N. 1977. Global synchroneity of late Quaternary coccolith datum levels validation by oxygen isotopes. *Geology* 5(7): 400-04.

Trimborn S, Langer G, Rost B. 2007. Effect of varying calcium concentrations and light intensities on calcification and photosynthesis in *Emiliania huxleyi*. *Limnol Oceanogr* 52(5): 2285-93.

Tyrrell T, Merico A 2004. *Emiliania huxleyi*: Bloom observations and the conditions that induce them. *Coccolithophores: From Molecular Processes to Global Impact*, 75-97.

Vaughn KC, Campbell EO, Hasegawa J, Owen HA, Renzaglia KS. 1990. The pyrenoid is the site of ribulose 1,5-bisphosphate carboxylase/oxygenase accumulation in the hornwort (Bryophyta, Anthocerotae) chloroplast. *Protoplasma* 156(3): 117-29.

Wahlund TM, Hadaegh AR, Clark R, Nguyen B, Fanelli M, et al. 2004. Analysis of expressed sequence tags from calcifying cells of marine coccolithophorid (*Emiliania huxleyi*). *Marine Biotechnol* 6(3): 278-90.

Weiss RF. 1974. Carbon dioxide in water and seawater: The solubility of a non-ideal gas. *Mar Chem* 2: 203-15.

Westbroek P, De Jong E, Van der Wal P, Borman A, De Vrind J, et al. 1984. Mechanism of calcification in the marine alga *Emiliania huxleyi* [and Discussion]. *Phil Trans R Soc B* 304(1121): 435-44.

Wilson WH, Tarran GA, Schroeder D, Cox M, Oke J, et al. 2002. Isolation of viruses responsible for the demise of an *Emiliania huxleyi* bloom in the English Channel. *Journal of the Marine Biological Association of the UK* 82(3): 369-77.

Winter A, Henderiks J, Beaufort L, Rickaby REM, Brown CW. 2013. Poleward expansion of the coccolithophore *Emiliania huxleyi*. *J Plankton Res* 36(2): 316-25.

Wolf-Gladrow DA, Riebesell U, Burkhardt S, Bijma J. 1999. Direct effects of CO_2 concentration on growth and isotopic composition of marine plankton. *Tellus B* 51(2): 461-76.

Wolf-Gladrow DA, Zeebe RE, Klaas C, Körtzinger A, Dickson AG. 2007. Total alkalinity: The explicit conservative expression and its application to biogeochemical processes. *Mar Chem* 106(1-2): 287-300.

Xing T, Gao K, Beardall J. 2015. Response of growth and photosynthesis of *Emiliania huxleyi* to visible and UV irradiances under different light regimes. *Photochem Photobiol*

Young JR, Davis SA, Bown PR, Mann S. 1999. Coccolith ultrastructure and biomineralisation. *J Struct Biol* 126(3): 195-215.

Young JR, Henriksen K. 2003. Biomineralization within vesicles: The calcite of coccoliths. *Rev Mineral Geochem* 54(7): 189-215.

Zeebe RE, Wolf-Gladrow DA. 2001. *CO_2 in seawater: equilibrium, kinetics, isotopes*: Elsevier Science B.V.

Zeebe RE, Westbroek P. 2003. A simple model for the $CaCO_3$ saturation state of the ocean: The "Strangelove," the "Neritan," and the "Cretan" Ocean. *Geochem Geophy Geosy* 4(12): 1-26.

Ziveri P, Passaro M, Incarbona A, Milazzo M, Rodolfo-Metalpa R, et al. 2014. Decline in coccolithophore diversity and impact on coccolith morphogenesis along a natural CO_2 gradient. *Biol Bull* 226(3): 282-90.

Zondervan I, Rost B, Riebesell U. 2002. Effect of CO_2 concentration on the PIC/POC ratio in the coccolithophore *Emiliania huxleyi* grown under light-limiting conditions and different daylengths. *J Exp Mar Biol Ecol* 272(1): 55-70.

Erklärung

Hiermit erkläre ich, dass ich die Doktorarbeit mit dem Titel:

Process understanding of photosynthetic fluxes underlying ocean acidification responses in the coccolithophore *Emiliania huxleyi*

selbständig verfasst und geschrieben habe und außer den angegebenen Quellen keine weiteren Hilfsmittel verwendet habe.

Bei dieser veröffentlichen Version meiner Dissertation handelt es sich um eine überarbeitete, aber inhaltlich unveränderte Version der Doktorarbeit. In Kapitel 3 wurde die in der Zwischenzeit veröffentlichte formatierte Version der Publikation II verwendet.

Dorothee Kottmeier